

Arbeitsbericht NAB 22-02

**TBO Stadel-2-1:
Data Report**

**Dossier IV
Microfacies, Bio- and Chemo-
stratigraphic Analysis**

September 2022

S. Wohlwend, H.R. Bläsi, S. Feist-Burkhardt,
B. Hostettler, U. Menkveld-Gfeller,
V. Dietze & G. Deplazes

**National Cooperative
for the Disposal of
Radioactive Waste**

Hardstrasse 73
P.O. Box
5430 Wettingen
Switzerland
Tel. +41 56 437 11 11

nagra.ch

Arbeitsbericht

NAB 22-02

**TBO Stadel-2-1:
Data Report**

**Dossier IV
Microfacies, Bio- and Chemo-
stratigraphic Analysis**

September 2022

S. Wohlwend¹, H.R. Bläsi², S. Feist-Burkhardt^{3,4},
B. Hostettler⁵, U. Menkveld-Gfeller⁵,
V. Dietze⁶ & G. Deplazes⁷

¹Geological Institute, ETH Zurich

²Geo-Consulting, Wünnewil, Switzerland

³SFB Geological Consulting & Services, Ober-Ramstadt, Germany

⁴Département des Sciences de la Terre, Université de Genève

⁵Natural History Museum Bern

⁶Nördlingen, Germany

⁷Nagra

Keywords:

STA2-1, Nördlich Lägern, TBO, deep drilling campaign,
microfacies, lithostratigraphy, biostratigraphy, ammonite
stratigraphy, palynostratigraphy, chemostratigraphy,
dinoflagellate cysts, stable carbon isotopes

**National Cooperative
for the Disposal of
Radioactive Waste**

Hardstrasse 73
P.O. Box
5430 Wettingen
Switzerland
Tel. +41 56 437 11 11

nagra.ch

Nagra Arbeitsberichte ("Working Reports") present the results of work in progress that have not necessarily been subject to a comprehensive review. They are intended to provide rapid dissemination of current information.

This NAB aims at reporting drilling results at an early stage. Additional borehole-specific data will be published elsewhere.

In the event of inconsistencies between dossiers of this NAB, the dossier addressing the specific topic takes priority. In the event of discrepancies between Nagra reports, the chronologically later report is generally considered to be correct. Data sets and interpretations laid out in this NAB may be revised in subsequent reports. The reasoning leading to these revisions will be detailed there.

This report was finalised in June 2023.

This Dossier was prepared by a project team consisting of:

S. Wohlwend (sampling, chemostratigraphy, conceptualisation and compilation)

H.R. Bläsi (microfacies)

S. Feist-Burkhardt (palynostratigraphy)

B. Hostettler, U. Menkveld-Gfeller, V. Dietze (ammonite stratigraphy)

G. Deplazes (project management and conceptualisation)

Editorial work: P. Blaser and M. Unger

The Dossier has greatly benefitted from technical discussions with, and reviews by, external and internal experts. Their input and work are very much appreciated.

Copyright © 2022 by Nagra, Wettingen (Switzerland) / All rights reserved.

All parts of this work are protected by copyright. Any utilisation outwith the remit of the copyright law is unlawful and liable to prosecution. This applies in particular to translations, storage and processing in electronic systems and programs, microfilms, reproductions, etc.

Table of Contents

Table of Contents	I
List of Tables.....	II
List of Figures	II
List of Appendices	III
1 Introduction	1
1.1 Context.....	1
1.2 Location and specifications of the borehole	2
1.3 Documentation structure for the STA2-1 borehole	5
1.4 Scope and objectives of this dossier	6
2 Methods	9
2.1 Microfacies	9
2.2 Ammonite preparation	11
2.3 Palynological sample preparation and quantitative analysis	11
2.4 Chemostratigraphy.....	12
3 Results.....	15
3.1 Microfacies	15
3.2 Ammonite stratigraphy	23
3.3 Palynostratigraphy	29
3.4 Chemostratigraphy.....	38
4 Definition of specific lithostratigraphic boundaries	53
5 Conclusion	57
6 References.....	59

List of Tables

Tab. 1-1:	General information about the STA2-1 borehole	2
Tab. 1-2:	List of dossiers included in NAB 22-02	5
Tab. 3-1:	Microfacies analysis from STA2-1 (1'225.80 – 521.15 m; numbers in vol.-%.....	21
Tab. 3-2:	Ammonite and other macrofossil determination from STA2-1	27
Tab. 3-3:	List of analysed palynology samples from STA2-1	37

List of Figures

Fig. 1-1:	Tectonic overview map with the three siting regions under investigation	1
Fig. 1-2:	Overview map of the investigation area in the Nördlich Lägern siting region with the location of the STA2-1 borehole in relation to the boreholes Weiach-1, BUL1-1, STA3-1 and BAC1-1	3
Fig. 1-3:	Lithostratigraphic profile and casing scheme for the STA2-1 borehole.....	4
Fig. 1-4:	Stadel-2-1 stratigraphy with core depth in metres [m MD].....	7
Fig. 1-5:	Lithostratigraphy plot (1:5'000) from the Mesozoic succession with the individual sampling intervals for thin sections, macrofossils, palynological analysis and chemostratigraphy	8
Fig. 3-1:	Zones and subzones which are documented by ammonites in STA2-1.....	28
Fig. 3-2:	Bulk rock (carbonate) isotopic data from the Lias Group	40
Fig. 3-3:	Organic isotopic data from the Lias Group	41
Fig. 3-4:	Bulk rock (carb.) isotopic data from the lower Dogger Group – mainly Opalinus Clay	44
Fig. 3-5:	Organic isotopic data from the lower Dogger Group – mainly Opalinus Clay	45
Fig. 3-6:	Bulk rock (carbonate) isotopic data from the upper part of the Dogger Group.....	48
Fig. 3-7:	Organic isotopic data from the upper part of the Dogger Group.....	49
Fig. 3-8:	Whole bulk rock (carbonate) isotopic data from STA2-1	50
Fig. 3-9:	Whole organic isotopic data from STA2-1.....	51

List of Appendices

Appendix A:	List of all samples	A-1
Appendix A1:	List of all thin sections from STA2-1 (1'225.80 – 521.15 m).....	A-2
Appendix A2:	List of all sampled macrofossils from STA2-1 (915.45 – 718.61 m)	A-3
Appendix A3:	List of other provisionally determined conspicuous macrofossils from STA2-1 (931.67 – 697.40 m).....	A-4
Appendix A4:	List of all palynological samples from STA2-1 (905.83 – 726.25 m)	A-5
Appendix B:	Photos microfacies	B-1
Appendix C:	Plates of ammonites and other macrofossils	C-1
Plate I:	STA2-1 (915.45 m, core pictures)	C-3
Plate II:	STA2-1 (915.45 m).....	C-5
Plate III:	STA2-1 (911.39 – 905.84 m).....	C-7
Plate IV:	STA2-1 (905.31 – 850.57 m).....	C-9
Plate V:	STA2-1 (805.58 – 774.05 m).....	C-11
Plate VI:	STA2-1 (734.84 – 728.84 m).....	C-13
Plate VII:	STA2-1 (727.08 – 718.61 m).....	C-15
Appendix D:	Palynostratigraphy (in the digital version)	D-1
Appendix D1:	Range Chart: Quantitative stratigraphic distribution of Middle Jurassic palynomorphs in the Stadel-2-1 borehole	
Appendix D2:	Depth/Age plot: Stadel-2-1 borehole	
Appendix E:	Chemostratigraphy	E-1
Appendix E1:	List of all geochemical samples and results mainly drilled from specific calcareous beds in the Opalinus Clay and its confining units.....	E-2

1 Introduction

1.1 Context

To provide input for site selection and the safety case for deep geological repositories for radioactive waste, Nagra has drilled a series of deep boreholes ("Tiefbohrungen", TBO) in Northern Switzerland. The aim of the drilling campaign is to characterise the deep underground of the three remaining siting regions located at the edge of the Northern Alpine Molasse Basin (Fig. 1-1).

In this report, we present the results from the Stadel-2-1 borehole.

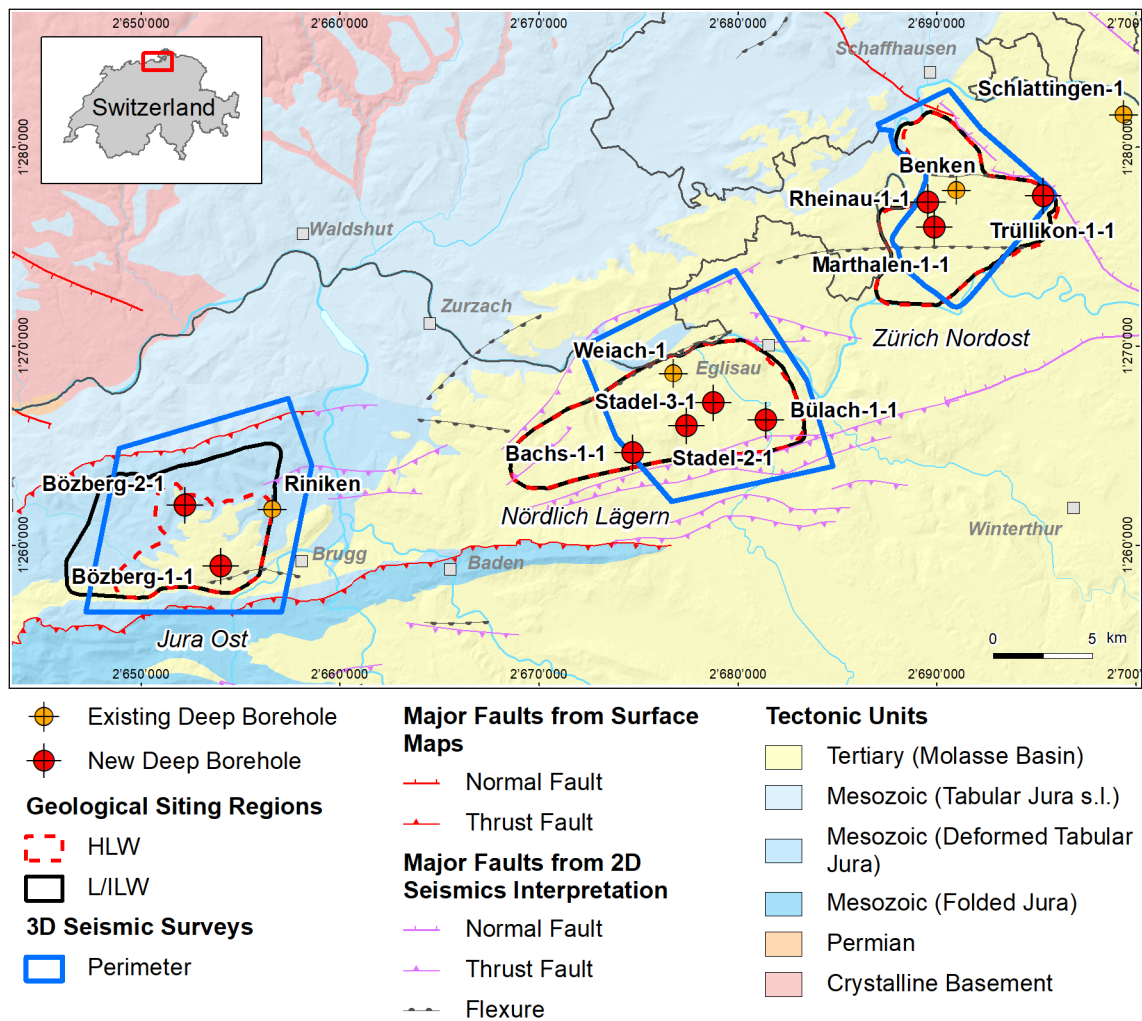


Fig. 1-1: Tectonic overview map with the three siting regions under investigation

1.2 Location and specifications of the borehole

The Stadel-2-1 (STA2-1) exploratory borehole is the seventh borehole drilled within the framework of the TBO project. The drill site is located in the central part of the Nördlich Lägern siting region (Fig. 1-2). The vertical borehole reached a final depth of 1'288.12 m (MD)¹. The borehole specifications are provided in Tab. 1-1.

Tab. 1-1: General information about the STA2-1 borehole

Siting region	Nördlich Lägern
Municipality	Stadel (Canton Zürich / ZH), Switzerland
Drill site	Stadel-2 (STA2)
Borehole	Stadel-2-1 (STA2-1)
Coordinates	LV95: 2'677'447.617 / 1'265'987.019
Elevation	Ground level = top of rig cellar: 417.977 m above sea level (asl)
Borehole depth	1'288.12 m measured depth (MD) below ground level (bgl)
Drilling period	25th January – 8th July 2021 (spud date to end of rig release)
Drilling company	Daldrup & Söhne AG
Drilling rig	Wirth B 152t
Drilling fluid	Water-based mud with various amounts of different components such as ² : 0 – 670 m: Bentonite & polymers 670 – 1'051 m: Potassium silicate & polymers 1'051 – 1'117 m: Water & polymers 1'117 – 1'288.12 m: Sodium chloride brine & polymers

The lithostratigraphic profile and the casing scheme are shown in Fig. 1-3. The main lithostratigraphic boundaries in the STA2-1 borehole are shown in Fig. 1-4.

¹ Measured depth (MD) refers to the position along the borehole trajectory, starting at ground level, which for this borehole is the top of the rig cellar. For a perfectly vertical borehole, MD below ground level (bgl) and true vertical depth (TVD) are the same. In all Dossiers depth refers to MD unless stated otherwise.

² For detailed information see Dossier I.

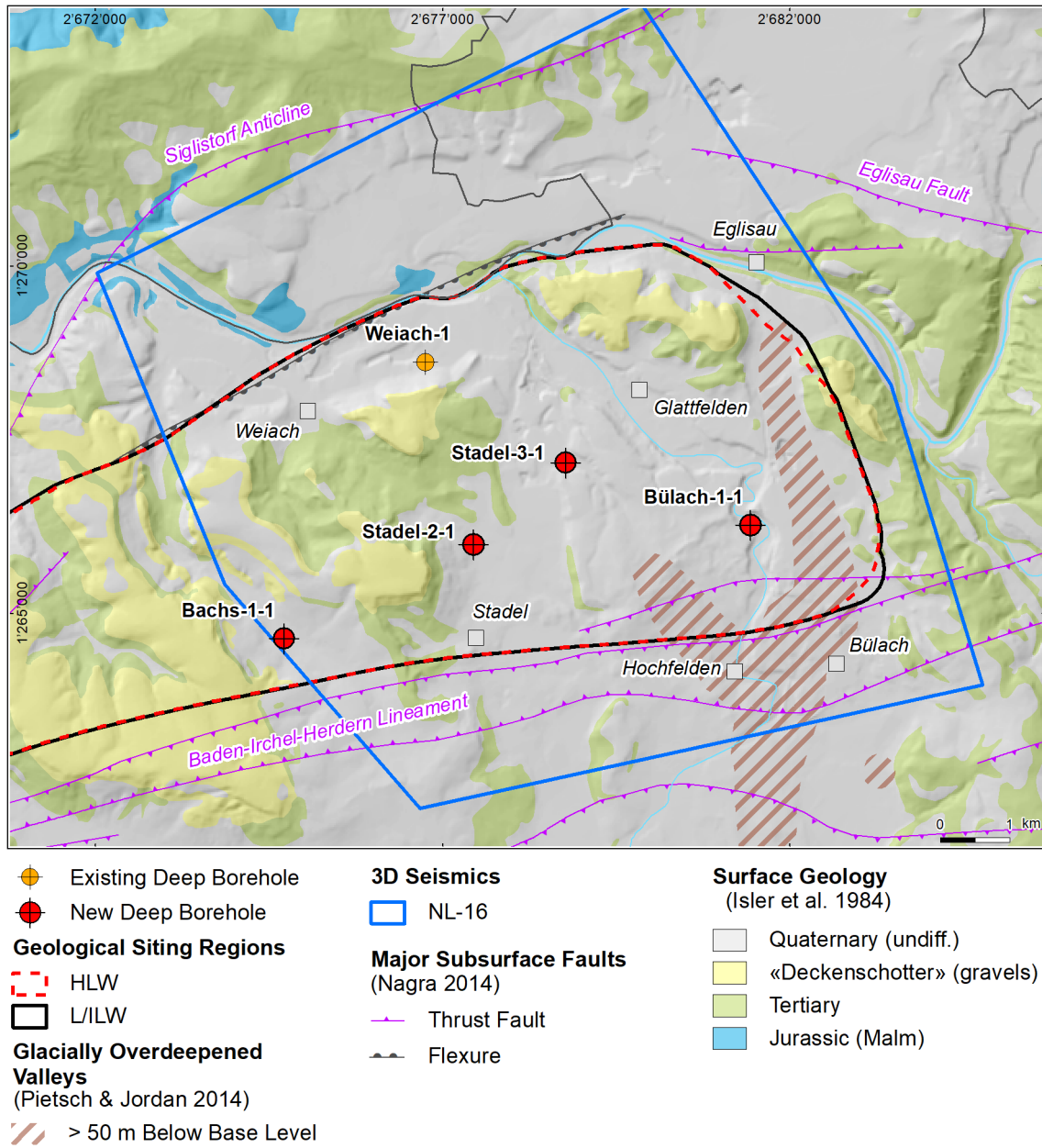


Fig. 1-2: Overview map of the investigation area in the Nördlich Lägern siting region with the location of the STA2-1 borehole in relation to the boreholes Weiach-1, BUL1-1, STA3-1 and BAC1-1

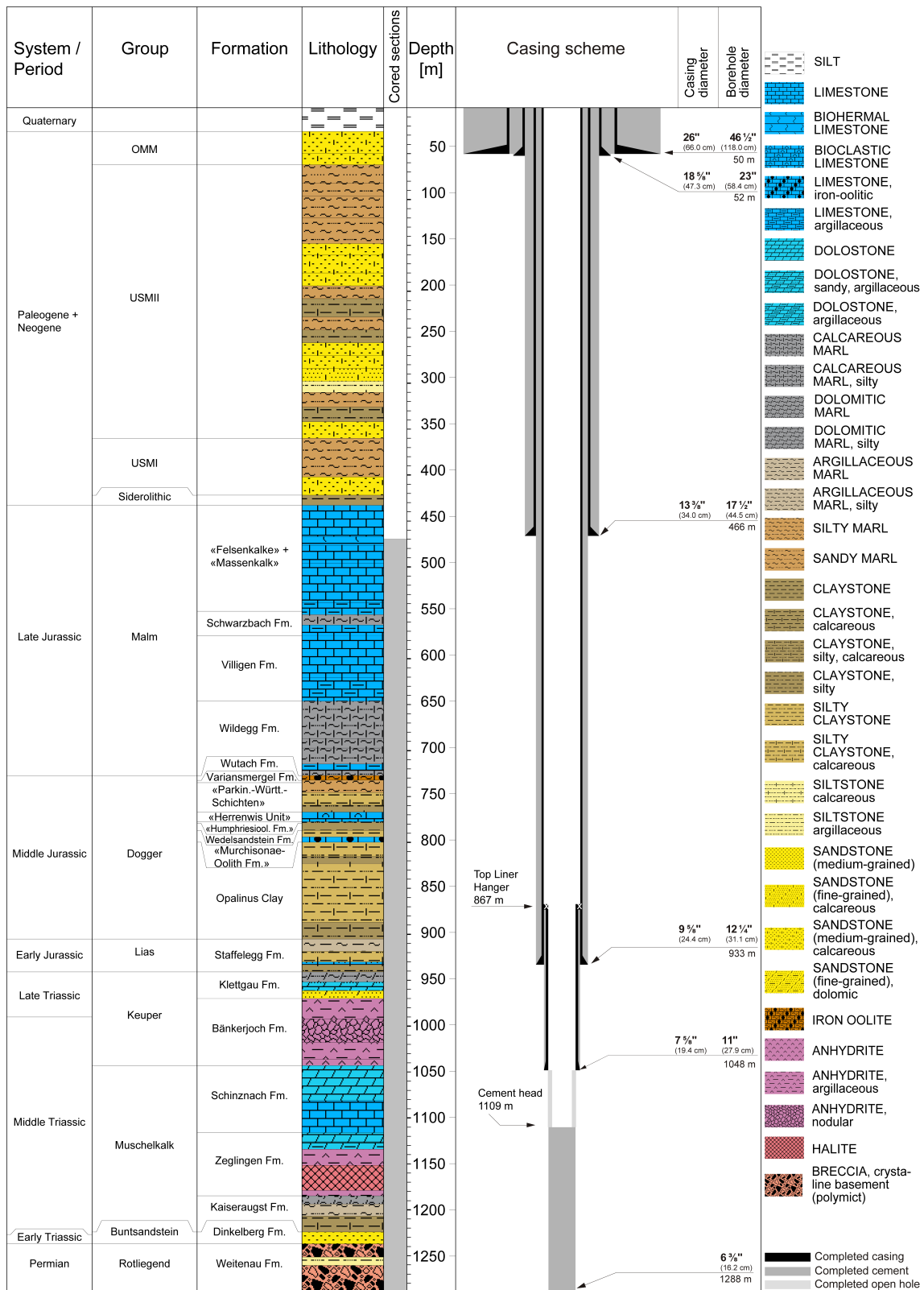


Fig. 1-3: Lithostratigraphic profile and casing scheme for the STA2-1 borehole³

³ For detailed information see Dossier I and III.

1.3 Documentation structure for the STA2-1 borehole

NAB 22-02 documents the majority of the investigations carried out in the STA2-1 borehole, including laboratory investigations on core material. The NAB comprises a series of stand-alone dossiers addressing individual topics and a final dossier with a summary composite plot (Tab. 1-2).

This documentation aims at early publication of the data collected in the STA2-1 borehole. It includes most of the data available approximately one year after completion of the borehole. Some analyses are still ongoing (e.g. diffusion experiments, analysis of veins, hydrochemical interpretation of water samples) and results will be published in separate reports.

The current borehole report will provide an important basis for the integration of datasets from different boreholes. The integration and interpretation of the results in the wider geological context will be documented later in separate geoscientific reports.

Tab. 1-2: List of dossiers included in NAB 22-02

Black indicates the dossier at hand.

Dossier	Title	Authors
I	TBO Stadel-2-1: Drilling	P. Hinterholzer-Reisegger
II	TBO Stadel-2-1: Core Photography	D. Kaehr & M. Gysi
III	TBO Stadel-2-1: Lithostratigraphy	P. Jordan, P. Schürch, H. Naef, M. Schwarz, R. Felber, T. Ibele & H.P. Weber
IV	TBO Stadel-2-1: Microfacies, Bio- and Chemostratigraphic Analysis	S. Wohlwend, H.R. Bläsi, S. Feist-Burkhardt, B. Hostettler, U. Menkveld-Gfeller, V. Dietze & G. Deplazes
V	TBO Stadel-2-1: Structural Geology	A. Ebert, S. Cioldi, E. Hägerstedt & H.P. Weber
VI	TBO Stadel-2-1: Wireline Logging, Micro-hydraulic Fracturing and Pressure-meter Testing	J. Gonus, E. Bailey, J. Desroches & R. Garrard
VII	TBO Stadel-2-1: Hydraulic Packer Testing	R. Schwarz, R. Beauheim, S.M.L. Hardie & A. Pechstein
VIII	TBO Stadel-2-1: Rock Properties, Porewater Characterisation and Natural Tracer Profiles	C. Zwahlen, L. Aschwanden, E. Gaucher, T. Gimmi, A. Jenni, M. Kiczka, U. Mäder, M. Mazurek, D. Roos, D. Rufer, H.N. Waber, P. Wersin & D. Traber
IX	TBO Stadel-2-1: Rock-mechanical and Geomechanical Laboratory Testing	E. Crisci, L. Laloui & S. Giger
X	TBO Stadel-2-1: Petrophysical Log Analysis	S. Marnat & J.K. Becker
	TBO Stadel-2-1: Summary Plot	Nagra

1.4 Scope and objectives of this dossier

The dossier at hand complements the lithostratigraphic report (Dossier III) on the STA2-1 borehole. The report documents data on microfacies analysis, ammonite- and palynostratigraphy as well as detailed geochemical (C, O and N isotopes) analyses. Preliminary results of these analyses already existed at data-freeze (30.09.2021), two months after the end of drilling operations and were integrated into the lithostratigraphic discussion and lithostratigraphic boundary definition (Dossier III).

The objectives of this report focusing on the Opalinus Clay and its confining units are:

- to specify the macroscopic description by a detailed microfacies analysis (components, matrix, cements),
- to allow a microfacies comparison of specific horizons, for example hardgrounds of the upper Opalinus Clay,
- to provide additional data on the diagenetic history of the sediment,
- to recover macrofossils from the stratigraphic interval of interest which are significant for facies changes and chronostratigraphic data,
- to compile an additional independent dataset of palynomorphs for chronostratigraphic data,
- to provide detailed geochemical (C, O and N isotopes) analyses with one metre spacing from the stratigraphic interval of interest,
- to allow a chemostratigraphic correlation (stable isotopes) with other deep boreholes in the three siting regions,
- to support the definition of the lithostratigraphic units.

The detailed stratigraphy of the STA2-1 borehole with core depth in metres can be found in Fig. 1-4. The stratigraphic intervals of interest for the different investigations (microfacies analysis, ammonite- and palynostratigraphy and geochemical analyses) and their specific sampling intervals are visualised in Fig. 1-5 with respect to the 1:5'000 lithostratigraphic profile.

All depths labelled with metres [m] in this report refer to "m MD core depth" if not stated otherwise.

TBO STADEL-2-1					
System / Period	Group	Formation	Metres MD	Member / Sub-unit	
Quaternary			26		
Paleogene / Neogene	OMM		62		
	USM	USM II	360		
		USM I	422		
	Siderolithic		433.0		
Jurassic	Late	Malm	«Felsenkalke» + «Massenkalk»	548.35	
			Schwarzbach Fm.	575.08	
			Villigen Fm.	591.16	Wangental Mb.
				592.38	«Knollen Bed»
				620.37	Küssaburg Mb.
	646.23	Hornbuck Mb.			
	Middle	Dogger	Wildeggen Fm.	726.36	Effingen Mb.
				727.18	Birmenstorf Mb. and «Glaukonitsandmergel Bed»
			Wutach Fm.	732.16	
			Variansmergel Fm.	734.92	
			«Parkinsoni-Württembergica-Sch.»	767.02	
			«Herrenwis Unit»	777.54	
			«Humphriesioolith Fm.»	779.34	
			Wedelsandstein Fm.	786.85	
			«Murchisonae-Oolith Fm.»	799.67	
			Opalinus Clay	823.50	«Sub-unit with silty calcareous beds»
		839.72	«Upper silty sub-unit»		
		886.97	«Mixed clay-silt-carbonate sub-unit»		
		905.20	«Clay-rich sub-unit»		
	Early	Lias	Staffelegg Fm.	909.98	Gross Wolf Mb.
				916.14	Rietheim Mb.
				918.46	Grünscholzh Holz Mb., Breitenmatt Mb. and Rickenbach Mb.
				930.24	Frick Mb.
				933.16	Beggingen Mb.
940.89				Schambelen Mb.	
951.85				Gruhalde Mb.	
957.62				Seebi Mb.	
959.06				Gruhalde Mb.	
961.46				Gansingen Mb.	
Triassic	Late	Keuper	969.87	Ergolz Mb.	
			992.22	«Claystone with anhydrite nodules»	
			1'017.72	«Cyclic sequence»	
			1'036.19	«Thin-layered anhydrite and claystone sequence»	
			1'039.72	«Banded massive anhydrite»	
			1'043.07	«Dolomite and anhydrite»	
			1'047.48	Asp Mb.	
	Middle	Muschelkalk	Bänkerjoch Fm.	1'081.00	Stamberg Mb.
				1'090.78	Liedertswil Mb.
				1'116.01	Leutschenberg Mb. and Kienberg Mb.
			Schinznach Fm.	1'125.93	«Dolomitzone»
				1'151.45	«Obere Sulfatzone»
				1'178.88	«Salzlager»
				1'184.72	«Untere Sulfatzone»
Kaiseraugst Fm.	1'193.73	«Orbicularismergel»			
	1'217.00	«Wellenmergel»			
	1'224.20	«Wellendolomit»			
1226	Bsst.	Dinkelberg Fm.	1'237.01		
Permian	Rotlieg.	Weitenau Fm.	1'288.12	Final depth	

Fig. 1-4: Stadel-2-1 stratigraphy with core depth in metres [m MD]

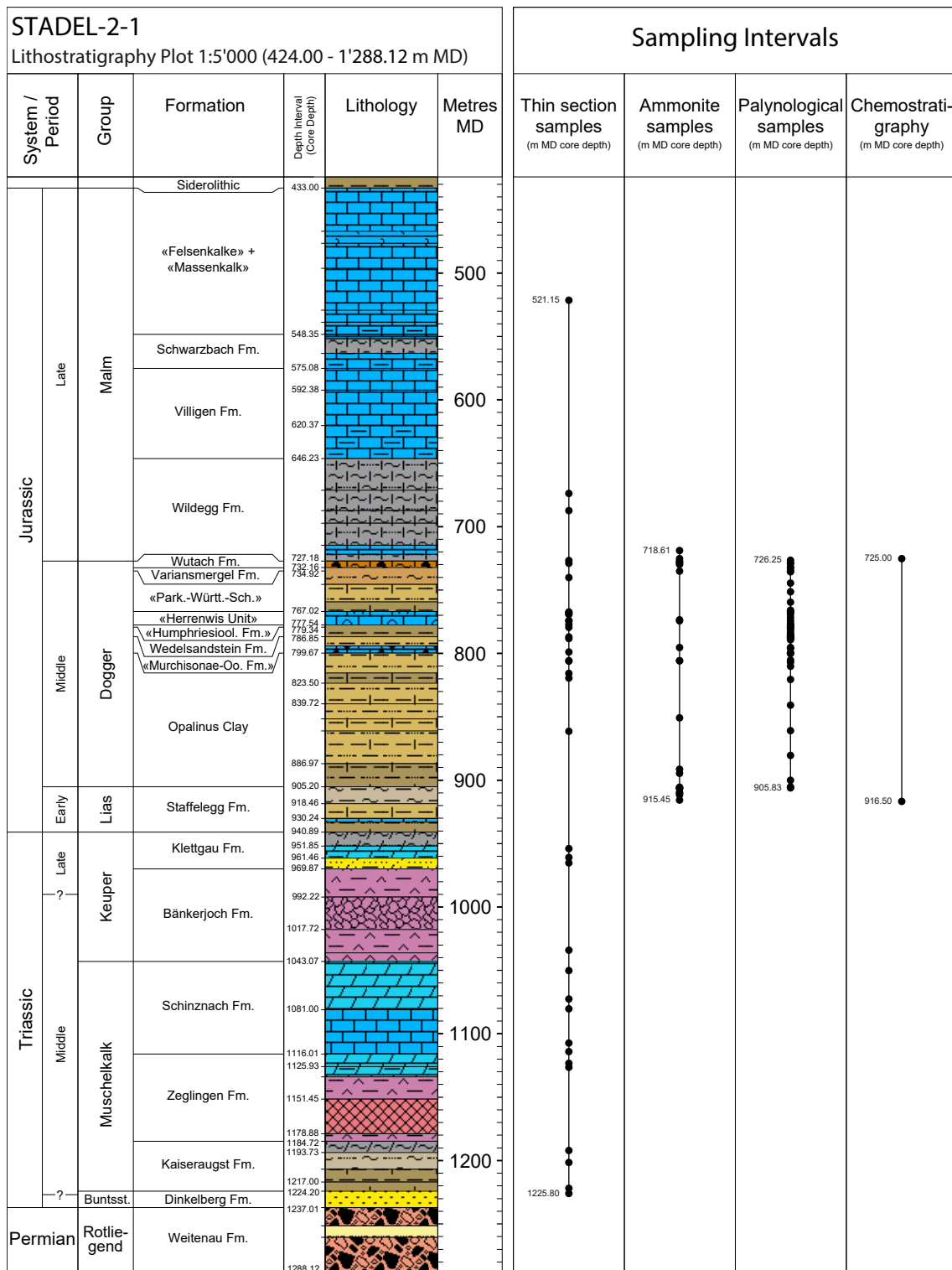


Fig. 1-5: Lithostratigraphy plot (1:5'000) from the Mesozoic succession with the individual sampling intervals for thin sections, macrofossils, palynological analysis and chemostratigraphy

1:5'000 stratigraphic plot modified from Dossier III.

2 Methods

2.1 Microfacies

Thin section preparation

All 37 thin sections (TS) were cut edgewise from the core so that the long side is parallel to the coring direction and therefore covers as much of the stratigraphy as possible. The mean depth of the thin section corresponds to the Sample ID. Therefore, thin sections containing lithological boundaries may have Sample IDs that fall into only one of the two described intervals. However, the lower or upper range on the thin section still covers the interval. A list of all thin sections with their sampling range and Sample ID can be found in Appendix A1 of this report.

The thin sections from calcareous lithologies with a standard length of 4 cm were prepared at the University of Basel. Lithologies sensitive to water such as claystones and argillaceous sediments (swelling of clay minerals) or evaporates (dissolution of evaporitic minerals) were prepared by the Thin Section Lab (TSL) using petroleum, they are only 3 cm long. For better identification of the carbonate minerals calcite, Fe-calcite and Fe-dolomite, the left half of the thin sections was stained applying the technique of Dickson (1965). Thin sections with a macroscopic porosity were impregnated during preparation using a blue coloured epoxy resin to estimate the percentage of their porosity.

Thin section analyses

The thin sections were analysed using a Zeiss polarisation microscope. First, all allochemical components, biogenic particles, siliciclastics, matrix and diagenetic alterations as neomorphic minerals, cements and replacements were studied. Then, to obtain the percentage of the components etc., 100 points were counted with a net micrometre ocular. For detrital quartz-bearing thin sections, the average grain size was evaluated in millimetres. To count inhomogeneous sediments, two different sections were looked at and averaged. A selection of 18 thin section photographs for microfacies analysis is documented in Appendix B (Figs. B-1 to B-18).

Components, matrix and cements (definitions)

To describe thin sections, several allochemical components (described below) were counted, and their numbers are documented in Section 3.1 ('Microfacies'). Some of the specific terms used for the components or matrix are explained as follows:

Clay matrix, micrite, microsparite (or pseudosparite): Sedimented mud consisting of clay minerals, other very small silicate grains, heavy minerals (i.e. clay matrix) and/or microcrystalline carbonate ooze (i.e. micrite). Microsparite is defined as a mosaic of small calcite crystals formed by aggrading neomorphism; originally, it was micrite and not a diagenetic pore-filling cement. Alternatively, microsparite could also be the product of dedolomitisation as seen in the «Felsenkalke» and «Massenkalk».

Dolomitic matrix: primary microcrystalline dolostone ooze.

Limonitic matrix: Calcite micrite mixed with microcrystalline limonitic grains grown during diagenesis.

Limonitic echinoderms, limonitic bivalves: Fragments, parts of echinoderms and bivalves, with limonite filling the skeletal structure of the fossil.

Pellets, peloids, aggregates: the column of pellets also contains aggregates (lumps); that means "carbonate grains of various kinds are clumped together to form compound grains" (Bathurst 1975).

Fe-stromatolites and stromatolitic clasts: Iron-mineralised microbial mats and/or microbial clasts.

Fe-ooids or iron-ooids: Limonitic/goethitic or chamositic ooids, with a visible concentric structure; some iron-ooids are replaced by calcite (calcitic iron-ooids), a few of them show relicts of iron mineral layers (see STA2-1-819.20, Fig. B-6, Appendix B).

Intraclasts: Rock fragments of early diagenetic cemented sediment, reworked and sedimented in the same sedimentary environment.

Calcite cement (sparite): "Normal" cement, calcite crystals grown – filled in – within the primary pore space or in leached components. In this column, the amount of calcite crystal pseudomorphs after gypsum was noted.

"Stellate cement": Calcite "cement" grown within the matrix and not filling primary or secondary pore space. The calcite crystals form small "stellates", i.e. a habitus typical for "hiatus beds" (firm-, hardgrounds; Wetzel & Allia 2000) or "hiatus concretions" (Voigt 1968).

Cone-in-cone calcite: Rows of piled calcite cones grown during diagenesis which were named "Tutenmergel" in the Swabian realm.

(Fe)-Dolomite: Normally dolomite rhombohedrons that originated during diagenesis; in special cases, the dolomite replaces gypsum crystals that were sedimented as detrital gypsum crystals. In some cases, the rhombohedrons consist of iron-dolomite, which are stained blue after the thin section staining.

Dedolomite: Calcite replacement of dolomite: each single dolomite rhombohedron is replaced by a few smaller calcite crystals. When it was a total dolostone and the calcitic replacement has been completed, the result is a thoroughly crystalline, sparitic/microsparitic limestone. In addition, another dedolomite type exists with larger calcite crystals jointly replacing a few dolomite crystals, thus forming a calcite mosaic similar to marble.

Anhydrite: Present in various forms: as a rock-forming mineral, as a vein mineral, mainly replacing "Fasergips", and as cement in sandstones (e.g. Ergolz Member of the Klettgau Formation).

Quartz cement: Authigenic quartz rims grown during diagenesis around detrital quartz grains; quartz/chalcedony in silicified bivalves (MAR1-1-569.18; Wohlwend et al. 2021c).

Porosity: Thin sections with a macroscopic porosity were impregnated during preparation using a blue coloured epoxy resin to estimate the volume percentage (vol.-%) of their porosity.

Hardground: Thin sections from hardgrounds document synsedimentarily cemented and lithified carbonate layers which have been exposed on the seafloor. During that time period, the hardgrounds are therefore mostly encrusted and bored by organisms and may consist of early marine calcite cements and are in parts mineralised by iron and manganese oxides or calcium phosphates.

2.2 Ammonite preparation

The STA2-1 cores were carefully examined for macrofossils at the Würenlingen (Canton Aargau) core storage facility. The cores were examined for ammonites and other macrofossils on the bedding and fractured surfaces as well as on the outer surface of the core; the core itself was not broken open. A list of all 23 samples with their sampling range and Sample ID can be found in Appendix A2 of this report. In addition to ammonites, other conspicuous fossils were identified to the extent possible and entered in the list (Appendix A3), even when they were not subsequently, or only occasionally, recovered. The ammonites were then secured from the core and brought to Glovelier where they were prepared and documented. Afterwards they were archived in the earth sciences collection of the Natural History Museum in Bern.

For the preparation, we used mechanical methods such as air tools and fine sandblasting equipment as well as a chemical etching method using potassium hydroxide (KOH). Sodium hydrogen carbonate was mainly used as abrasive. Residual material from the ammonite sample taken between 905.81 m and 905.84 m was used as material for a palynological sample (905.83 m; marked in grey in Appendix A4). Before being photographed, ammonium chloride steam was applied to the fossils to compensate for variation in contrast caused by different colouring. A selection of ammonites and additional macrofossils is documented on seven plates (Plate I – VII) in Appendix C.

The names of several ammonite taxa are followed by a question mark, for example in *Pleydellia?* sp. The question mark after the genus name was used to indicate a question regarding the correct taxonomical assignment of the species to the genus.

2.3 Palynological sample preparation and quantitative analysis

Palynological processing of the rock samples was carried out by PLS Palynological Laboratory Services Ltd. (Holyhead, Anglesey, LL65 4RJ, UK). Processing follows the standard protocol using concentrated HCl and concentrated HF, followed by a short oxidation with HNO₃ and, if necessary, treatment with ultrasound (e.g. Wood et al. 1996). The residues are sieved at a mesh size of 15 µm. Residues are mounted on microscope slides and analysed using transmitted light microscopy. A list of all samples with their sampling range and Sample ID can be found in Appendix A4 of this report.

Two consecutive counts were carried out in the quantitative microscopic analysis. In a first count 200 grains of all palynomorphs were counted and the number of dinoflagellate cysts was noted (column 'DA *Dinocysts (count 1)*' in Appendix D1). In a consecutive second count, only dinoflagellate cysts were counted until a total of 100 dinoflagellate cysts was reached. The remainder of the slide was checked for additional, out of count species. Taxa recorded out of count are marked with a '+', questionably identified taxa are marked with a '?' in the range chart. Occurrences of fungal remains are recorded semi-quantitatively (R = Rare, O = Occasional, C = Common, A = Abundant, S = Superabundant).

Results are illustrated using the software package StrataBugs v2.1 (Appendices D1 and D2). Numerical age dates used for the Composite Standard and the Depth/Age plot are in line with those of the *Geologic Time Scale 2016* (Ogg et al. 2016). On the range chart (Appendix D1), several abbreviations are used (AC = Acritarchs, ALBO = Algae, *Botryococcus* and *Pediastrum*, ALPR = Algae, Prasinophytes, ALZY = Algae, Zygnematophyceae, DA = Dinocyst abundance, DC = Dinoflagellate cysts, FT = Foraminiferal test linings, FU = Fungi, MP = Miscellaneous palynomorphs, SP = Spores and pollen. Several dinoflagellate cyst taxa contain a question mark in the name, as for example in *Evansia? eschachensis*. The question mark after the genus name indicates uncertainty regarding the correct taxonomical assignment of the species to the genus.

2.4 Chemostratigraphy

The sampling of the STA2-1 borehole focused primarily on the Dogger and Lias Groups and therefore primarily on clay mineral-rich layers of the Opalinus Clay. The sampling resolution was one metre, except for some intervals with denser sampling density (mainly hardgrounds, condensed intervals and the Rietheim Member of the Staffelegg Formation). All 306 samples were drilled with a micro-drill. In general, clay mineral-rich lithologies were sampled. Diagenetic calcite and siderite veins and nodules were avoided. The drilled powder amounted to around 1 g of material. A list of specific samples ($n = 21$) with results mainly from calcareous beds and calcareous concretions, as well as a macrofossil (gryphaea) can be found in Appendix E1 of this report.

Inorganic (carbonate) analyses

243 samples were analysed for **stable carbon** ($\delta^{13}\text{C}_{\text{carb}}$) and **oxygen isotope** ($\delta^{18}\text{O}_{\text{carb}}$) of bulk carbonate, 222 continuous samples (roughly in metre resolution) and additional 21 samples from specific calcareous beds and concretions in the Opalinus Clay (Appendix E1). Varying amounts of powder to reach approximately 120 μg of carbonate in the vial were weighed using a Mettler Toledo MT5 Fact microbalance in 12 ml vacutainers. The headspace was flushed with pure He, and then the samples were reacted with 100% phosphoric acid at 72 °C in a ThermoFisher GasBench II carbonate device connected to a ThermoFisher Delta V PLUS mass spectrometer. The instrument is calibrated with international carbonate standards NBS19 and NBS18 distributed by the International Atomic Energy Agency (IAEA), Vienna and internal standards (MS2 "Carrara marble"; $\delta^{13}\text{C}_{\text{carb}} = 2.16 \text{ ‰}$, $\delta^{18}\text{O}_{\text{carb}} = -1.85 \text{ ‰}$). The reproducibility of the measurements based on replicated standards was $\pm 0.05 \text{ ‰}$ for $\delta^{13}\text{C}_{\text{carb}}$ and $\pm 0.06 \text{ ‰}$ for $\delta^{18}\text{O}_{\text{carb}}$. All isotope measurements were performed at the Stable Isotope Laboratory of the ETH Zurich (Geological Institute). The isotope values are reported in the conventional delta notation with respect to the Vienna Pee Dee Belemnite (VPDB).

The **Total Carbonate content** (TCarb) was calculated based on a calibration using extracted CO_2 from the known weight of the internal standard material (MS2), which is composed to 100% of carbonate (calcite). The mean area of the m/z 44 peak (corresponding to the most abundant isotopologue $^{12}\text{C}^{16}\text{O}_2$) in the mass spectrometer allows the carbonate content to be estimated from the individual bulk rock samples. The individual uncertainty for TCarb, represents the average from all standard deviations from the MS2 and is $\pm 5.67\%$. However, the TCarb values calculated from the reaction of the phosphoric acid with the bulk rock, only reflect the carbonate that was able to react during the reaction time (~ 60 min). However, ankerite and especially siderite, for example, roughly require 60 h reaction time for full dissolution at 70 °C (Fernandez et al. 2016). Therefore, the calculated carbonate content (TCarb) does not completely represent the total amount of all different carbonates. The data reflect a mixed signal composed mostly of calcite and dolomite with a smaller component of the other more resistant carbonates (see also Wohlwend et al. 2019).

Organic analyses

The powders remaining after inorganic analysis from 185 samples were decarbonated in quantities of less than 1 g in 10 ml of 3 M HCl for 12 h in 15 ml centrifuge tubes, to ensure the complete removal of carbonate. For neutralisation purposes, the residue was subsequently washed three times with deionised water, and then centrifuged and decanted. After drying at 70 °C in an oven for at least 72 h the samples were homogenised with a mortar and pestle. Depending on the

organic carbon content of each specific sample, a different amount was weighed in a tin capsule using a Mettler Toledo MT5 Fact microbalance, so that approximately the same amount of organic carbon was always measured.

$\delta^{13}\text{C}_{\text{org}}$ and $\delta^{15}\text{N}_{\text{org}}$ were measured by flash combustion on a ThermoFisher Scientific FlashEA elemental analyser connected to a Delta V isotope ratio mass spectrometer (IRMS) operated in continuous flow mode. The samples were combusted in an O_2 atmosphere in a quartz reactor at 1'020 °C packed with $(\text{Co}_3\text{O}_4)\text{Ag}$ and Cr_2O_3 to form CO_2 , N_2 , NO_x and H_2O . These gases were then transferred through a reduction reactor containing elemental Cu at 600 °C to remove excess O_2 and to reduce NO_x to N_2 . H_2O and SO_x were subsequently removed using anhydrous $\text{Mg}(\text{ClO}_4)_2$ and elemental Ag. Then, N_2 and CO_2 were separated in a packed gas chromatographic column and analysed for their isotopic composition using the IRMS. Isotope ratios are reported in conventional delta notation with respect to atmospheric N_2 (AIR) and VPDB standards, respectively. The methods were calibrated with the International Atomic Energy Agency (IAEA)-N1 ($\delta^{15}\text{N} = 0.45 \text{ ‰}$), IAEA-N2 ($\delta^{15}\text{N} = +20.41 \text{ ‰}$) and IAEA-N3 ($\delta^{15}\text{N} = +4.72 \text{ ‰}$) reference materials for nitrogen, and NBS22 ($\delta^{13}\text{C} = -30.03 \text{ ‰}$) and IAEA-CH-6 ($\delta^{13}\text{C} = -10.46 \text{ ‰}$) for carbon. Reproducibility of the measurements is better than $\pm 0.2 \text{ ‰}$ for both nitrogen and carbon. Reproducibility and accuracy of the measurements are based on replicate analyses of the internal laboratory standards atropine, peptone and nicotinamide. All geochemical measurements were performed at the Stable Isotope Laboratory of the ETH Zurich (Geological Institute).

The **Total Organic Carbon** ($\text{TOC}_{\text{decarb}}$) and **Total Nitrogen** ($\text{TN}_{\text{decarb}}$) contents of the decarbonised samples were calculated based on the known carbon and nitrogen contents of atropine (70.56 wt.-% C, 4.84 wt.-% N). The individual uncertainty for $\text{TOC}_{\text{decarb}}$ represents the average from all standard deviations from atropine during that calculation and is $\pm 0.73 \text{ ‰}$, respectively $\pm 0.12 \text{ ‰}$ for the $\text{TN}_{\text{decarb}}$. The calculated $\text{TN}_{\text{decarb}}$ reflects a mixture of bound inorganic and organic nitrogen and therefore also contains ammonium, which substitutes for K^+ in the interlayer exchange sites of illite (Scheffer & Schachtschnabel 1984).

The **Carbon-to-Nitrogen ratio** (C/N ratio) is a ratio of the mass of carbon to the mass of nitrogen. In this study, the ratio was calculated using the $\text{TOC}_{\text{decarb}}$ and the $\text{TN}_{\text{decarb}}$. As mentioned above, the C/N ratios can also be influenced by inorganic nitrogen in the form of soil-derived ammonium (Scheffer & Schachtschnabel 1984). Due to this inorganic nitrogen, the C/N ratios of sediments containing additional inorganic nitrogen will decrease. Therefore, C/N ratios are referred to as organic carbon/total nitrogen ($\text{TOC}_{\text{decarb}}/\text{TN}_{\text{decarb}}$) giving the ratio of the C and N masses of the decarbonised samples ($\text{C}_{\text{org}}/\text{N}_{\text{org}}$). The calculated ratios allow to distinguish between marine ($\text{C/N} \leq 10$; Parsons 1975) *versus* terrigenous matter ($\text{C/N} \geq 12$; Kukul 1971) in marine sediments.

$$\frac{C_{\text{org}}}{N_{\text{org}}} = \frac{\text{TOC}_{\text{decarb}}}{\text{TN}_{\text{decarb}}} * \frac{\text{atomic mass (C)}}{\text{atomic mass (N)}} = \frac{\text{TOC}_{\text{decarb}}}{\text{TN}_{\text{decarb}}} * \frac{14.007}{12.011}$$

The **Total Organic Carbon** (TOC) of the whole/bulk sample was calculated using the semi-quantitative carbonate content (TCarb) and semi-quantitative $\text{TOC}_{\text{decarb}}$ content based on the following equation:

$$\text{TOC} = (1 - \text{TCarb}) * \text{TOC}_{\text{decarb}}$$

3 Results

3.1 Microfacies

Dinkelberg Formation (STA2-1-1225.80)

The Dinkelberg Formation consists of numerous different sandstones, which differ in their components, but also in their cementation. Thin section STA2-1-1225.80 is a quartz-sandstone, composed of closely joined quartz sand components (74 vol.-%; Tab. 3-1 for all vol.-% data in this section) and quartz cement (12 vol.-%). Diagenetic pressure-solution between the quartz grains (concave-convex grain contacts) induced the high percentage of quartz components. Anhydrite cement (8 vol.-%) fills a rest of the original pore space. The 6 vol.-% porosity could be caused eventually by thin section preparation (clay matrix washed out).

Kaiseraugst Formation (STA2-1-1221.70, 1201.33, 1191.87)

The three samples represent the three informal members of the Kaiseraugst Formation: STA2-1-1221.70 the «Wellendolomit», STA2-1-1201.33 the «Wellenmergel» and STA2-1-1191.87 the «Orbicularismergel».

Thin section STA2-1-1221.70 is a sandstone (dolomitic) (Fig. B-1; Appendix B for all figures in this section), consisting of quartz sand (45 vol.-%), dolomite cement (35 vol.-%), quartz cement (8 vol.-%), anhydrite cement (5 vol.-%), echinoderms (3 vol.-%), which are enclosed in dolomite crystals, as well as some porosity (4 vol.-%).

STA2-1-1201.33, taken from a calcareous bed, intercalated in an argillaceous marl succession, is a bioclastic limestone (Fig. B-2), composed of numerous thin-shelled bivalves (36 vol.-%), which are cemented by calcite (38 vol.-%). Few echinoderms (3 vol.-%) are also present. Dolomite (8 vol.-%), big anhydrite crystals (12 vol.-%) and ore minerals (3 vol.-%, column of pyrite), which could be sphalerites, complete the cementation.

Thin section STA2-1-1191.87, taken from the anhydrite bed, which occurs in the lower «Orbicularismergel», shows small fibrous anhydrite nodules and anhydrite needles, crystallised in a dolomitic, argillaceous matrix. The following composition results: anhydrite (72 vol.-%), argillaceous matrix (15 vol.-%) and dolomite (13 vol.-%).

Zeglingen Formation (STA2-1-1126.26, 1123.09)

Both samples STA2-1-1126.26 and 1123.09 are pure or nearly pure anhydrites (98 vol.-%, resp. 92 vol.-%). STA2-1-1126.26 contains also dispersed dolomite rhombohedrons (2 vol.-%), STA2-1-1123.09 on the other hand some dolomitic matrix (8 vol.-%), or it may be, that these are dolomitic rock fragments (8 vol.-%).

Schinznach Formation (STA2-1-1113.87, 1107.13, 1080.14, 1072.39, 1049.97)

Numerous different shallow water carbonates mark the Schinznach Formation. Five different beds were selected for a microfacies analyse.

Thin section STA2-1-1113.87, about 2 m above the lower limit to the Schinznach Formation, is still affected by the evaporites of the underlying unit: anhydrite (45 vol.-%) nodules penetrate the bioclastic limestone. Codiacean green algae nodules (14 vol.-% (other biogenes), Fig. B-3) are the dominant components. Micritic pellets (18 vol.-%) and echinoderms (6 vol.-%) are further components. All components are cemented by clear calcite (17 vol.-%).

STA2-1-1107.13 on the contrary is a micritic, bioclastic limestone, consisting of small bioclasts, sometimes only single calcite prisms of bivalve shells and micrite matrix (32 vol.-%). Bivalves (16 vol.-%), echinoderms (8 vol.-%), other biogenes (4 vol.-%) and pellets (28 vol.-%), as well as dolomite rhombohedrons (4 vol.-%) and anhydrite (8 vol.-%) form this limestone.

The three thin sections STA2-1-1080.14, 1072.39 and 1049.97 were taken from the Stammerberg Member. They are now all dolostones. The question arises as to what their original composition was before dolomitisation?

STA2-1-1080.14 consists mostly of fine crystalline dolomite (58 vol.-%), then a layer of thin shelled bivalves (10 vol.-%), furthermore dolomicritic matrix (8 vol.-%), bigger calcite (10 vol.-%) and anhydrite crystals (5 vol.-%) and some porosity (9 vol.-%).

STA2-1-1072.39 was primary an oolite. Now, with a mineralogical view, it is a dolostone with dolomite rhombohedrons (15 vol.-%), which are not part of the ooids and bivalves, fine-crystalline quartz (8 vol.-%), few anhydrite crystals (5 vol.-%) and some pores (9 vol.-%). But the original components are still recognisable: ooids (52 vol.-%, Fig. B-4) and bivalves (11 vol.-%), but both now dolomitic, so therefore it is now a dolostone.

STA2-1-1049.97 includes a lot of micritic and microsparitic pellets (22 vol.-%), bivalves (4 vol.-%) and other biogenes (3 vol.-%), sedimented with micrite (now dolomicritic matrix, 52 vol.-%). Single anhydrite crystals (7 vol.-%), fine-crystalline quartz (4 vol.-%) and pores (8 vol.-%) are present too.

Bänkerjoch Formation (STA2-1-1033.88)

Similar, as it was seen for example in STA3-1, the Bänkerjoch Formation contains in their lower sections calcareous marls and limestone beds: STA2-1-1033.88 shows a laminated limestone, consisting of calcite rosettes (spheres), which are pseudomorph after multiple twinned gypsum crystals (see Fig. B-4 in STA3-1; Wohlwend et al. 2023). Calcite (83 vol.-%, noted in the column of calcite cement), anhydrite (5 vol.-%) and clay matrix (12 vol.-%) are the constituent of this bed.

Klettgau Formation (STA2-1-965.02, 960.69, 953.72)

The three thin sections taken from the Klettgau Formation derive from three individual members: Ergolz Member (STA2-1-965.02), Gansingen Member (STA2-1-960.69) and Seebi Member (STA2-1-953.72).

The thin section from the Ergolz Member (STA2-1-965.02) is a fine grained, argillaceous sandstone with 75 vol.-% quartz and silicate rock fragments (Tab. 3-1), micas (3 vol.-%), clay matrix (18 vol.-%) and anhydrite cement (4 vol.-%).

The thin section from the Gansingen Member (STA2-1-960.69) shows a laminated dolostone (microbial mat), composed of dolomicrite (50 vol.-%) with little dolomite rhombohedrons (35 vol.-%), few quartz silt grains (4 vol.-%) and a fenestrate fabric, which is partly filled with anhydrite (5 vol.-%) and partly open (porosity: 6 vol.-%).

The thin section from the Seebi Member (STA2-1-953.72) is a sandy, argillaceous, brecciated dolostone: dolomite rhombohedrons (40 vol.-%), dolomicrite (26 vol.-%), claystone (22 vol.-%) and silt to coarse sand sized quartz (12 vol.-%).

Opalinus Clay (STA2-1-861.18, 819.20, 815.50, 805.86, 805.50)

The Opalinus Clay of STA2-1 contains calcareous horizons in equivalent stratigraphic positions as in STA3-1. For comparison, we analysed five of these calcareous beds.

STA2-1-861.18 is a pyritic, bioclastic calcareous marl (silty) with calcareous nodules. Strange micritic nodules (14 vol.-%, Fig. B-5), echinoderms (13 vol.-%), bivalves (7 vol.-%), other biogenes (2 vol.-%), quartz silt (13 vol.-%), pyrite (5 vol.-%) and mica (2 vol.-%). All components "swim" in a sideritic (20 vol.-%) clay matrix (22 vol.-%).

Thin section STA2-1-819.20 shows a multi-layered hardground with an iron-oolite layer, a bioclastic marl layer and iron-oolitic, bioclastic marl layers. Overall, the composition is: iron-oolids (replaced by calcite; 26 vol.-%), echinoderms (8 vol.-%), bivalves (7 vol.-%), quartz silt (6 vol.-%), pyrite (4 vol.-%) and a marly and micritic (22 vol.-%), sideritic (18 vol.-%) matrix with "stellate calcite" (9 vol.-%). All iron-oolids are now calcitic (Fig. B-6). The here mentioned calcitic iron-oolids (also applies for the following thin section description, STA2-1-815.50 and thin section STA2-1-779.21) have been noted in the "Fe-oolids" column in Tab. 3-1 with an asterisk behind the number.

Thin section STA2-1-815.50 was taken from a marly, bioclastic "hiatus bed", consisting of numerous echinoderms (27 vol.-%), bivalves (9 vol.-%), other biogenes (3 vol.-%), iron-oolids (10 vol.-%), iron-oolitic intraclasts (5 vol.-%), quartz silt (5 vol.-%) and a siderite-rich (20 vol.-%) clay matrix (10 vol.-%) with some pyrite (4 vol.-%). Most of the iron-oolids are replaced completely by calcite, but few have preserved their chamosite core (Fig. B-7).

STA2-1-805.86 is a bioclastic limestone, rich in echinoderms (26 vol.-%), thick-shelled bivalves (22 vol.-%), serpulids (3 vol.-%), other biogenes (3 vol.-%), intraclasts (4 vol.-%) and quartz sand (5 vol.-%). The components are embedded in micrite (10 vol.-%) with "stellate calcite" (10 vol.-%), calcite cement (6 vol.-%), siderite (8 vol.-%) and pyrite (3 vol.-%).

An iron-stromatolitic horizon and iron-oolids characterise the uppermost limestone of the Opalinus Clay (STA2-1-805.50). This hardground is composed of iron-oolids (10 vol.-%, Fig. B-8), iron-stromatolite (3 vol.-%), echinoderms (15 vol.-%), bivalves (12 vol.-%), limonitic

bioclasts (11 vol.-%), other biogenes and serpulids (5 vol.-%), as well as some quartz sand (6 vol.-%), then micrite matrix (8 vol.-%), "stellate calcite" (14 vol.-%), siderite (5 vol.-%) and pyrite (3 vol.-%).

«Murchisonae-Oolith Formation» (STA2-1-798.65, 788.06)

Both samples are bioclastic limestones with iron-oooids and limonitic components. In detail, however, they differ significantly in the number and type of components. The lower one (STA2-1-798.65) comes from the lowermost red-brown limonitic section, the upper (STA2-1-788.06) from the limestone among the uppermost marly section.

STA2-1-798.65 consists of echinoderm skeletal elements (24 vol.-%), bivalves (7 vol.-%), limonitic biogenes (8 vol.-%), other biogenes (3 vol.-%) and iron-oooids (17 vol.-%, counted together with the limonitic pellets, because they are hardly to distinguish) (Fig. B-9). The iron-oooids are rather small with sizes of 0.1 – 0.3 mm. In addition, quartz sand (5 vol.-%), micrite matrix (5 vol.-%), calcite cement (10 vol.-%), as well as numerous iron-dolomite rhombohedrons (19 vol.-%) and a bit of celestine (or a similar mineral) crystals (2 vol.-%, listed in column anhydrite, gypsum in Tab. 3-1) are present.

Thin section STA2-1-788.06 primarily differs in the type of the iron-oooids, in the quartz content and in the absence of iron-dolomite. The sample consists of echinoderm skeletal elements (22 vol.-%), bivalves (12 vol.-%), limonitic biogenes (5 vol.-%), other biogenes (4 vol.-%) and iron-oooids (10 vol.-%). Most of the iron-oooids are echinoderm plates with a small ooidal cortex (Fig. B-10) and they are relatively big (0.6-2 mm). Quartz sand (18 vol.-%), micrite matrix (14 vol.-%), calcite cement (4 vol.-%), "stellate calcite" (9 vol.-%) and pyrite (2 vol.-%) complete the composition.

Wedelsandstein Formation (STA2-1-786.78)

Thin section STA2-1-786.78, taken at the base of the formation, shows another iron-oolitic, bioclastic limestone. Iron-oooids (21 vol.-%), echinoderms (14 vol.-%), bivalves (10 vol.-%), limonitic biogenes (6 vol.-%), other biogenes (3 vol.-%), intraclasts (4 vol.-%), limonitic nodules (3 vol.-%), quartz silt (7 vol.-%), micrite matrix (23 vol.-%), "stellate calcite" (5 vol.-%) and pyrite (4 vol.-%) compose the sample. The iron-oooids persist still of iron-minerals and have calcite cement rims (Fig. B-11).

«Humphriesioolith Formation» (STA2-1-779.21)

The only bed of the «Humphriesioolith Formation» analysed in a thin section (STA2-1-779.21) is also a bioclastic limestone: echinoderms (17 vol.-%), bivalves (14 vol.-%), other biogenes (4 vol.-%), calcitic iron-oooids (8 vol.-%), intraclasts (4 vol.-%), limonitic nodules (4 vol.-%), quartz sand (8 vol.-%), pyrite (6 vol.-%), glauconite (2 vol.-%), micrite matrix (10 vol.-%) and "stellate calcite" (23 vol.-%) are the "components" of this "hiatus bed" (Fig. B-12).

«Herrenwis Unit» (STA2-1-776.92, 773.98, 773.90, 768.87, 768.73, 767.60, 767.02)

The «Herrenwis Unit» of STA2-1 is composed of bioclastic limestones (e.g., STA2-1-776.92, 773.98, 768.87 and 767.73) and several marly interlayers (e.g., STA2-1-773.90 and 768.73). The four bioclastic limestones differ in their content of bioclasts versus matrix and their content of

coral clasts. The uppermost sample, with an iron-stromatolitic hardground, comes from the top of the «Herrenwis Unit».

STA2-1-776.92 and 773.98 consists of echinoderm skeletal elements (15, resp. 18 vol.-%), bivalves (18, resp. 22 vol.-%), other biogenes, e.g. several foraminifera (6, resp. 9 vol.-%), 5 vol.-% coral clasts in STA2-1-776.92 and 5 vol.-% serpulids in STA2-1-773.98, as well as pellets (7, resp. 0 vol.-%). The components are embedded in microsparitic matrix (40, resp. 44 vol.-%) and in the case of STA2-1-776.92 additional with some calcite cement (5 vol.-%) and iron-dolomite (4 vol.-%). STA2-1-773.98 also contains 2 vol.-% pyrite. The two beds, from which the thin sections were taken, differ in their bioclasts size: STA2-1-773.98 is obvious coarse-grained, with bivalves > 1 cm, and in addition, these are overgrown by serpulids (Fig. B-13).

The two calcareous marl interlayers (STA2-1-773.90 and 768.73) contain echinoderm skeletal elements (20, resp. 24 vol.-%), bivalves (28, resp. 13 vol.-%), other biogenes (5, resp. 4 vol.-%) and little quartz silt (6, resp. 7 vol.-%). STA2-1-768.73 also contains coral clasts (20 vol.-%) and calcite cement (4 vol.-%), whereas STA2-1-773.90 intraclasts (5 vol.-%) and pellets (7 vol.-%). The components are closely packed in a marly matrix (24, resp. 26 vol.-%, Fig. B-14) with few pyrite (3, resp. 2 vol.-%) and mica (2 vol.-%).

The upper two bioclastic limestones (STA2-1-768.87 and 767.60, Fig. B-15), are composed of echinoderms (17, resp. 16 vol.-%), bivalves (22, resp. 8 vol.-%), coral clasts (19, resp. 24 vol.-%), other biogenes (5, resp. 4 vol.-%), pellets (STA2-1-768.87) (5 vol.-%) and microsparite (originally micrite) (24, resp. 28 vol.-%), as well as some calcite cement (5, resp. 12 vol.-%), dolomite rhombohedrons (3, resp. 5 vol.-%) and pyrite (STA2-1-767.60) (3 vol.-%).

The top of the bioclastic limestone succession, also containing clast of corals, is at least partially covered by the thin section (STA2-1-767.02). The lower part documents a limonitic crust or an iron-stromatolite. The upper part, overlaying the iron-stromatolite, contains a layer with numberless biogene components, especially belemnites (Fig. B-16). The thin section STA2-1-767.02 consists of echinoderms (17 vol.-%), bivalves (6 vol.-%), coral clasts (17 vol.-%), other biogenes, especially belemnites (13 vol.-%), iron-stromatolite (7 vol.-%), intraclasts (5 vol.-%), micrite matrix (18 vol.-%), calcite cement (14 vol.-%) and pyrite (3 vol.-%).

«Parkinsoni-Württembergica Schichten» (STA2-1-739.90)

Thin section STA2-1-739.90 documents the composition of one of the many calcareous beds, intercalated in the argillaceous to marly formation of the «Parkinsoni-Württembergica Schichten». It is a silty bioclastic limestone, consisting of echinoderm- (13 vol.-%) and bivalve-components (16 vol.-%) and quartz silt (24 vol.-%), as well as few other biogenes (3 vol.-%) and pyrite (4 vol.-%). Particularly striking is the cementation with "stellate calcite" (40 vol.-%, Fig. B-17), typical for a "hiatus bed".

Wutach Formation (STA2-1-728.68)

The analysed iron-oolitic bed with the thin section STA2-1-728.68 can be characterised as a micritic, bioclastic limestone with thin-shelled bivalves clasts (17 vol.-%), echinoderms (6 vol.-%) and iron-oooids (16 vol.-%). The iron-oooids have sizes of 0.05 – 1.5 mm, are scattered, and some of them have calcite rims. Few other biogenes (2 vol.-%), a bit quartz silt (2 vol.-%) and pyrite (3 vol.-%) are also present. All components have been sedimented together with a micrite matrix (51 vol.-%). Calcite cement (3 vol.-%) is found in calcite veins.

Wildegge Formation (STA2-1-726.46, 687.10, 673.55)

STA2-1-726.46 originates from the basal part of the Wildegge Formation, namely the Birmenstorf Member with the integrated «Glaukonitsandmergel Bed». It is a glauconitic, sandy marl with limonitic intraclasts. Glauconite (16 vol.-%), quartz sand (12 vol.-%), limonitic intraclasts (20 vol.-%), one of them with a limonitic crust, echinoderms (7 vol.-%), other biogenes (5 vol.-%, an ammonite clast with a glauconitic marl infill) and marly matrix (39 vol.-%) with few micas (1 vol.-%).

The two thin sections STA2-1-687.10 and 673.55 come from limestone beds, intercalated in the marly succession of the Wildegge Formation. They consist of micrite matrix (78, resp. 67 vol.-%) with few tiny (0.01 – 0.05 mm) biogene components (total 6, resp. 11 vol.-% echinoderm- and bivalve-clasts), pellets (8, resp. 17 vol.-%), as well as quartz silt (STA2-1-673.55: 5 vol.-%), dolomite rhombohedrons (STA2-1-687.10: 5 vol.-%) and pyrite (STA2-1-687.10: 3 vol.-%).

Siderolithic infilling in «Felsenkalke» and «Massenkalk» (STA2-1-521.15)

The thin section sample STA2-1-521.15 was taken out of a sandy claystone karst filling (Siderolithic Group), about 88 m below the top of the Malm Group. Spheroidal claystone components (up to 1 mm in size) (19 of 34 vol.-%, counted together with the limonitic clasts in the column of intraclasts), limonitic clasts (15 of 34 vol.-%), few iron-pisoids ("Bohnerz", listed in column Fe-ooids in Tab. 3-1) (5 vol.-%) and quartz sand (20 vol.-%), as well as clay matrix (40 vol.-%) form this curious sediment (Fig. B-18).

3.2 Ammonite stratigraphy

Twenty-three macrofossil specimens were recovered from STA2-1, twenty-one of which are ammonite specimens. The sample at depth 773.24 m (Appendix A2) contains two individual ammonites at 773.26 m and 773.23 m, however both could not be extracted because there was no separation between the rock matrix and the fossil, and the rock matrix did not react to potassium hydroxide.

Several ammonites were unfortunately so damaged by drilling or sampling that the genus or species could not be determined. Typically, the ammonites are distributed differently over the individual time periods drilled by the borehole. They are relatively common in the Toarcian and Early Aalenian, where ammonite fragments and cross sections are locally common in the range between 909.95 m and 905.35 m. In the Late Aalenian and in the Early Bajocian no ammonites were found. Also, from the Early Bathonian there is only one ammonite. From the Bathonian and the Callovian there are several ammonites, which often cannot be determined because of the size or the preservation. Somewhat more frequent are the ammonites again in the Middle Oxfordian. Due to the generally small sample size and the poor, often incomplete preservation of the ammonites, a more-or-less large uncertainty in the age determinations must be expected, and this can have an effect on the biostratigraphic classification.

The names of several ammonite taxa are followed by a question mark, for example in *Leioceras?* sp. The question mark after the genus name was used to indicate a question regarding the correct taxonomical assignment of the species to the genus.

We documented a selection of ammonites and additional macrofossils with photographs on seven plates (Plates I – VII) in Appendix C. In addition to ammonites, other conspicuous fossils were identified to the extent possible (Appendix A3), even when they were not subsequently, or only occasionally, recovered.

In general, the more ammonites are present in a specific profile section, the more precisely the biostratigraphic classification of that section can be determined (Tab. 3-2). Furthermore, it must be considered that not all ammonites have the same index value and that the state of preservation of the objects also plays an important role in the biostratigraphic determination. In this respect, a certain error must always be expected. This error is in the range of about one ammonite Subzone (SZ) but can be as high as one ammonite Zone (Z) when the available data is insufficient.

Staffelegg Formation

915.45 m: Crocodile. The truncated fragment of a crocodile is somewhat compressed. The cavities of the bones (e.g. armour-plates) are filled with calcite. Age: Early Toarcian. Lithology: the crocodile is in a calcareous concretion formed in a laminated bituminous mudstone (core photographs on Plate I, Figs. 1 and 2 in Appendix C). After preparation, the crocodile can probably be assigned to the species *Pelagosaurus typus* (Bronn, 1842). This is likely to represent the first record of this species in the Swiss Jura. The stratigraphic position only a few centimetres below the «Unterer Stein» *sensu* Kuhn & Etter (1994) is not surprising, since two specimens of the genus *Pelagosaurus* were discovered in the same position in the quarry of the Holcim GmbH at Dormettingen (Germany) by members of the Fondation paléontologique jurassienne (FPJ, Glovelier). The crocodile is documented on Plate II, Figs. 1 to 5 (Appendix C, for all figures in this section) in different preparation stages.

- 911.39 m: *Dactyloceras* sp. Flattened steinkern with preserved periostracum. Age: probably Falciferum Zone. Lithology: dark bituminous claystone, somewhat micaceous. The ammonite is figured on Plate III, Fig. 1.
- 909.95 m: *Hildoceras* sp.? Truncated steinkern with calcitic inner coils. Age: probably Variabilis Zone. Lithology: dark grey, bioclastic limestone (slightly argillaceous) with burrows. Other fossils are belemnites. The ammonite fragment is illustrated on Plate III, Figs. 2a and 2b.
- 909.50 m: Ammonite indet. Truncated phosphorite steinkern. Age: Toarcian. Lithology: grey, bioclastic (echinoderms, bivalves) limestone (argillaceous) with sporadic pyrite. Other fossils include belemnites and bivalves. The ammonite is not illustrated.
- 906.42 m: *Cotteswoldia* ex gr. *aalensis* (Zieten, 1830). Somewhat flattened steinkern. Age: Aalensis Zone, Aalensis Subzone. Lithology: grey calcareous marl with some bioclasts consisting mainly of echinoderm skeletal elements. Other fossils comprise ammonites and ammonite fragments. The ammonite is illustrated on Plate III, Fig. 3.
- 906.16 m: *Cotteswoldia* sp. Incomplete phosphorite steinkern. Age: Aalensis Zone, probably Aalensis Subzone. Lithology: grey bioclastic limestone (argillaceous). The bioclasts consist mainly of crinoid skeletal elements. Other fossils are ammonites and belemnites. The ammonite is illustrated on Plate III, Fig. 4.
- 905.84 m: *Cotteswoldia* aff. *fluitans* (Dumortier, 1874). Incomplete phosphorite steinkern Age: Aalensis Zone, Aalensis Subzone. Lithology: grey bioclastic marl. The bioclastic remains comprise shell fragments and echinoderm skeletal elements. Other fossils are belemnites. The ammonite is illustrated on Plate III, Fig. 5.
- 905.31 m: *Pleydellia* ex gr. *buckmani* (Maubeuge, 1947). Two flattened steinkern. One specimen is preserved with three-dimensional phosphoritic body chamber. Age: Aalensis Zone, Torulosum Subzone. Lithology: grey bioclastic marl. The bioclasts comprise shell fragments and echinoderm skeletal elements. Other fossils are ammonites. The ammonites are illustrated on Plate IV, Fig. 1.

Opalinus Clay

- 894.34 m: *Leioceras* ex gr. *subglabrum* (Buckman, 1902). Flattened steinkern, body chamber partly preserved in three dimensions. Age: Opalinum Zone, Opalinum Subzone. Lithology: dark grey, somewhat silty claystone. The ammonite is illustrated on Plate IV, Fig. 2.
- 891.13 m: *Leioceras* ex gr. *opalinum* (Reinecke, 1818). Flattened specimen with healed injury in body chamber area. Age: Opalinum Zone, Opalinum Subzone. Lithology: dark grey, claystone (slightly calcareous) with sulfidic burrows. The ammonite is illustrated on Plate IV, Fig. 3.
- 850.57 m: *Leioceras* ex gr. *subglabrum* (Buckman, 1902). Flattened argillaceous steinkern. Age: Opalinum Zone, Opalinum Subzone. Lithology: dark, somewhat silty claystone. The ammonite is illustrated on Plate IV, Fig. 4.

- 805.52 m: *Leioceras?* indet. Flattened specimen with calcitic shell preservation. Too little of the ammonite is preserved for a determination and age classification. Lithology: dark grey bioclastic limestone with very small iron-oolites. The bioclastic remains comprise, among other fragments, skeletal elements from echinoderms. The ammonite is not illustrated.
- 805.58 m: *Leioceras* ex gr. *bifidatum?* (Buckman, 1899). Flattened specimen with calcitic shell preservation. Age: Opalinum Zone, probably Bifidatum Subzone. Lithology: dark grey bioclastic limestone with very small iron-oolites. The bioclastic remains include echinoderm skeletal elements. The ammonite is illustrated on Plate V, Fig. 1.

«Murchisonae-Oolith Fm»

- 795.11 m: *Staufenia* ex gr. *staufensis?* (Oppel, 1856). Truncated steinkern with eroded upper side. Age: probably Bradfordensis Zone, probably Bradfordensis Subzone. Lithology: dark grey to black bioclastic marl with light, green-brown, iron-oolite-bearing, partly bored intraclasts. The iron-oolites are < 1 mm in diameter. Other fossils are bivalves (*Plagiostoma* u.a.) shell fragments. The ammonite is illustrated on Plate V, Figs. 2a and 2b.

«Herrenwis Unit»

- 774.05 m: *Pedina* sp. Age: Bajocian. The echinoderm (sea urchin) is illustrated on Plate V, Fig. 3.
- 773.24 m: The sampled interval (773.28 – 773.21 m) contains two ammonites at 773.26 m and at 773.23 m. The preparation of both was unsuccessful, because there was no separation between the rock matrix and the fossil, and the rock matrix did not react to potassium hydroxide, so no reliable determination can be given for either, they are not illustrated.

Variansmergel Formation

- 734.84 m *Parkinsonia* (*Oraniceras*) sp. Flattened steinkern. Age: Zigzag Zone. Lithology: dark grey bioclastic marl with limonitised components. Other fossils are a belemnite and a rhynchonellid. The ammonite is illustrated on Plate VI, Fig. 1.

Wutach Formation

- 729.58 m: Pseudoperisphinctidae indet. Truncated ammonite, steinkern. Age: Bathonian to Callovian. Lithology: dark, rust-red iron-oolites with large limonitic/goethitic iron-oolites (diameters up to just 2 mm). Other fossils: shell fragments from large ammonites, belemnites, and partly preserved bivalves, gastropods, and brachiopods. The ammonite is not illustrated.
- 728.80 m: *Macrocephalites* sp. Truncated ammonite with partial shell preservation and mineralised phragmocone. Age: Bathonian to Callovian. Lithology: dark, rust-red iron-oolites with large limonitic/goethitic iron-oolites (diameters up to just 2 mm). Other fossils: shell fragments of large ammonites, belemnites and gastropods. The ammonite is illustrated on Plate VI, Figs. 2a and 2b.

727.51 m: Reineckeidae indet. somewhat truncated specimen. Age: Callovian. Lithology: light-grey, limestone (iron-oolitic, argillaceous). The iron-oids are limonitic/goethitic. The ooids exhibit diameters up to 1.5 mm. Other fossils are bivalves and a questionable brachiopod. The ammonite is not illustrated.

Wildegge Formation

727.08 m: *Trimarginites* ex gr. *arolicus*? (Oppel, 1863). Flattened steinkern. Age: Transversarium or Bifurcatus Zone. Lithology: dark-grey, mica-bearing calcareous marl with small, brown, partly phosphoritic intraclasts. Other fossils include a bivalve (*Grammatodon* sp.) and an ammonite. The ammonite is illustrated on Plate VII, Fig. 1.

725.00 m: *Perisphinctes* sp. Macroconch. Flattened, truncated steinkern. Age: Transversarium Zone. Lithology: dark-grey calcareous marl with some glauconite. The ammonite is illustrated on Plate VII, Fig. 2.

718.61 m: *Glochiceras* ex gr. *tectum* (Ziegler, 1958). Age: Transversarium or Bifurcatus Zone. Lithology: grey, somewhat bioclastic-bearing, bioturbated limestone (argillaceous). The ammonite is illustrated on Plate VII, Fig. 3.

Tab. 3-2: Ammonite and other macrofossil determination from STA2-1

Depth [m MD]	Identification	Ammonite Zone (Subzone) or Age
718.61	<i>Glochiceras</i> ex gr. <i>tectum</i> (Ziegler, 1958)	Transversarium or Bifurcatus Zone
725.00	<i>Perisphinctes</i> sp.	Transversarium Zone
727.08	<i>Trimarginites</i> ex gr. <i>arolicus</i> ? (Oppel, 1863)	Transversarium or Bifurcatus Zone
727.51	Reineckeidae indet.	Callovian
728.80	<i>Macrocephalites</i> sp.	Bathonian to Callovian
729.58	Pseudoperisphinctidae indet.	Bathonian to Callovian
734.84	<i>Parkinsonia</i> (<i>Oraniceras</i>) sp.	Zigzag Zone
773.23	Ammonite indet. (not preparable)	
773.26	Ammonite indet. (not preparable)	
774.05	<i>Pedina</i> sp.	Bajocian
795.11	<i>Staufenia</i> ex gr. <i>staufensis</i> ? (Oppel, 1856)	Bradfordensis Zone? (Bradfordensis SZ?)
805.52	<i>Leioceras</i> indet.	indet.
805.58	<i>Leioceras</i> ex gr. <i>bifidatum</i> ? (Buckman, 1899)	Opalinum Zone (Bifidatum Subzone?)
850.57	<i>Leioceras</i> ex gr. <i>subglabrum</i> (Buckman, 1902)	Opalinum Zone (Opalinum Subzone)
891.13	<i>Leioceras</i> ex gr. <i>opalinum</i>	Opalinum Zone (Opalinum Subzone)
894.34	<i>Leioceras</i> ex gr. <i>subglabrum</i> (Buckman, 1902)	Opalinum Zone (Opalinum Subzone)
905.31	<i>Pleydellia</i> ex gr. <i>buckmani</i> (Maubeuge, 1947)	Aalensis Zone (Torulosum Subzone)
905.84	<i>Cotteswoldia</i> aff. <i>fluitans</i> (Dumortier, 1874)	Aalensis Zone (Aalensis Subzone)
906.16	<i>Cotteswoldia</i> sp.	Aalensis Zone (Aalensis Subzone?)
906.42	<i>Cotteswoldia</i> ex gr. <i>aalensis</i> (Zieten, 1830)	Aalensis Zone (Aalensis Subzone)
909.50	Ammonite indet.	Toarcian
909.95	<i>Hildoceras</i> sp.?	Variabilis Zone?
911.39	<i>Dactylioceras</i> sp.	Falciferum Zone?
915.45	Fragment of crocodile: <i>Pelagosaurus typus</i> (Bronn, 1842)	Early Toarcian

System	Stage	Zone	Subzone					
Jurassic	Late	Oxfordian	Bifurcatus [?]	Grossouvrei Stenocycloides				
			Transversarium	Rotoides Schilli Luciaiformis Parandieri				
				Plicatilis	Antecedens Vertebrale			
				Cordatum	Cordatum Costicardia Bukowski			
			Early	Mariae	Praecordatum Scarburgense			
					Middle	Late	Lamberti	Lamberti Henrici
			Athleta	Spinosum Proniae Phaeinum				
			Middle	Coronatum		Grossouvrei Obductum		
				Jason		Jason Medea		
			Early	Calloviense		Enodatum Calloviense		
	Koenigi	Galilaei Curtilobus Gowerianus						
	Herveyi	Kamptus Terebratus Keppleri						
		Middle		Late		Discus	Discus Hollandi	
	Orbis		Hannoveranus Blanazense					
	Hodsoni Morrisi Subcontractus Progracilis							
	Early		Zigzag	Tenuiplicatus Yeovilensis Macrescens Convergens Bomfordi				
				Late	Parkinsoni	Truellei Acris		
	Garantiana		Tetragona Garantiana Dichotoma					
			Niortense		Baculata Polygyralis Banksii			
	Humphriesianum				Blagdeni Humphriesianum Romani Pinguis			
			Early		Sauzei	Macrum Kumaterum		
	Laeviuscula					Laeviuscula Trigonalis		
	Middle	Bajocian	Ovale					
			Discites					
			Early		Late	Concavum	Formosum Concavum	
	Bradfordensis [?]	Gigantea Bradfordensis [?]						
	Middle	Murchisonae		Murchisonae Haugi				
				Opalinum	Bifidatum* [?] Opalinum			
	Jurassic	Late		Toarcian	Aalensis	Torulosum Aalensis		
					Levesquei	Moorei Levesquei		
						Insigne	Dispansum Insigne	
					Thouarsense	Fallaciosum Thouarsense		
						Variabilis [?]		
					Early	Bifrons	Crassum Fibulatum Commune	
			Falciferum [?]				Falcifer Elegans Exaratum Elegantulum	
			Middle		Pliensbachian	Late	Tenuicostatum	Semicelatum Clevelandicum Paltum
							Spinatum	Hawskerense Apyrenum Gibbosus
						Early	Margaritatus	Subnodosus Stokesi
		Davoei		Figulinum Capricornus Maculatum				
		Early		Ibex		Luridum Valdani Masseanum		
						Jamesoni	Jamesoni Brevispina Polymorphus Taylori	
		Late		Sinemurian			Raricostatum	Aplanatum Macdonnelli Raricostatum Densinodulum
						Oxynotum	Oxynotum Simpsoni	
						Obtusum	Denotatus Stellare Obtusum	
							Turneri	Turneri Sauzeanum Scipionanum
			Early		Semicostatum	Charlesi Bucklandi Rotiforme Conybeari		
						Hettangian	Angulata	Complanata Extranodosa
Liasicus			Laquaeus Portlocki					
Planorbis			Johnstoni Planorbis					

STA2-1

Grey highlighted zones and subzones are documented in the drill core with ammonites. Fields with additional interrogation points are not surely proven with ammonites.

Biostratigraphy modified after Cariou & Hanzpergue (1997)
* after Dietze et al. (2021), former «Comptum» Subzone

Fig. 3-1: Zones and subzones which are documented by ammonites in STA2-1

3.3 Palynostratigraphy

The 45 studied samples yielded mostly a good palynological residue with rich and diverse palynofloras. Preservation is good. The palynomorph assemblages are mainly composed of dinoflagellate cysts and pollen and spores. Minor components are prasinophytes, acritarchs, foraminiferal test linings and green algae (e.g. *Botryococcus*). A total of 175 dinoflagellate cyst taxa, 20 other aquatic palynomorphs and 52 pollen and spore taxa are recorded.

Some reworked sporomorphs (*Densosporites* spp., *Ovalipollis* spp., *Ricciisporites tuberculatus*) indicate erosion of Triassic sediments in the source area. Other reworking is indicated by the occurrence of a few single specimens of the dinoflagellate cyst *Luehndea spinosa*, a typical Early Jurassic species with a main distribution in the Late Pliensbachian and earliest Toarcian.

The studied samples from the STA2-1 core are dated to span the interval from the latest Toarcian to the Oxfordian. There are 21 sample intervals differentiated and, where possible, assigned to ammonite biostratigraphy. A list of the analysed samples and the age dating of each sample is given in Tab. 3-3. The indicated ages, zones (Z) and subzones (SZ) for each sample are the result of the palynostratigraphical analysis and interpretation. The results of the quantitative analysis are illustrated in a Range Chart (Appendix D1). A Depth/Age plot is illustrated in Appendix D2.

Sample 905.83 m (1 sample): Late Toarcian, Aalensis Zone to Early Aalenian, Opalinum Zone, Opalinum Subzone

The palynoflora in this sample is characterised by the very high abundance of one dinoflagellate cyst species, *Evansia?* cf. *granochagrinata*. The species dominates the palynoflora, reaching 58% of all palynomorphs counted. Other dinoflagellate cysts present, though in low numbers, are a few representatives of the families Phallocystaceae (*Andreedinium* sp. 2, *Dodekovia* spp., *Weiachia* spp.) and Valvaediniaceae (*Comparodinium punctatum*, *Valvaedinium* spp., *V. brevipellitum*, *V. cavum*, *V. sphaerechinatum*) as well as questionable *Hystriochodinium?* sp. in Feist-Burkhardt & Pross (2020), *Kallosphaeridium praussii*, *Mancodinium semitabulatum*, *Nannoceratopsis* spp., *N. gracilis* s.l., *Scrinocassis limbicavatus*, *S. priscus*, *S. weberi* and *Wittnaudinium minutum*.

The sample interval is defined by the dominant occurrence (superabundance) of *Evansia?* cf. *granochagrinata*.

The composition of the dinoflagellate cyst assemblage is typical for the interval straddling the Toarcian/Aalenian boundary. *Evansia?* cf. *granochagrinata* has its FAD (First Appearance Datum) in the Late Toarcian, probably Levesquei Zone. *Kallosphaeridium praussii* first appears in the Late Toarcian Aalensis Zone. The very high abundance or dominance of *Evansia?* cf. *granochagrinata* is typical for an age of the sample straddling the Toarcian/Aalenian boundary (Aalensis Zone to Opalinum Zone, Opalinum Subzone). This characteristic bioevent at the Early to Middle Jurassic boundary defines the palynostratigraphic unit A of Feist-Burkhardt & Pross (2010).

Sample interval 905.04 – 809.91 m (7 samples): Early Aalenian, Opalinum Zone, Opalinum Subzone

Dinoflagellate cyst assemblages of this sample interval are moderately rich and diverse. They are composed of common to abundant *Evansia?* cf. *granochagrinata*, diverse Phallocystaceae (*Andreedinium* spp., *Andreedinium* sp. 2, *Dodekovia* spp., *D. bullula*, *D. knertensis*, *D. pseudochytroeides*, *D. syzygia*, *Ovalicysta hiata*, *Parvocysta? tricornuta*, *Phallocysta? frommernensis*, *Reutlingia cardobarbata*, *R. cracens*, *R. nasuta*, *Susadinium scrofoides*, *Weiachia* spp.) and

Valvaeodiniaceae (questionable *Comparodinium punctatum*, *Valvaeodinium* spp., *V. brevepeltitum*, *V. cavum*, *V. sphaerechinatum*, *V. spongiosum*), species of *Nannoceratopsis* (*Nannoceratopsis* spp., *N. dictyambonis*, *Nannoceratopsis gracilis* s.s. and s.l., *N. plegas brevicornis*, *N. plegas plegas*, *Nannoceratopsis* sp. B in Feist 1987, *Nannoceratopsis* sp. 1, *N. triangulata*, *N. tricerias*) and *Scriniocassis* (*S. limbicavatus*, *S. priscus*, *S. weberi*) as well as *Hystrichodinium?* sp. in Feist-Burkhardt & Pross (2010), *Kallosphaeridium praussii*, *Manco-dinium semitabulatum*, *Wallogdinium laganum* and *Witnaudinium minutum*. The species *Evansia?* cf. *granochagrinata* is still superabundant in the sample at the base of the interval but its abundance decreases up section. *Phallocysta?* *frommernensis* occurs regularly throughout the interval. Last occurrences at the top of the interval are those of unquestionable *Nannoceratopsis triangulata*, *Phallocysta?* *frommernensis* and unquestionable *Wallogdinium laganum*. In the sample at the top of the interval there are the first occurrences of *Nannoceratopsis plegas brevicornis*, *N. plegas plegas*, *Nannoceratopsis* sp. 1 and *N. tricerias*.

The interval is defined as from the first to the last occurrence of *Phallocysta?* *frommernensis*.

According to Feist-Burkhardt & Pross (2010) there are four marker species for the Early Aalenian Opalinuston Formation (Germany stratigraphy): *Kallosphaeridium praussii*, *Phallocysta?* *frommernensis*, *Nannoceratopsis triangulata* and *Wallogdinium laganum*. All four marker species occur in this interval. An acme of *Phallocysta?* *frommernensis* defines the palynostratigraphical unit B of Feist-Burkhardt & Pross (2010) of the Opalinuston Formation (German stratigraphy).

The sample interval is dated Early Aalenian Opalinum Zone, Opalinum Subzone, and corresponds largely to palynostratigraphic unit B of Feist-Burkhardt & Pross (2010).

The occurrence of *Luehndea spinosa* (840.57 m and 809.91 m) indicates reworking of Early Jurassic Late Pliensbachian to earliest Toarcian sediments in the source area.

Sample interval 806.62 – 799.90 m (3 samples): Early Aalenian, Opalinum Zone, Opalinum to possibly Bifidatum Subzone

Assemblages in this interval are reduced in diversity of the phallocystacean dinoflagellate cysts. The base of the interval is characterised by the first common occurrences of several subspecies of *Nannoceratopsis plegas* (*N. plegas brevicornis*, *N. plegas plegas*). *Nannoceratopsis plegas dictyornata* first occurs in sample 805.01 m. Last occurrences in this interval include *Evansia?* cf. *granochagrinata*, *Nannoceratopsis tricerias*, questionable *N. triangulata*, *Scriniocassis weberi* and questionable *Wallogdinium laganum*.

The interval is defined from the first common and diverse occurrences of subspecies of *Nannoceratopsis plegas* to the first occurrence of *Batiacasphaera* spp. and questionable *Evansia?* *spongogranulata* in the interval above.

The common occurrence of subspecies of *Nannoceratopsis plegas* and the increase in diversity of *Nannoceratopsis* species in general has been observed to be typical from the upper part of the Opalinum Zone onwards. The LADs (Last Appearance Datums) of *Nannoceratopsis triangulata*, *Scriniocassis weberi* and *Wallogdinium laganum* are considered to be at the top of the Opalinum Zone. The FAD of the genus *Batiacasphaera* is in the upper part of the Opalinum Zone and that of *Evansia?* *spongogranulata* is in the Murchisonae Zone.

The interval is interpreted Opalinum Zone, Opalinum to possibly Bifidatum Subzone.

The occurrence of *Luehndea spinosa* (805.01 m) indicates reworking of Early Jurassic Late Pliensbachian to earliest Toarcian sediments in the source area.

Sample 799.55 m (1 sample): Early Aalenian, ?Opalinum Zone to Middle Aalenian, ?Murchisonae Zone

The assemblage in this sample is still quite similar to the interval below, but it shows the first occurrences of *Batiacasphaera* spp. and questionable *Evansia? spongogranulata*. The last occurrence of *Scriniocassis weberi* is recorded in this sample with some questionable specimens.

The interval is defined by the first occurrences of *Batiacasphaera* spp. and questionable *Evansia? spongogranulata* to the last occurrence of questionable *Scriniocassis weberi*.

The genus *Batiacasphaera* has its FAD in the upper part of the Opalinum Zone with *Batiacasphaera* sp. A often being abundant in the Bifidatum Subzone of Opalinum Zone. The FAD of *Evansia? spongogranulata* is in the Murchisonae Zone. The LAD of *Scriniocassis weberi* is considered to be at the top of the Opalinum Zone.

The sample is dated questionably Opalinum Zone to questionably Murchisonae Zone.

Sample interval 799.11 – 795.79 m (2 samples): Middle Aalenian, Murchisonae to Bradfordensis Zone

The dinoflagellate cyst assemblages in this interval are still quite similar to below. In addition, there are the first few questionable specimens of *Dissiliodinium* spp. and *D. lichenoides* as well as *Evansia? spongogranulata*. The genus *Scriniocassis* is represented by *S. limbicavatus* and *S. priscus*.

The interval is defined by the first occurrences of *Evansia? spongogranulata* and questionable *Dissiliodinium* spp. to the first unquestionable occurrences of *Dissiliodinium* spp. in the interval above.

The FAD of *Evansia? spongogranulata* is in the Murchisonae Zone, that of *Dissiliodinium* spp. is within the Bradfordensis Zone. The LADs of *Scriniocassis limbicavatus* and *S. priscus* are at the top of Bradfordensis Zone.

The interval is interpreted Murchisonae to Bradfordensis Zone.

Sample interval 795.07 – 789.01 m (2 samples): Middle Aalenian, Bradfordensis Zone

Assemblages in this interval are still quite similar to below. At the base of the interval there are the first few unequivocal specimens of *Dissiliodinium* spp. and *D. lichenoides*. Last occurrences in this interval are *Scriniocassis priscus* at the top and *S. limbicavatus* in the sample at 795.07 m. *Nannoceratopsis dictyambonis* is superabundant at the top of the interval.

The interval is defined by the first occurrence of unequivocal *Dissiliodinium* spp. to the last occurrence of *Scriniocassis priscus*.

The FAD of *Dissiliodinium* spp. is within the Bradfordensis Zone. The LAD of *Scriniocassis priscus* is at the top of Bradfordensis Zone.

The interval is dated Bradfordensis Zone.

Sample interval 787.95 – 786.01 m (4 samples): Late Aalenian, Concavum Zone to ?Early Bajocian, ?Discites Zone

Assemblages in this interval differ from the interval below. *Dissiliodinium* spp. and *D. lichenoides* are common to abundant. At the base of the interval the first occurrence of *Evansia? eschachensis* is recorded. *Pareodinia* spp. first occurs a little further up in the section. Further regularly occurring taxa are i.a. common *Andreedinium elongatum*, *Hystrichodinium? sp.*, *Moesiodinium raileanui*, *N. dictyambonis* and *Nannoceratopsis* sp. B. *N. dictyambonis* is super-abundant at the top of the interval.

The interval is defined by the first occurrence of *Evansia? eschachensis* to the first occurrences of *Dissiliodinium* aff. *giganteum* and questionable *D. giganteum* in the interval above.

The FADs of *Evansia? eschachensis* and *Pareodinia* spp. are in the Concavum Zone, those of *Dissiliodinium* aff. *giganteum* and *D. giganteum* in the Discites and the Ovale Zone, respectively. The LAD of *Nannoceratopsis* sp. B is in the Discites Zone.

The interval is interpreted Concavum to questionably Discites Zone.

The occurrence of *Luehndea spinosa* (787.04 m) indicates reworking of Early Jurassic Late Pliensbachian to earliest Toarcian sediments in the source area.

Sample 785.55 m (1 sample): Early Bajocian, Discites Zone to ?Ovale Zone

In addition to the species known from below, the sample shows the first occurrence of abundant *Dissiliodinium* aff. *giganteum* and a few single specimens of questionable *Dissiliodinium giganteum*. *Nannoceratopsis* sp. B has its last occurrence in this sample.

The interval is defined by the co-occurrence of *Dissiliodinium* aff. *giganteum* and *Nannoceratopsis* sp. B on the one hand, and questionable *Dissiliodinium giganteum* on the other.

The FAD of *Dissiliodinium* aff. *giganteum* is in the Discites Zone, the LAD of *Nannoceratopsis* sp. B is also in the Discites Zone. The FAD of *Dissiliodinium giganteum* is in the Ovale Zone.

The interval is interpreted Discites to questionably Ovale Zone.

Sample 784.24 m (1 sample): Early Bajocian, Ovale Zone

The assemblage in this sample is similar to the interval below with i.a. abundant specimens of the genus *Dissiliodinium*. First occurrences in the sample show *Durotrigia* spp., *Moesiodinium* sp. 2 and *Reutlingia gochtii*, last occurring are *Andreedinium elongatum*, *Evansia? eschachensis* and *Nannoceratopsis dictyambonis*. The spore *Lycopodiumsporites gristhorpensis* has also its first occurrence.

The interval is defined by the co-occurrence of questionable *Dissiliodinium giganteum* and *Lycopodiumsporites gristhorpensis* on the one hand and *Andreedinium elongatum* and *Evansia? eschachensis* on the other.

The FADs of *Dissiliodinium giganteum* and *Lycopodiumsporites gristhorpensis* are in the Ovale Zone. The LADs of *Andreedinium elongatum* and *Evansia? eschachensis* are also in the Ovale Zone.

The sample is dated Ovale Zone.

Sample interval 782.98 – 777.71 m (5 samples): Early Bajocian, Laeviuscula Zone

Assemblages in this interval show the first occurrences of *Batiacasphaera laevigata*, *Cavatodissiliodinium hansgochtii*, *Durotrigia daveyi* and *Gongylodinium erymnoteichon*. *Dissiliodinium giganteum* shows an acme in the samples from 782.98 to 779.43 m. Last occurrences in this interval have *Evansia? spongogranulata*, *Hystrichodinium? sp.* and *Moesiodinium raileanui*.

The interval is defined by the first occurrence of *Batiacasphaera laevigata* at the base of the interval to the first occurrence of *Kallosphaeridium hypornatum* in the interval above.

The FADs of *Batiacasphaera laevigata* and *Cavatodissiliodinium hansgochtii* are in the Laeviuscula Zone. The LAD of *Hystrichodinium? sp.* is also in the Laeviuscula Zone. The FAD of *Kallosphaeridium hypornatum* is in the Sauzei Zone.

The interval is dated Laeviuscula Zone.

Sample interval 777.39 – 771.37 m (4 samples): Early Bajocian, Sauzei Zone

Assemblages in this interval show the first occurrence of *Kallosphaeridium hypornatum*. Last occurrences in this interval have *Cavatodissiliodinium hansgochtii* and *Dissiliodinium giganteum*.

The interval is defined from the first occurrence of *Kallosphaeridium hypornatum* to the first occurrences of questionable *Phallocysta thomasii* and *Valensiella/Ellipsoidictyum spp.* in the interval above.

The FAD of *Kallosphaeridium hypornatum* is in the Sauzei Zone. The FADs of *Phallocysta thomasii* and *Valensiella/Ellipsoidictyum spp.* are in the Humphriesianum Zone.

The interval is dated Sauzei Zone.

Sample 768.76 m (1 sample): Early Bajocian, Sauzei to Humphriesianum Zone

The assemblage in this sample shows the first occurrences of questionable *Cavatodissiliodinium spp.*, questionable *Phallocysta thomasii* and *Valensiella/Ellipsoidictyum spp.* The species *Evansia? spongogranulata* and *Phallocysta thomasii* occur for the last time in this sample with questionable specimens.

The interval is defined by the co-occurrence of questionable *Evansia? spongogranulata* and questionable *Phallocysta thomasii*.

The LAD of *Evansia? spongogranulata* is in the Sauzei Zone. The range of *Phallocysta thomasii* is considered to be restricted to the Romani and Humphriesianum Subzones of the Humphriesianum Zone.

Based on the co-occurrence of the taxa mentioned the interval is interpreted Sauzei to Humphriesianum Zone.

Sample 767.40 m (1 sample): Late Bajocian, Niortense Zone

The assemblage in this sample is characterised by numerous first occurrences including *Acanthaulax crista*, *Ctenidodinium continuum*, *Endoscrinium asymmetricum*, *Gonyaulacysta pectinigera*, *Meiourogonyaulax superornata*, *M. valensii* and *Rhynchodiniopsis? regalis*. *Nannoceratopsis gracilis* s.l. has its last occurrence in this sample.

The interval is defined by the first occurrences of *Ctenidodinium continuum*, *Endoscrinium asymmetricum* and *Gonyaulacysta pectinigera* to the last occurrence of *Nannoceratopsis gracilis* s.l.

Ctenidodinium continuum, *Endoscrinium asymmetricum* and *Gonyaulacysta pectinigera* all have their FAD in the Niortense Zone. The LAD of *Nannoceratopsis gracilis* s.l. is also in the Niortense Zone.

The sample is dated Niortense Zone.

Sample 766.95 m (1 sample): Late Bajocian, Garantiana to Parkinsoni Zone

The sample shows further numerous first occurrences including *Atopodinium polygonale*, *Bradleyella adela*, *Ctenidodinium sellwoodii* group, *Gongylocladus hocneratum*, questionable *Gonyaulacysta eisenackii*, *Korystocysta gochtii*, *Nannoceratopsis spiculata* and *Valvaeodinium spinosum*.

The interval is defined by the first occurrence of *Ctenidodinium sellwoodii* and questionable *Gonyaulacysta eisenackii* to the first occurrence of *Sirmiodiniopsis* sp. in Feist-Burkhardt & Wille (1992) in the interval above.

The FAD of *Ctenidodinium sellwoodii* is in the Garantiana Zone, the FADs of *Gonyaulacysta eisenackii* and *Sirmiodiniopsis* sp. are in the Parkinsoni Zone.

The sample is interpreted Garantiana to Parkinsoni Zone.

Sample interval 765.64 – 744.27 m (4 samples): Late Bajocian, Parkinsoni Zone

The dinoflagellate cyst assemblages are quite similar to those from below with *Acanthaulax crispera* consistently occurring up to the top of the interval. Representatives of the genus *Ctenidodinium* are abundant. A single questionable specimen of *Ctenidodinium combazii* is considered to be not *in situ*. First occurrences in this interval include *Sirmiodiniopsis* sp. in Feist-Burkhardt & Wille (1992) at the base of the interval and occurring regularly throughout, and *Ambonosphaera* sp. 1 occurring in the top two samples. Questionable *Orobodinium automobile* is recorded at the top of the interval.

The interval is defined by the first occurrence of *Sirmiodiniopsis* sp. at the base of the interval to the last occurrence of *Acanthaulax crispera* at the base of the interval above.

The FAD of *Sirmiodiniopsis* sp. is in the Parkinsoni Zone. The LAD of *Acanthaulax crispera* is also in the Parkinsoni Zone.

The interval is dated Parkinsoni Zone.

Sample 735.37 m (1 sample): Late Bajocian, Parkinsoni Zone to Early Bathonian, Zigzag Zone

The assemblage in this sample is still similar to below with *Acanthaulax crispera*, *Endoscrinium asymmetricum* and *Meiourogonyaulax valensii* occurring for the last time. First occurrences include questionable *Ctenidodinium combazii*, unequivocal *Orobodinium automobile*, *Lithodinia* spp. and *Tubotuberella dangeardii*.

The interval is defined by the last occurrence of *Acanthaulax crispa* to the first occurrence of *Tubotuberella dangeardii*.

The LAD of *Acanthaulax crispa* is in the Parkinsoni Zone. The LADs of *Endoscrinium asymmetricum* and *Meiourogonyaualax valensii* are in the Zigzag Zone. The FADs of *Ctenidodinium combazii* and *Orobodinium automobile* are within the upper part of the Parkinsoni Zone, that of *Tubotuberella dangeardii* is in the Zigzag Zone.

The sample is dated Parkinsoni to Zigzag Zone.

Sample interval 734.66 – 732.31 m (2 samples): Early Bathonian, Zigzag Zone, Tenuiplicatus Subzone to Middle Bathonian, Morrissi Zone

Assemblages in this interval are characterised by abundant and diverse representatives of the genus *Ctenidodinium*, including common to abundant *Ct. combazii*. First occurrences include *Cleistosphaeridium* spp. at the base of the interval and *Lithodinia jurassica* and *Atopodinium prostaticum* higher up. *Dissiliodinium minimum* is very abundant at the base. Last occurrences at the top of the interval show *Carpathodinium predae* and *Gongylocladus hocneratum*.

The interval is defined by the first occurrence of *Cleistosphaeridium* spp. to the last occurrence of *Carpathodinium predae*.

The FAD of the first chorate dinoflagellate cyst, *Cleistosphaeridium ehrenbergii*, is in the Tenuiplicatus Subzone of Zigzag Zone. The LAD of *Carpathodinium predae* is in the Morrissi Zone.

The interval is interpreted Tenuiplicatus Subzone of the Zigzag Zone to Morrissi Zone.

Sample 731.76 m (1 sample): Late Bathonian, Hodsoni Zone

The assemblage in this sample is similar to below with abundant and diverse representatives of the genus *Ctenidodinium*. In addition, there are the first occurrences of the first complex skolochorate dinocysts indet. and *Nannoceratopsis pellucida*. *Ctenidodinium combazii* is super-abundant and occurs for the last time in this sample. Last occurring is also *Rhynchodiniopsis? regalis*.

The interval is defined by the last occurrence of *Carpathodinium predae* in the interval below to the last occurrence of *Rhynchodiniopsis? regalis*.

The LAD of *Carpathodinium predae* is in the Morrissi Zone. The LAD of *Rhynchodiniopsis? regalis* is in the Hodsoni Zone.

The sample is dated Hodsoni Zone.

Sample 728.87 m (1 sample): Early Callovian, Herveyi Zone

Composition of the dinoflagellate cyst assemblage in this sample is very different to below. Abundance of representatives of the genus *Ctenidodinium* has strongly decreased. *Ctenidodinium combazii* is not recorded anymore. Chorate dinoflagellate cysts are common. There are several first occurrences, i.a. *Hapsidaulax margarethae*, *Korystocysta pachyderma*, questionable *Limbodinium absidatum*, *Lithodinia caytonensis*, *Rhynchodiniopsis cladophora*, *Sentusidinium? varispinosum*, *Sirmiodiniopsis orbis*, *Sirmiodinium grossii* and *Stephanelytron scarburghense*.

Last occurring in this sample are i.a. *Atopodinium polygonale*, *Gonyaulacysta pectinigera*, *Rigaudella filamentosa* and *Valvaeodinium vermicylindratum*.

The interval is defined by the first occurrences of *Lithodinia caytonensis*, *Rhynchodiniopsis cladophora*, *Sentusidinium? varispinosum*, *Sirmiodinium grossii* and *Stephanelytron scarburghense* to the last occurrences of *Atopodinium polygonale* and *Gonyaulacysta pectinigera*.

The FADs of *Lithodinia caytonensis*, *Rhynchodiniopsis cladophora*, *Sentusidinium? varispinosum*, *Sirmiodinium grossii* and *Stephanelytron scarburghense* are in the Herveyi Zone. The LADs of *Atopodinium polygonale* and *Gonyaulacysta pectinigera* are also in the Herveyi Zone.

The sample is dated Herveyi Zone.

Sample 728.46 m (1 sample): Early Callovian, Koenigi to Calloviense Zone

The assemblage differs to the one below in showing i.a. the first occurrences of abundant *Mendicodinium groenlandicum*, *Stephanelytron caytonense* and *St. redcliffense*. Last occurrences include *Aldorfia aldorfensis*, *Hapsidaulax margarethae*, *Lithodinia caytonensis*, *Nannoceratopsis spiculata*, *Orobodinium automobile*, *Sentusidinium? varispinosum* and *Wanaea indotata*.

The interval is defined by the first occurrence of *Mendicodinium groenlandicum* to the last occurrences of *Aldorfia aldorfensis* and *Sentusidinium? varispinosum*.

The FAD of *Mendicodinium groenlandicum* is in the Koenigi Zone. The LADs of *Aldorfia aldorfensis* and *Sentusidinium? varispinosum* are in the Calloviense Zone.

The sample is dated Koenigi to Calloviense Zone.

Sample 726.25 m (1 sample): Middle Oxfordian, Transversarium Zone

Composition of the dinoflagellate cyst assemblage in this sample is very different to below. Complex skolochorate dinocysts are abundant, specimens of *Ctenidodinium* are rare. There are numerous first occurrences. These include *Acanthaulax granulata/venusta* spp., *Compositosphaeridium polonicum*, *Endoscrinium galeritum*, *Glossodinium dimorphum*, *Gonyaulacysta dualis*, *Leptodinium arcuatum*, *L. mirabile*, *L. subtile* and *Neuffenia willei*. Other important taxa present in the sample are *Rigaudella aemula* and *Scriniodinium crystallinum*.

The interval is defined by the first occurrence of *Leptodinium subtile* to the last occurrence of *Compositosphaeridium polonicum*.

The FAD of *Leptodinium subtile* is in the Transversarium Zone. The LAD of *Compositosphaeridium polonicum* is also in the Transversarium Zone.

The sample is dated Transversarium Zone.

Tab. 3-3: List of analysed palynology samples from STA2-1

The indicated ages, zones and subzones for each sample are the result of the palynostratigraphical analysis and interpretation.

Depth [m MD]	Age	Zone & Subzone
726.25	Middle Oxfordian	Transversarium Zone
728.46	Early Callovian	Calloviense – Koenigi Zone
728.87	Early Callovian	Herveyi Zone
731.76	Late Bathonian	Hodsoni Zone
732.31	Middle – Early Bathonian	Morrisi Zone – Zigzag Zone (Tenuiplicatus SZ)
734.66	Middle – Early Bathonian	Morrisi Zone – Zigzag Zone (Tenuiplicatus SZ)
735.37	E. Bathonian – L. Bajocian	Zigzag – Parkinsoni Zone
744.27	Late Bajocian	Parkinsoni Zone
751.13	Late Bajocian	Parkinsoni Zone
759.36	Late Bajocian	Parkinsoni Zone
765.64	Late Bajocian	Parkinsoni Zone
766.95	Late Bajocian	Parkinsoni – Garantiana Zone
767.40	Late Bajocian	Niortense Zone
768.76	Early Bajocian	Humphriesianum – Sauzei Zone
771.37	Early Bajocian	Sauzei Zone
773.79	Early Bajocian	Sauzei Zone
775.75	Early Bajocian	Sauzei Zone
777.39	Early Bajocian	Sauzei Zone
777.71	Early Bajocian	Laeviuscula Zone
779.13	Early Bajocian	Laeviuscula Zone
779.43	Early Bajocian	Laeviuscula Zone
781.07	Early Bajocian	Laeviuscula Zone
782.98	Early Bajocian	Laeviuscula Zone
784.24	Early Bajocian	Ovale Zone
785.55	Early Bajocian	?Ovale – Discites Zone
786.01	E. Bajocian – L. Aalenian	?Discites – Concavum Zone
786.53	E. Bajocian – L. Aalenian	?Discites – Concavum Zone
787.04	E. Bajocian – L. Aalenian	?Discites – Concavum Zone
787.95	E. Bajocian – L. Aalenian	?Discites – Concavum Zone
789.01	Middle Aalenian	Bradfordensis Zone
795.07	Middle Aalenian	Bradfordensis Zone
795.79	Middle Aalenian	Bradfordensis – Murchisonae Zone
799.11	Middle Aalenian	Bradfordensis – Murchisonae Zone
799.55	Middle – Early Aalenian	?Murchisonae – ?Opalinum Zone
799.90	Early Aalenian	Opalinum Zone (possibly Bifidatum – Opalinum SZ)
805.01	Early Aalenian	Opalinum Zone (possibly Bifidatum – Opalinum SZ)
806.62	Early Aalenian	Opalinum Zone (possibly Bifidatum – Opalinum SZ)
809.91	Early Aalenian	Opalinum Zone (Opalinum SZ)
820.30	Early Aalenian	Opalinum Zone (Opalinum SZ)
840.57	Early Aalenian	Opalinum Zone (Opalinum SZ)
860.70	Early Aalenian	Opalinum Zone (Opalinum SZ)
880.24	Early Aalenian	Opalinum Zone (Opalinum SZ)
899.83	Early Aalenian	Opalinum Zone (Opalinum SZ)
905.04	Early Aalenian	Opalinum Zone (Opalinum SZ)
905.83	E. Aalenian – L. Toarcian	Opalinum (Opalinum SZ) – Aalensis Zone

3.4 Chemostratigraphy

The sampling of the STA2-1 cores focused primarily on the upper part of the Lias Group (Figs. 3-2 and 3-3) and Dogger Group (Figs. 3-4 to 3-7) and, therefore inter alia on clay mineral-rich layers of the Opalinus Clay. The summary Figs. 3-8 and 3-9 illustrate the fully analysed interval from the upper part of the Staffelegg Formation up to the lowermost part of the Wildeggen Formation (916.50 – 725.00 m). The data presented here (applies for all subsequent figures in this section) is shown in comparison to other data collected during the drilling campaign: Stratigraphic profile after Dossier III, Dry Clay (values in wt.-%, vertical axis in m MD log depth, logging has a significant offset to the core depth; *cf.* Dossier X), XRD measurements (horizontal bars; calcite: blue, dolomite and ankerite: green, siderite: red; *cf.* Dossier VIII) and C(org) measurements also with blue horizontal bars (*cf.* Dossier VIII). In addition, formation boundaries were highlighted with black lines and other formal or informal subintervals with grey lines. The following stratigraphic abbreviations were used in Figs. 3-2 to 3-9: F. = Frick Member; G.B.R = Grünschlholz Member, Breitenmatt Member and Rickenbach Member; Rieth. = Rietheim Member; G. W. = Gross Wolf Member; «M.-O. Fm.» = «Murchisonae-Oolith Formation»; Wedelsst. = Wedelsandstein Formation; «H.o.» = «Humphriesioolith Formation»; «H.U.» = «Herrenwis Unit»; Var. = Variansmergel Formation.

In addition to the continuous samples (roughly in metre resolution), some specific samples were taken (Appendix E1) to complete the information about the calcareous beds and macrofossils. Some of the firm- to hardground samples were drilled directly from the remaining thin section blocks to correlate the bulk geochemical data with the microfacies analysis. All these data points are distinguished in different colours on Figs. 3-2, 3-4 and 3-6 (in light blue: calcareous samples (firm- and hardgrounds, "hiatus beds", calcareous and sideritic concretions); in violet: septarian nodules; in green the macrofossil) but may not be shown on the individual plots because of the data ranges (see Appendix E1 for data).

The data will be discussed in three intervals: Lias Group, the lower part of the Dogger Group – mainly Opalinus Clay and the upper part of the Dogger Group. Not all data are discussed to the same extent as for example the $\delta^{18}\text{O}_{\text{carb}}$ and $\delta^{15}\text{N}_{\text{org}}$ data. The oxygen isotopes are strongly influenced by diagenesis. This can be exemplarily shown with the measured belemnites in the Lias Group in MAR1-1 (green points in Figure 3-2 in Wohlwend et al. 2021c). These are 3 to 4 ‰ more positive than the marlier bulk rock and therefore much less diagenetically overprinted. The nitrogen isotopes may not be as meaningful in some cases, because the combined $\delta^{13}\text{C}_{\text{org}}$ and $\delta^{15}\text{N}_{\text{org}}$ measurements showed a too low concentration of N in most of the measurements.

Although, the calculated carbonate content (TCarb) is only a semi-quantitative method, the values presented here correspond quite good to the XRD values measured at the University of Bern (*cf.* Dossier VIII). The XRD data are illustrated in the following Figs. 3-2, 3-4 and 3-6 to provide a visual comparison between the data presented here and those from Dossier VIII. As discussed in Wohlwend et al. (2019) based on measurements from the BDB-1 borehole at the Mont Terri Rock Laboratory, the values calculated here follow nicely the calcite and dolomite wt.-% with an additional mixed signal from the other carbonates (mainly siderite). Because during the reaction time of 60 min at 72 °C, a complete reaction for example for siderite does not take place. The TCarb values are slightly too low in siderite-rich successions (red bars in the XRD data), which is often the case in the «Mixed clay-silt-carbonate sub-unit» (886.97 – 839.72 m; Fig. 3-4).

In contrast to the carbonate measurements (bulk samples), the organic measurements were not always measured in metre resolution, depending on the variability of the expected isotope data and the TCarb content. If no major isotope changes were expected, as for example during the middle part of the Opalinus Clay, only every second sample (mainly 2 m interval) was analysed. Of the entire «Herrenwis Unit» only the more argillaceous interlayers were analysed.

Lias Group

Starting from the bottom up (Fig. 3-2), the oldest sediments measured belong to the Early Jurassic (probably Late Pliensbachian). The lowermost two measurements (916.50 m and 916.25 m) belong to the uppermost combined Grünscholzhof Member, Breitenmatt Member and Rickenbach Member. The following ones, between 916.06 m and 905.25 m, represent the upper two members of the Staffelegg Formation. They show larger variations in their individual data, which can be explained by the overall higher sampling resolution in the Lias Group (some intervals in the Rietheim Member with around 25 cm spacing) as well as by the nodular calcareous lithology of the Gross Wolf Member.

The semi-quantitative carbonate content (TCarb, Fig. 3-2) represents the lithological variations in the Rietheim Member and the hanging Gross Wolf Member up to the Opalinus Clay. In the Rietheim Member the TCARB values show an overall increasing trend from normal sediment of about 16 wt.-% to maximum values slightly above 60 wt.-%. The interval from the base of the Rietheim Member and up to the «Unterer Stein» (916.06 – 915.00 m), clearly contains less carbonate than the hanging interval to the top of the Rietheim Member. The whole succession is interrupted by higher values measured from the three calcareous interbeds in the middle part («Unterer Stein»: 915.39 – 915.17 m, «Homogene Kalkbänke»: 914.79 – 914.69 m and «Oberer Stein»: 914.09 – 913.76 m). The uppermost more calcareous interval was not sampled (questionable «Monotishank» between 910.89 – 910.77 m). The nomenclature of these beds is *sensu* Kuhn & Etter (1994). The TCARB data from these three beds is documented in Appendix E1 and marked by blue dots in Fig. 3-2. The overlying Gross Wolf Member shows similar values as in the succession below, but only those measured from the argillaceous to calcareous marl sediment. Although, the calcareous nodules to nodular layers, which are typical for the Gross Wolf Member clearly show higher values, as shown by the uppermost two samples at 905.75 m (77.0 wt.-%) and 905.25 m (70.5 wt.-%). They clearly document the lithological boundary at 905.20 m to the above laying formation of the argillaceous Opalinus Clay with TCARB values around 8 – 9 wt.-%.

The $\delta^{13}\text{C}_{\text{carb}}$ values document at the base of the Rietheim Member a negative trend with the most negative value (-2.2 ‰ at 915.50 m) just below the «Unterer Stein». The negative trend is subsequently followed by a rapid increase. The most positive $\delta^{13}\text{C}_{\text{carb}}$ value thereafter was documented slightly above the «Oberer Stein» with +1.9 ‰ at 913.04 m. Further up to the top of the Gross Wolf Member the values show a continuous decreasing trend to values around +0.4 ‰ at 906.25 m, followed by two more negative values from the two mentioned more calcareous samples at the top of the Gross Wolf Member. The negative trend then continues into the lowermost Opalinus Clay. The discussed negative carbon isotope excursion (CIE) up to the «Unterer Stein» represents one of the major Mesozoic perturbations of the carbon cycle. The one in the Rietheim Member can be correlated with the global Toarcian-CIE (T-CIE). In many places the T-CIE is also linked with an organic-rich succession (also in STA2-1, discussion follows below), and therefore was deposited during the Toarcian-Oceanic Anoxic Event (T-OAE).

The negative T-CIE can also be seen by the $\delta^{13}\text{C}_{\text{org}}$ values (Fig. 3-3). The most negative one, with a value of -32.8 ‰ at 915.50 m, was measured from the same sample as the most negative one from the $\delta^{13}\text{C}_{\text{carb}}$. The following rapid positive shift is also clearly documented in the organic matter, where the most positive value (-26.4 ‰) was measured from the sample drilled from the «Oberer Stein» at 914.00 m. The $\delta^{13}\text{C}_{\text{org}}$ values document at the very base of the Rietheim Member a fast shift to negative values, like in BUL1-1 (Wohlwend et al. 2021a) and STA3-1 (Wohlwend et al. 2023). The roughly 25 cm spacing through the T-CIE from STA2-1 is clearly not high enough in comparison with BUL1-1, where it was documented in much more detail with several negative shifts similar to the compilation made by Ruebsam & Al-Husseini (2020).

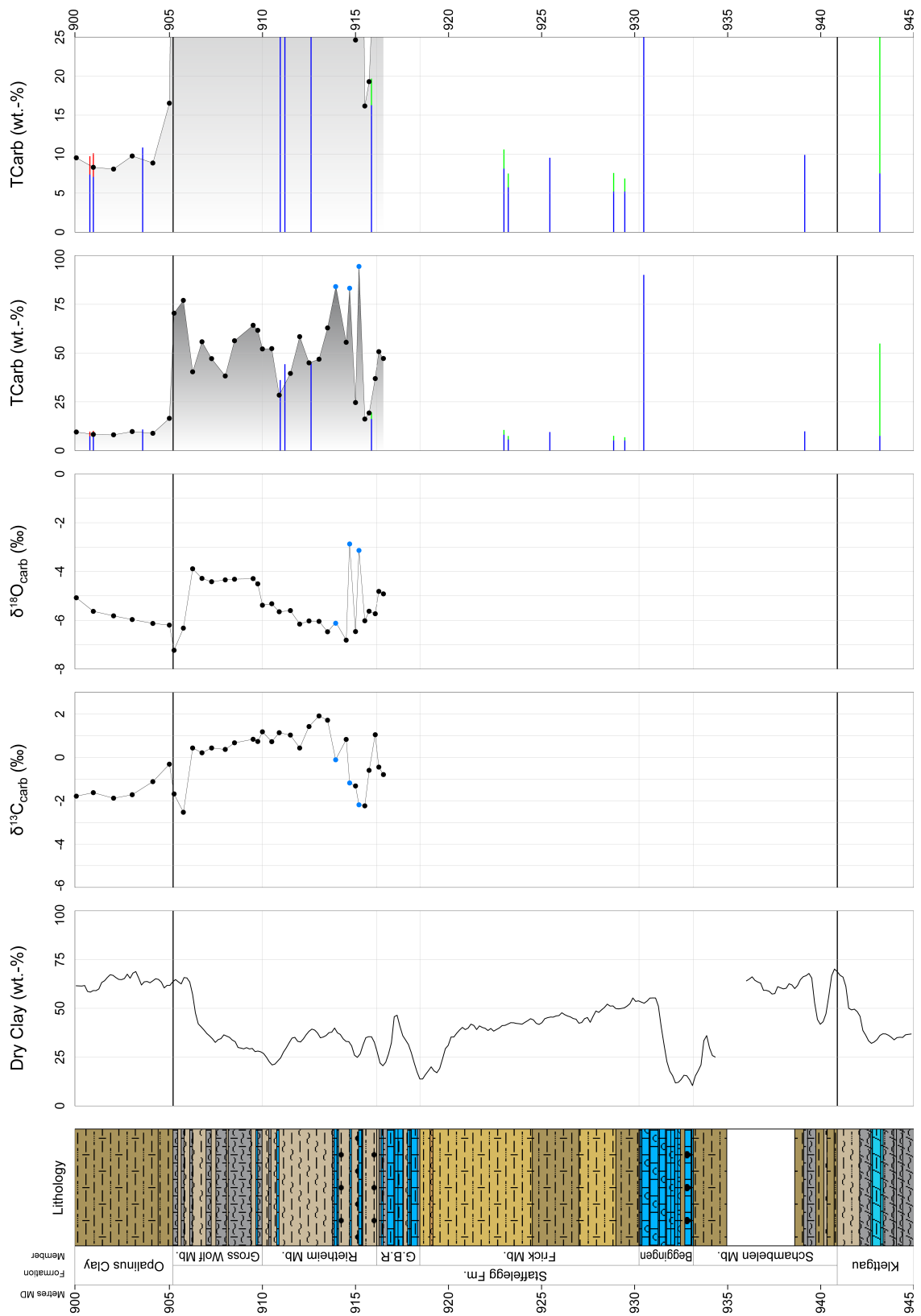


Fig. 3-2: Bulk rock (carbonate) isotopic data from the Lias Group

Geochemical data from 916.50 – 900.00 m, additional explanations and references see text at the beginning of Section 3.4.

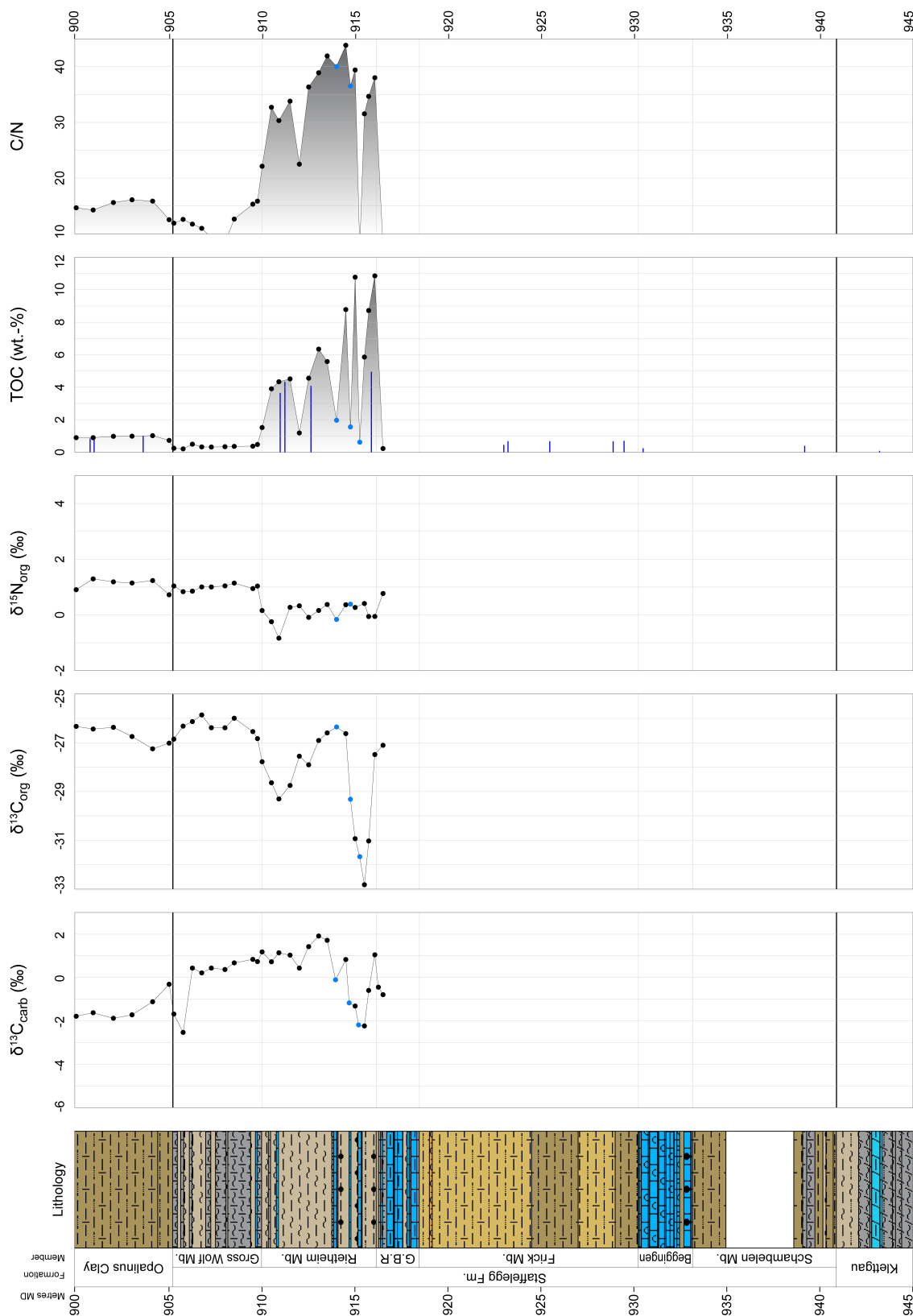


Fig. 3-3: Organic isotopic data from the Lias Group
 Geochemical data from 916.50 – 900.00 m, additional explanations and references see text at the beginning of Section 3.4.

The Rietheim Member is very bituminous and is itself defined by the occurrence of bituminous shale. The TOC as well as the C/N ratio (both Fig. 3-3) limit the range of the member. Both proxies show very increased values in the Rietheim Member. The highest TOC value with 10.9 wt.-% was measured in the more argillaceous interval below the «Unterer Stein» at 916.06 m and a similar one just above the calcareous bed with 10.8 wt.-% at 915.00 m. The average range of the semi-quantitative TOC content lies between 1.2 and 8.7 wt.-%, whereby the three calcareous beds document lower TOC values around 1 wt.-%. The Rietheim Member, as mentioned above, clearly can be assigned as a black shale deposit and the succession below the «Unterer Stein» with the higher TOC was deposited during the T-OAE. The hanging Gross Wolf Member has an obvious different lithological composition which is nicely documented by the very stable but much lower TOC content, which is below 0.5 wt.-%.

The C/N ratios show the same trend as the TOC with the highest ratios mainly measured contemporaneously with the bituminous lower and middle part of the Rietheim Member (ratios up to 44), compared to the overlying Gross Wolf Member with a much lower C/N ratio (9 – 16). Such high C/N ratios, measured in the Rietheim Member, are normally rather unusual for marine organic matter, which usually has values between 5 and 8 (e.g. Emerson & Hedges 1988, Meyers 1997) and would therefore pretend that the organic material would be of terrigenous source. However, such high C/N ratios were also reported from mid-Pleistocene sapropels from the Tyrrhenian Basin (Meyers & Bernasconi 2005) which are also clearly produced by marine organic matter. Van Mooy et al. (2002) proposed a model for these very unusual C/N ratios in which they determined from sediment trap studies that suboxic microbial degradation via denitrification preferentially utilises nitrogen-rich amino acids and hence leaves a larger proportion of the nitrogen-poor organic matter components intact than under oxic conditions. C/N values of the surviving organic matter necessarily rise.

Lower part of the Dogger Group – mainly Opalinus Clay

The interval described in the following section, the lower part of the Dogger Group (Opalinus Clay, «Murchisonae-Oolith Formation» and the transition into the lower part of the Wedelsandstein Formation), is also the interval at the main focus of these investigations (Figs. 3-4 and 3-5).

The semi-quantitative carbonate content (TCarb) values from the more homogeneous clay mineral-dominated lithologies (mainly Opalinus Clay) are rather low and very stable compared to those from the underlying Staffelegg Formation (Fig. 3-4). In the lowermost succession of the Opalinus Clay («Clay-rich sub-unit»: 905.20 – 886.97 m), the average TCarb values decrease from around 17 wt.-% (905.00 m) to values around 9 wt.-% at 904.11 m. The carbonate content decreases further through the lowermost sub-unit and reaches the lowest value (5.5 wt.-% at 883.00 m) in the lower part of the «Mixed clay-silt-carbonate sub-unit» (886.97 – 839.72 m). Upsection, the TCarb seems to be somewhat higher than in the lower succession, but rarely exceeds 13 wt.-%. What is striking, however, is that the values fluctuate more from sample to sample. Some of the higher values can be explained by the sampling: sample at 882.00 m taken from a 1 cm thin bositra-rich interval (21.4 wt.-%), sample taken at 876.00 m was slightly more sideritic (23.0 wt.-%). The informal «Upper silty sub-unit» (839.72 – 823.50 m) shows slightly higher values reaching 14 wt.-% at 837.00 m, followed by a clearly less calcareous interval, analysed between 835.00 m to 833.11 m with values around 5 wt.-%. Another "outlier", reaching a TCarb value of 25.6 wt.-%, was sampled at 830.00 m from a sand- to silt-rich facies. In the above following informal «Sub-unit with silty calcareous beds» (823.50 – 799.67 m) a clear change in the carbonate content can be seen. The TCarb values are lower and similar to the lowermost succession of the Opalinus Clay and show several trends to more calcareous values, which are always bounded by calcareous bed (see also Appendix E1). The most prominent trend ends with the calcareous bed from 805.96 m to 805.47 m (see also Appendix E1). The succession above that calcareous bed and up to the top of the Opalinus Clay is again significantly less calcareous. In the above following «Murchisonae-Oolith Formation», three individual successions can be observed when looking at the TCarb contents: a very calcareous lower one with values between 82 and 94 wt.-%, a middle one with very low TCarb values between 3 and 5 wt.-% and an upper one, which is represented by two samples at 788.06 m (47 wt.-%) and 787.00 m (9 wt.-%). The middle one documents nicely the very monotonous and argillaceous succession from 794.04 m to 788.67 m.

The above-mentioned uppermost informal «Sub-unit with silty calcareous beds» comprises, as the name implies, several calcareous beds, mainly firm- to hardgrounds. Some of the samples analysed from these are classified as measurements from "hiatus beds" and calcareous concretions (see Appendix E1 for data and Section 3.1 for microfacies description). Additional calcareous beds can also be found in the lower part of the Opalinus Clay. They are all illustrated in Fig. 3-4 by thicker light blue lines ending with blue dots marking the TCarb values. In addition, also two septarian nodules (illustrated in violet: 892.01 m and 816.87 m) and one macrofossil (shell of a *Gryphaea* at 785.80 m; illustrated in green) were analysed. The calcareous beds (marked in blue) comprise TCarb values that are typical for calcareous marl (50 – 75 wt.-%) and limestone (75 – 100 wt.-%). The lower septarian nodule (892.01 m) and the calcareous concretion at 891.32 m belong to a level with typical calcareous concretions and septarian nodules in the «Clay-rich sub-unit», which can be correlated over several boreholes and siting regions (e.g. BUL1-1: Wohlwend et al. 2021a; TRU1-1: Wohlwend et al. 2021b; BOZ1-1: Wohlwend et al. 2022).

The $\delta^{13}\text{C}_{\text{carb}}$ data reveal two negative CIE or just negative intervals in the Opalinus Clay (Fig. 3-4): a lower negative CIE in the «Clay-rich sub-unit» and an upper CIE in the «Sub-unit with silty calcareous beds». The lower negative CIE starts with a clear decreasing trend in the lowermost 2 m at the base of Opalinus Clay, reaching than the most negative value (-4.7 ‰ at 892.00 m) within the horizon with the calcareous concretions and septarian nodules (892.32 – 891.26 m).

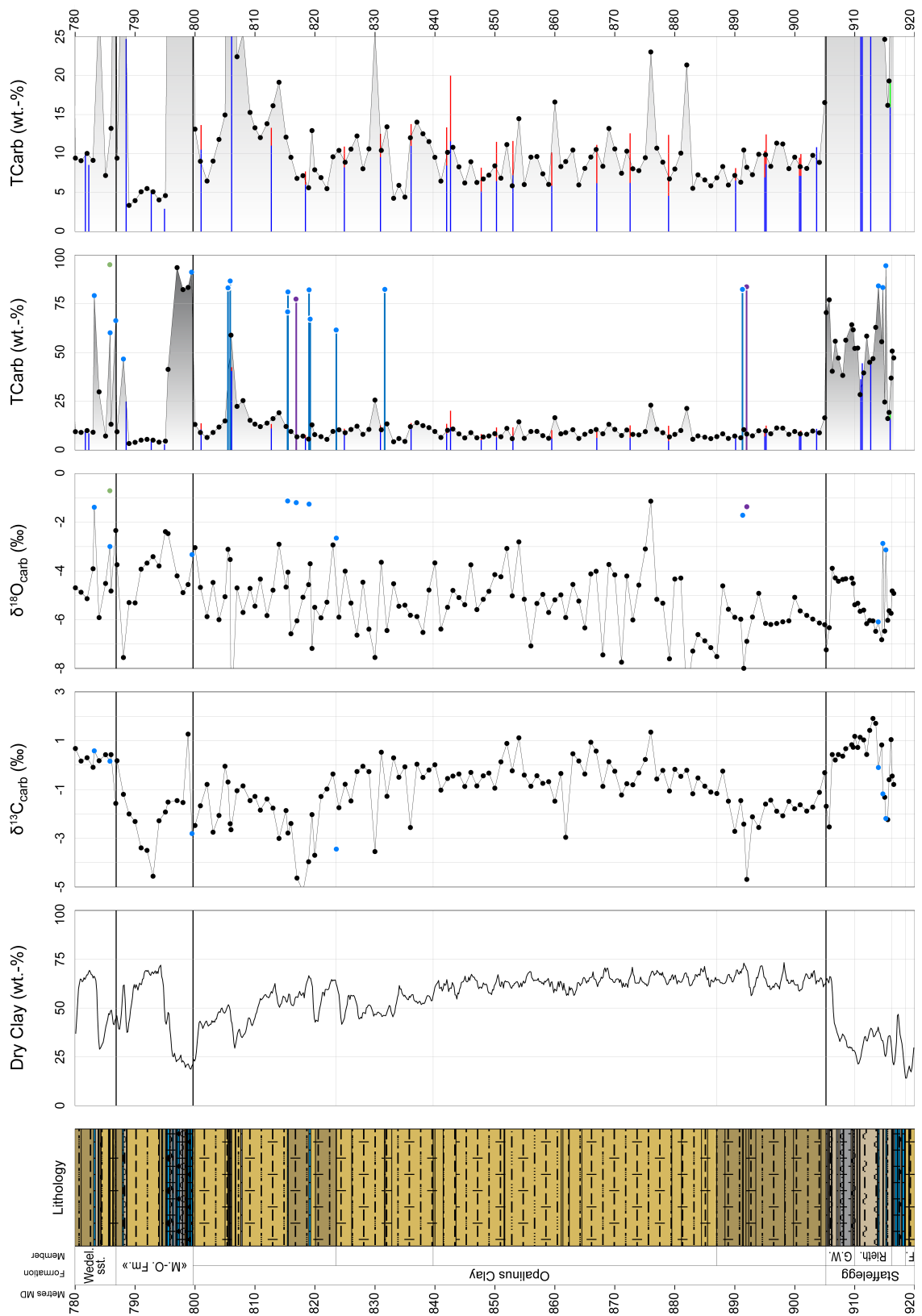


Fig. 3-4: Bulk rock (carb.) isotopic data from the lower Dogger Group – mainly Opalinus Clay
Geochemical data from 916.50 – 781.00 m, additional explanations and references see text at the beginning of Section 3.4.

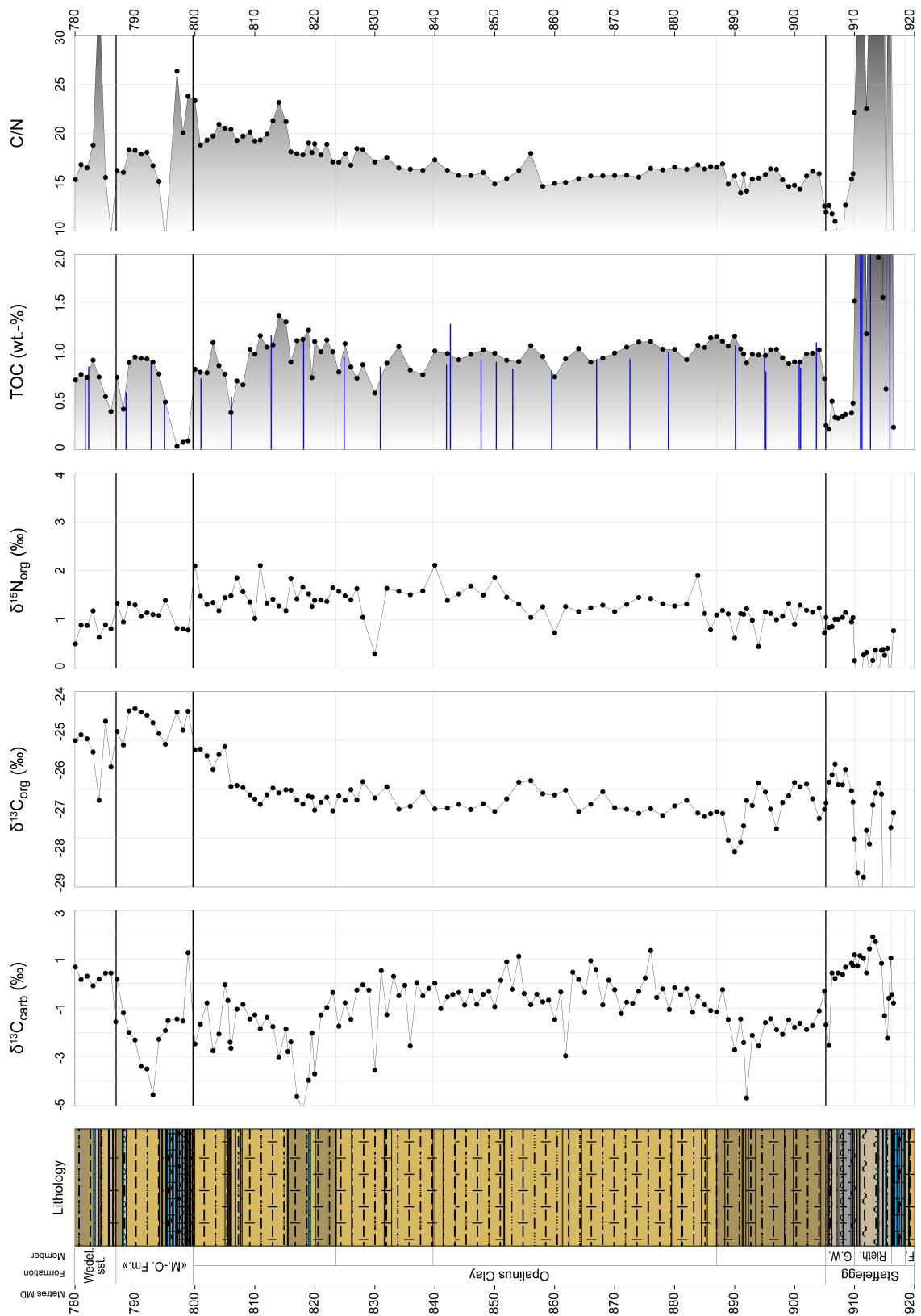


Fig. 3-5: Organic isotopic data from the lower Dogger Group – mainly Opalinus Clay
 Geochemical data from 916.50 – 781.00 m, additional explanations and references see text at the beginning of Section 3.4.

The above following increasing trend ends with values between -1 ‰ and 0 ‰. During almost the whole interval of the «Mixed clay-silt-carbonate sub-unit» and the «Upper silty sub-unit» above it, the $\delta^{13}\text{C}_{\text{carb}}$ data fluctuate with some more positive and some more negative outliers. In the uppermost part of the «Upper silty sub-unit» the C-isotope data decrease to values around -1.7 ‰. In the «Sub-unit with silty calcareous beds», the upper negative CIE can be observed with the most negative value of -5.12 ‰ at 818.00 m. The CIE is somehow bounded by two calcareous beds, which are located at: 819.28 – 819.00 m and 815.56 – 815.41 m (*cf.* Dossier III). Above the second mentioned calcareous bed, the $\delta^{13}\text{C}_{\text{carb}}$ values increase until reaching the uppermost calcareous bed (805.96 – 805.47 m) in the Opalinus Clay. Between this calcareous bed and the lithostratigraphic top of the Opalinus Clay the values fluctuate with a higher range. Crossing the lithological boundary to the hanging «Murchisonae-Oolith Formation», an additional negative CIE (-4.6 ‰ at 793.00 m) can be observed within the very monotonous and argillaceous succession in the middle part. Upsection, the $\delta^{13}\text{C}_{\text{carb}}$ value increases crossing the lithological boundary to the Wedelsandstein Formation to values slightly above 0 ‰.

The $\delta^{13}\text{C}_{\text{carb}}$ data from the calcareous beds and/or bored and reworked intraclasts document possibly an early diagenetic signal (e.g. Wetzel & Allia 2000). The calcareous concretions and all measured septarian nodules are the only macroscopic features with very negative $\delta^{13}\text{C}_{\text{carb}}$ values (-19.1 to -31.1 ‰, Appendix E1). However, very fine authigenic calcite was probably also precipitated in the very fine primary porosity of the Opalinus Clay as well as in the middle part of the «Murchisonae-Oolith Formation», which would lead to the more negative $\delta^{13}\text{C}_{\text{carb}}$ values in the lower and upper negative CIE in the Opalinus Clay and the one above (see also diagenetic discussion in Wohlwend et al. 2016).

The $\delta^{13}\text{C}_{\text{org}}$ data (Fig. 3-5) show a different picture compared to the $\delta^{13}\text{C}_{\text{carb}}$ values. The curve is relatively stable for the most part. The formation of the Opalinus Clay can be subdivided, based on $\delta^{13}\text{C}_{\text{org}}$ values, into four subintervals: The lowest interval (905.20 m – 888.00 m) can be described from the base of Opalinus Clay and includes the three progressively more negative CIE (-27.3 ‰ at 904.11 m, -27.5 ‰ at 896.99 m and -28.1 ‰ at 890.00 m). The most negative $\delta^{13}\text{C}_{\text{org}}$ value at 890.00 m is 2 m above the most negative $\delta^{13}\text{C}_{\text{carb}}$ value at 892.00 m. As already mentioned above, the most part in the middle (888.00 – 806.00 m) is rather stable but can be divided additionally into two subintervals. In the lower part a slight increasing trend is obvious, reaching values of -26.3 ‰ at 854.00 m. Above, the values are clearly shifted to more negative values around -27 ‰. From 812.00 m to 806.00 m the $\delta^{13}\text{C}_{\text{org}}$ data already start to increase slightly to values -26.4 ‰. The upper interval (805.00 – 799.67 m) is easily observed as the $\delta^{13}\text{C}_{\text{org}}$ data is shifted by +1 ‰ to more positive values. The shift or even jump in the organic C-isotopes happens with the uppermost calcareous bed (805.96 – 805.47 m) in the «Sub-unit with silty calcareous beds». The whole upper part until the top of the Opalinus Clay, as well as into the hanging «Murchisonae-Oolith Formation», shows a positive trend reaching the most positive value with -24.4 ‰ at 790.00 m.

The TOC as well as the C/N ratio will be discussed in the same paragraph. Both proxies document rather stable conditions throughout the lower part of the Opalinus Clay up to the top of the «Mixed clay-silt-carbonate sub-unit» at 840.00 m (TOC: ~ 1.0 wt.-%, C/N ratio ~ 15 to 16). From 838.00 m upwards, the C/N ratio starts to increase, reaching a peak value of 23 at 814.00 m just above the calcareous bed between 815.56 m and 815.41 m. With the same sample at 814.00 m also the TOC reaches a maximum with 1.4 wt.-%. In the upper part of the «Sub-unit with silty calcareous beds» both proxies show similar decreasing trends until the calcareous bed between 805.96 m and 805.47 m. In the «Murchisonae-Oolith Formation» the same three times subdivision, as discussed above by the TCarb data, can be seen with the TOC dataset. The middle part contains slightly higher TOC values close to 1 wt.-% compared to the contents below (almost 0 wt.-%) and above (two values at 0.4 and 0.7 wt.-%).

Upper part of the Dogger Group

The following described interval, the upper Dogger Group («Murchisonae-Oolith Formation», Wedelsandstein Formation, «Humphriesioolith Formation», «Herrenwis Unit», «Parkinsoni-Württembergica Schichten», Variansmergel Formation, Wutach Formation as well as the lower part of the Wildegge Formation), covers in time the whole Middle Aalenian to Middle Oxfordian substages (Figs. 3-6 and 3-7).

The semi-quantitative TCarb (Fig. 3-6) represents the alternation of silty claystone, argillaceous to calcareous marl and limestone intervals. The carbonate content curve thus roughly reflects the inverse Dry Clay content curve (*cf.* Dossier X). As mentioned above, the «Murchisonae-Oolith Formation» can be divided into three parts, with a very prominent calcareous lower part, a middle part represented by the very low TCarb values and an upper thin interval which is slightly more calcareous. The Wedelsandstein Formation, like the drilling in BUL1-1 (Wohlwend et al. 2021a) and STA3-1 (Wohlwend et al. 2023), is showing two increasing trends separated by a hardground at 783.37 – 783.10 m. However, it is striking that compared to STA3-1, the thickness of the Wedelsandstein Formation is much less in STA2-1. The lower interval is about the same, but the interval above the hardground is reduced to only 3.7 m compared to 18.7 m in STA3-1 and 14.5 m in BUL1-1. Reduction is probably the result of increased bottom currents which could lead to a winnowing effect. The 1.80 m thin «Humphriesioolith Formation» is overlain by the very calcareous 10.52 m thick bioclastic «Herrenwis Unit». The interval is therefore very pronounced in the TCarb and can be easily distinguished from the underlying and hanging formations. The «Parkinsoni-Württembergica-Schichten» start with a very low TCarb content around 10 wt.-% and document an overall trend to values around 40 wt.-% against the uppermost part. The three analysed samples from the Variansmergel Formation clearly document a return to a lower TCarb content before the content increases again in the above following Wutach Formation and Wildegge Formation with some fluctuations.

The $\delta^{13}\text{C}_{\text{carb}}$ data (Figs. 3-6 and 3-7) indicate in the Wedelsandstein Formation rather stable values around +0.5 ‰. This is somewhat different from STA3-1, where the values contain a slight increasing trend, which may be less obvious due to the significantly lower thickness in STA2-1 and is therefore more likely to appear stable. The values from the «Humphriesioolith Formation» and above all from the «Herrenwis Unit» reaching up to +2 ‰. The $\delta^{13}\text{C}_{\text{carb}}$ values from the above following «Parkinsoni-Württembergica-Schichten» are clearly lower and very stable between 0.4 and 0.7 ‰, with only one exception at the very base where the values are even more negative. In the iron-oid rich succession of the Wutach Formation the $\delta^{13}\text{C}_{\text{carb}}$ values start in the lower part quite stable around 0 ‰ and then from 729.52 m upwards the C-isotope data document a very prominent trend to even more positive values into the lowermost part of the Wildegge Formation. The several per mil positive shift to values around +3.1 ‰ with the uppermost sample taken at 725.00 m is typical for the Callovian/Oxfordian boundary and was already documented by Rais et al. (2007) in other locations as well as the Weiach borehole. The same positive trend was for example also documented during this campaign in the BUL1-1 borehole (Wohlwend et al. 2021a). The most positive $\delta^{13}\text{C}_{\text{carb}}$ values were normally in the Middle Oxfordian (Transversarium Zone; Rais et al. 2007).

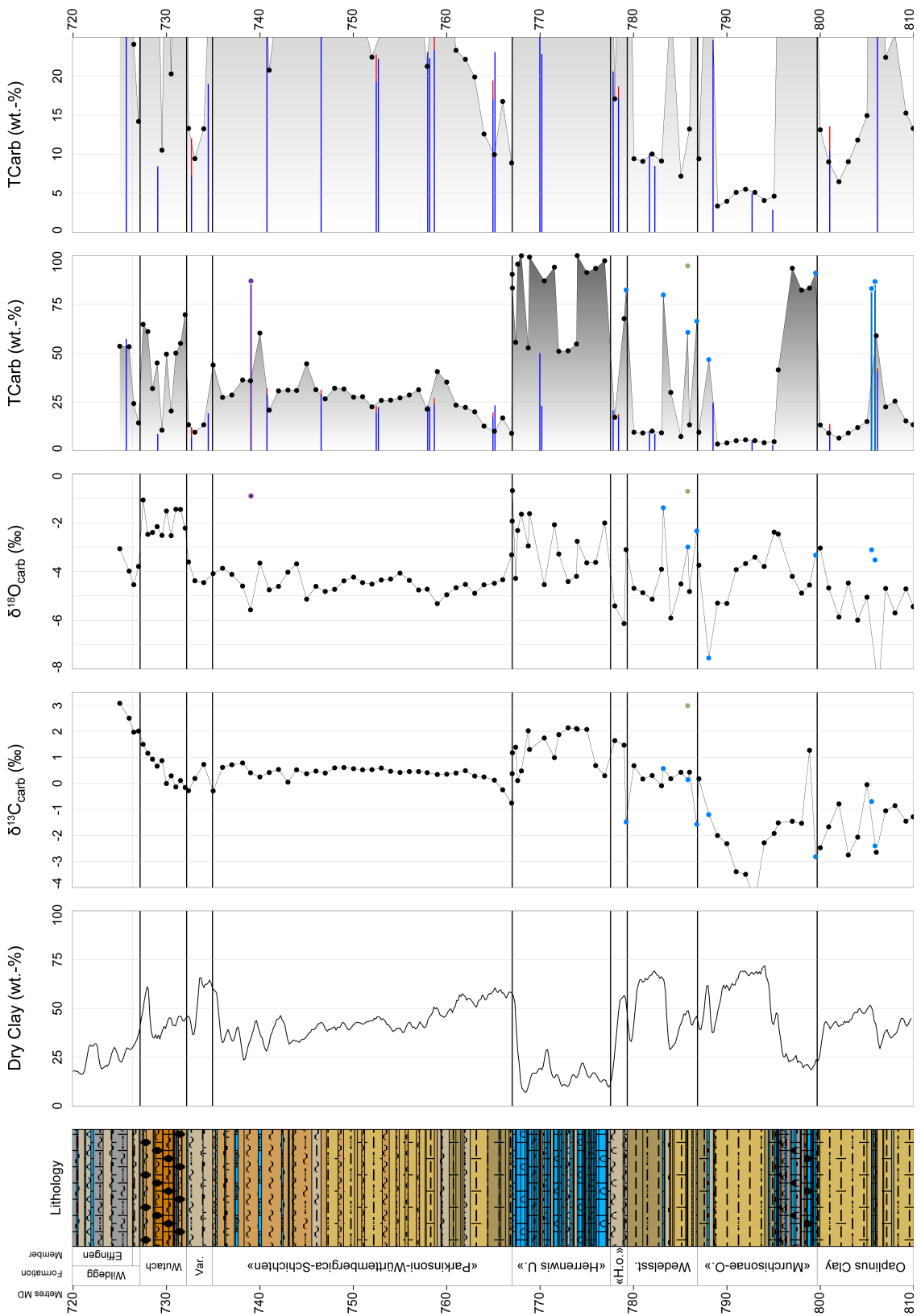


Fig. 3-6: Bulk rock (carbonate) isotopic data from the upper part of the Dogger Group
 Geochemical data from 810.00 – 725.00 m, additional explanations and references see text at the beginning of Section 3.4.

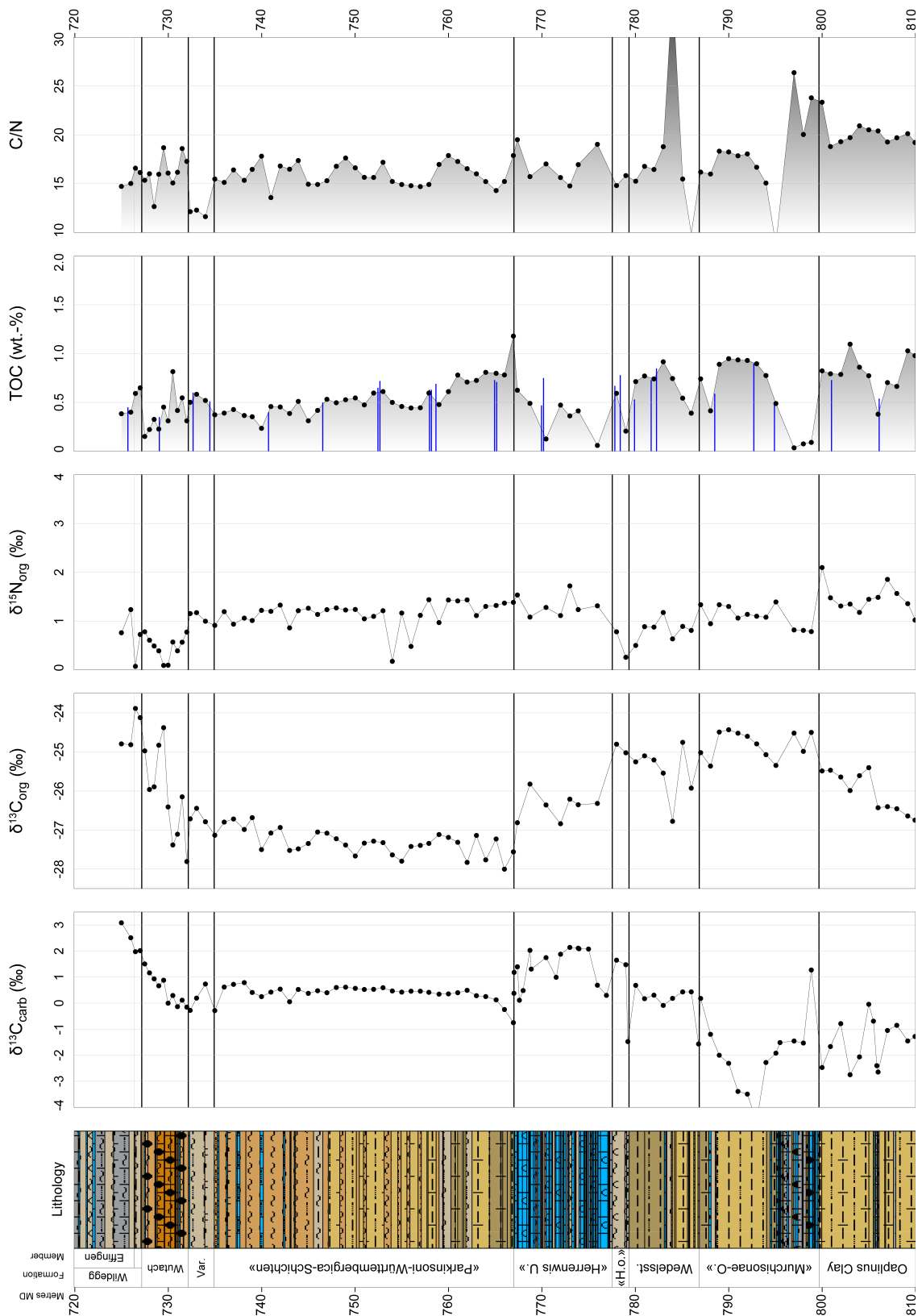


Fig. 3-7: Organic isotopic data from the upper part of the Dogger Group

Geochemical data from 810.00 – 725.00 m, additional explanations and references see text of Section 3.4.

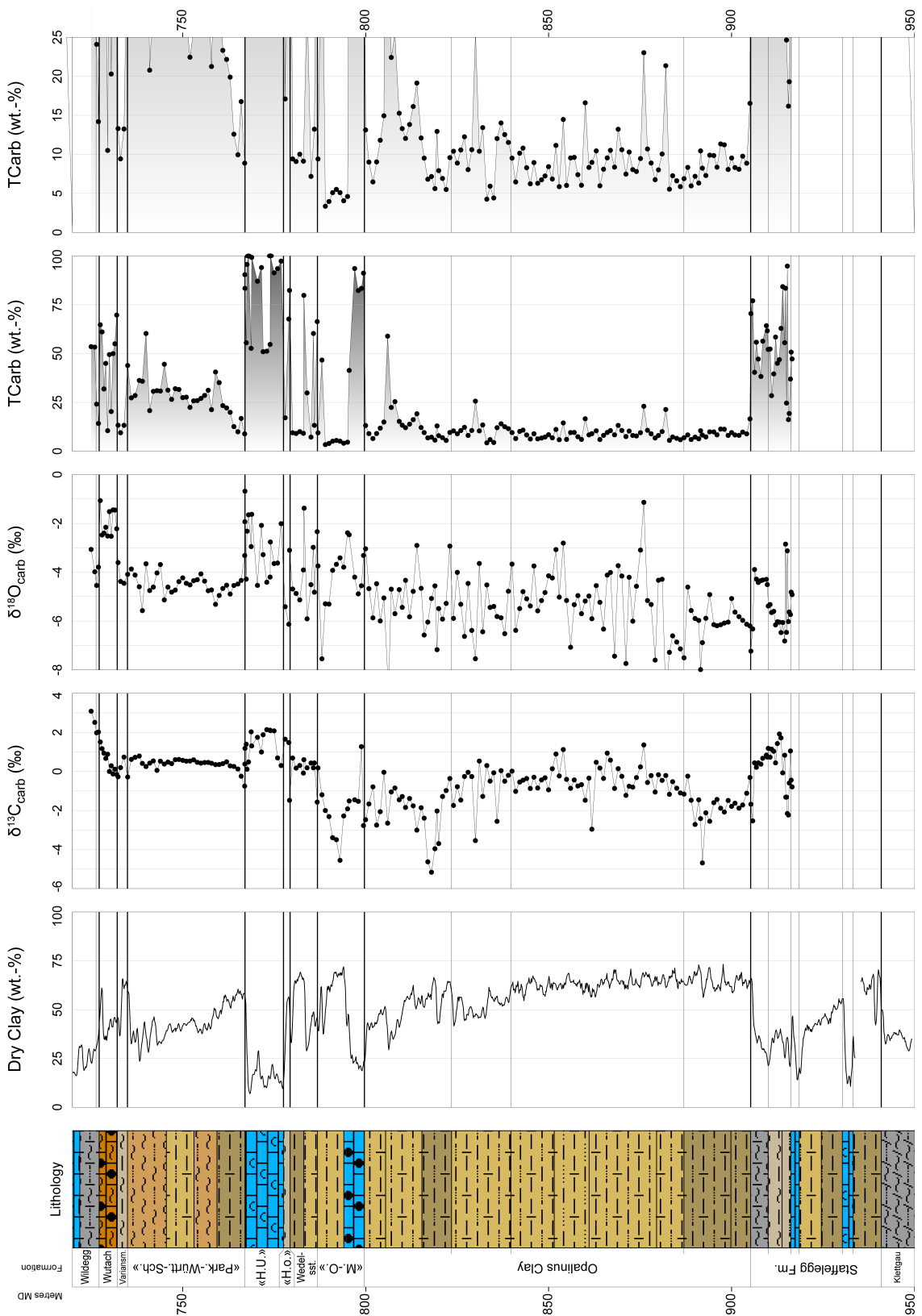


Fig. 3-8: Whole bulk rock (carbonate) isotopic data from STA2-1

Geochemical data from 916.50 – 725.00 m, additional explanations and references see text at the beginning of Section 3.4.

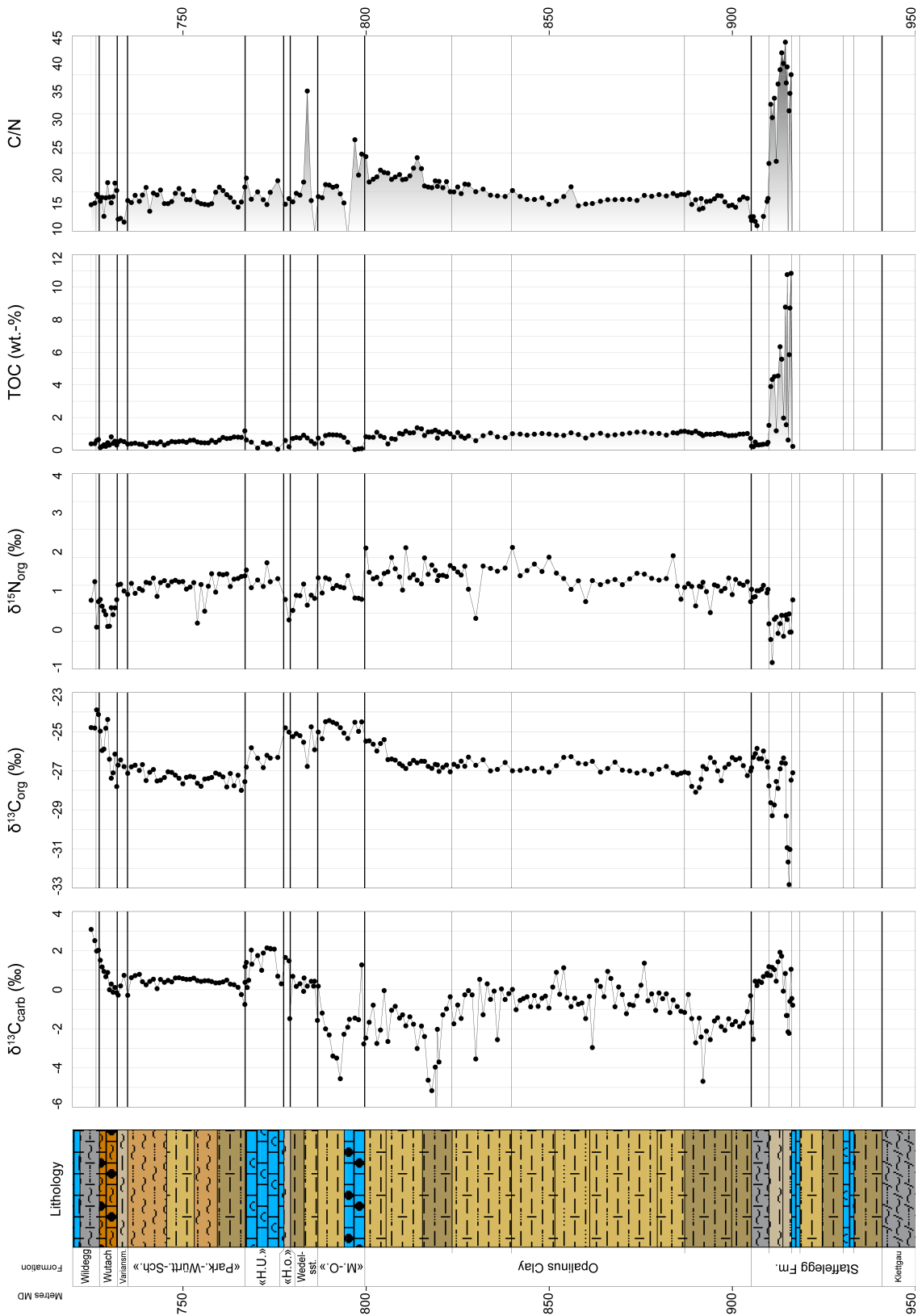


Fig. 3-9: Whole organic isotopic data from STA2-1
 Geochemical data from 916.50 – 725.00 m, additional explanations and references see text at the beginning of Section 3.4.

The $\delta^{13}\text{C}_{\text{org}}$ data (Fig. 3-7) document, as already mentioned above, very positive values in the middle interval of the «Murchisonae-Oolith Formation» (values up to -24.4 ‰ at 790.00 m). The above following lower part of the Wedelsandstein Formation is with the only five samples and the rather high range in the fluctuation difficult to discuss. However, the average data document a negative shift into the lower part of the Wedelsandstein Formation. In the upper part (above the hardground from 783.37 m to 783.10 m) the values increase again to more positive values. The trend goes on into the «Humphriesioolith Formation», reaching again values of -24.8 ‰ at 778.0 m. The $\delta^{13}\text{C}_{\text{org}}$ data from the overlying «Herrenwis Unit» are not showing the same resolution because there was not enough material for every organic measurement after the decarbonatisation of the limestone-rich succession. Though, the $\delta^{13}\text{C}_{\text{org}}$ data clearly show a decrease through the entire «Herrenwis Unit» into the lower part of the «Parkinsoni-Württembergica-Schichten», where the most negative value has been analysed at 766.00 m (-28.0 ‰). Upsection, the $\delta^{13}\text{C}_{\text{org}}$ data document a stable interval trough the lower and middle part of the «Parkinsoni-Württembergica-Schichten» before the values start to increase during the Variansmergel Formation.

Finally, also the $\delta^{13}\text{C}_{\text{org}}$ data document the very striking positive shift close to the Callovian/Oxfordian boundary from -27.4 ‰ at 730.50 m to -23.9 ‰ at 726.50 m, from the middle part of the Wutach Formation into the lower part of the Wildegg Formations. The C-isotope chemostratigraphic data ($\delta^{13}\text{C}_{\text{org}}$ as well as $\delta^{13}\text{C}_{\text{carb}}$) document, with the very large shifts, that the resolution in this very condensed succession is not high enough and that a lot of time is missing in such stratigraphic gaps.

In the middle part of the Wutach Formation two samples (729.52 m and 729.00 m), taken from very reddish, iron-oolitic and limonitic intervals, were tested because of a possible insufficient decarbonatisation. Similar cases and the resulting strange positive values in the $\delta^{13}\text{C}_{\text{org}}$ data have already been documented in other boreholes during this campaign (e.g. BOZ1-1; Wohlwend et al. 2022). The questioned samples have been decarbonised a second time for 12 h, but this time at 70 °C. However, the additional re-measurements document almost the same values as during the original analyses and therefore, the decarbonatisation seems to be good enough.

The C/N ratio as well as the TOC show less clear trends. The variations in the lithologies are also represented by higher variations throughout the upper part of the Dogger Group. Calcareous intervals (lower part of «Murchisonae-Oolith Formation» and «Herrenwis Unit») are clearly poorer in organic content. Overall, the TOC documents a decreasing trend up to the Wildegg Formation. The C/N ratio can be divided into two successions: a lower one with values around 20 in the upper part of the Opalinus Clay and lower part of the Murchisonae-Oolith Formation» and an upper one with values closer to 15 throughout the upper formations.

4 Definition of specific lithostratigraphic boundaries

The boundaries between stratigraphical units, as also shown in the stratigraphical logs of the lithostratigraphy report (Dossier III), were mostly defined by using lithological criteria. According to the guidelines on stratigraphical nomenclature of Remane et al. (2005), the definition of lithostratigraphical units should be based, both vertically and horizontally, on lithological variations regardless of their age. In fact, the formation boundaries, as used by Nagra for the ongoing borehole campaign of Stage 3 of the Sectoral Plan for Geological Repositories (Jordan & Deplazes 2019), were not always obvious in the borehole and definitions were difficult to apply, either because of the small core diameter or because of differences in facies. The exact location of some of the formation boundaries caused discussions during core description and the process of quality control. Most of the important data for questionable boundaries were already present before the data-freeze (30.09.2021) and were used for the log descriptions and drawings. In the following paragraphs, the underlying considerations are explained for providing a better understanding of how boundaries were demarcated. We are aware of the fact that several boundaries are no longer based on lithological criteria alone and that chronostratigraphic criteria (ammonite, palyno- and chemostratigraphy) are included in the definitions.

Opalinus Clay (905.20 – 799.67 m)

The *lower boundary* of the Opalinus Clay is set at 905.20 m at the uppermost surface of an argillaceous to calcareous marl interval from the underlying Staffelegg Formation, which is covered by claystone (silty, micaceous) (*cf.* Dossier III). The lithological boundary is therefore evident above all in the carbonate content (TCarb: Figs. 3-2 and 3-4). The values decrease from 71 wt.-%, measured from the uppermost sample (905.25 m) of the Gross Wolf Member, to 17 wt.-% at 905.00 m and then values only between 9 and 10 wt.-% were measured in the basal Opalinus Clay (Fig. 3-2). The lithological change between the Gross Wolf Member and the Opalinus Clay is also visible in the slight increase in TOC from values < 0.5 wt.-% to values around 1 wt.-% in the Opalinus Clay (Fig. 3-5).

The described ammonites (Section 3.2) document, within the resolution of the biostratigraphy, that the lithological boundary somehow coincides with the Toarcian / Aalenian stage boundary. The uppermost ammonite (*Pleydellia ex gr. buckmani*) from the Gross Wolf Member (depth: 905.31 m) yields Aalensis Zone (Torulosum Subzone). The lowermost sampled ammonite (*Leioceras ex gr. subglabrum*) from the basal Opalinus Clay, which is unfortunately not very ammonite rich (depth: 894.34 m), can be dated as Opalinum Zone (Opalinum Subzone). Although, the palynosample from 905.04 m already yields Opalinum Zone (Opalinum Subzone). Therefore, the stage boundary seems to practically coincide with the lithological boundary at 905.20 m.

The *upper boundary* of the Opalinus Clay is set at 799.67 m where a thick succession of dark grey silty claystone (calcareous) is overlain by medium grey bioclastic calcareous marl and bioclastic limestone, both sparsely iron-oolitic (*cf.* Dossier III). The boundary at 799.67 m documents a clear change in lithology, which is evident, for example, in the markedly higher carbonate content (TCarb) and is also supported by the analysis of FMI and GR logs.

The uppermost ammonite (*Leioceras ex gr. bifidatum?*) from the upper part of the Opalinus Clay (depth: 805.58 m) yields Opalinum Zone (questionable Bifidatum Subzone) and is therefore probably slightly younger than the rest of the Opalinus Clay. The three palynological samples, taken from the uppermost part of the Opalinus Clay at 806.62 m, 805.01 m and 799.90 m, document with the occurrence of subspecies of *Nannoceratopsis plegas* and the increase in diversity of *Nannoceratopsis* species an assemblage which is typical from the upper part of the

Opalinum Zone onwards. The interval is therefore interpreted Opalinum Zone (Opalinum to possibly Bifidatum Subzone). From the basinal bioclastic limestone beds from the following «Murchisonae-Oolith Formation» two palynosamples were taken at 799.55 m and 799.11 m. The lower one yields questionable Murchisonae Zone to questionable Opalinum Zone and is therefore not as meaningful. However, the upper sample at 799.11 m yields Murchisonae to Bradfordensis Zone. This age is also supported by the recovered *Staufenia* ex gr. *staufensis*? slightly above at 795.11 m.

The positive chemostratigraphic shift or even jump in the organic C-isotopes within the uppermost calcareous bed (805.96 – 805.47 m), is typical for the Bifidatum Subzone of the Opalinum Zone. The latter shift to even more positive $\delta^{13}\text{C}_{\text{org}}$ values at the lithological boundary fits to similar shifts (e.g., STA3-1; Wohlwend et al. 2023) found in the same biostratigraphic intervals. Although, in BUL1-1 the basal succession of the hanging «Murchisonae-Oolith Formation» is very condensed and therefore, the shift is more compressed to a peak (Wohlwend et al. 2021a).

«Murchisonae-Oolith Formation» (799.67 – 786.85 m)

The *lower boundary* of the «Murchisonae-Oolith Formation» is set at 799.67 m at the base of medium grey bioclastic calcareous marl and bioclastic limestone, both sparsely iron-oolitic (cf. Dossier III). This succession overlies typical clay-rich sediments from the Opalinus Clay and therefore, documents a clear change in lithology; see above for the detailed discussion about this boundary (upper boundary Opalinus Clay).

The *upper boundary* of the «Murchisonae-Oolith Formation», is defined per definition at the subface of the «Sowerbyi-Oolith», which forms the basal bed of the hanging Wedelsandstein Formation (Bloos et al. 2005). In the STA2-1 the lithological boundary was therefore defined at 786.85 m, at the base of the lowermost of three bioclastic calcareous marl beds with abundant iron-oooids and oysters (cf. Dossier III). The 15 cm thick bed (786.85 – 786.70 m) seems to correlate with the "Austernpflaster" of Weiach (539.17 – 538.10 m; Matter et al. 1988 and Bläsi et al. 2013) and a similar bed in STA3-1 (764.97 – 764.82 m; Schürch et al. 2023). All these "event-beds" may be linked to the «Sowerbyi-Oolith». Therefore, the top of the «Murchisonae-Oolith Formation» is set at 786.85 m.

The lower age of the «Murchisonae-Oolith Formation» is defined by palynomorphs and is interpreted as probably Murchisonae to Bradfordensis Zone (see discussion above). An additional ammonite from 795.11 m (*Staufenia* ex gr. *staufensis*?) yields probably Bradfordensis Subzone (Bradfordensis Zone?). In the middle and upper part of the formation no other ammonites were found. Therefore, the biostratigraphic interpretation in this upper succession is based only on palynomorphs. The palynosamples, taken at 795.07 m and 789.01 m, yield Bradfordensis Zone. The following four palynosamples, covering the lithological boundary (787.95 m, 787.04 m, 786.53 m and 786.01 m) yield all Concavum to questionable Discites Zone. Only the sample at 785.55 m is clearly younger of Early Bajocian and is dated as Discites to questionable Ovale Zone.

Wedelsandstein Formation (786.85 – 779.34 m)

The *lower boundary* of the Wedelsandstein Formation is set at the subface of the 15 cm thick oyster and iron-oid bearing bioclastic calcareous marl bed (786.85 – 786.70 m), which is believed to correspond to the «Sowerbyi-Oolith» and therefore defines the base of the Wedelsandstein Formation (German Stratigraphic Scheme; Bloos et al. 2005). See more detailed discussion for the boundary above (upper boundary of the «Murchisonae-Oolith Formation»).

The *upper boundary* of the Wedelsandstein Formation is set at 779.34 m at an erosional surface separating the overlying bioclastic calcareous marl with iron-ooids from the underlying silty claystone (*cf.* Dossier III). The lithological top is purely defined by the onset of iron-ooids and limonitic components and therefore solely based on lithological criteria.

As already mentioned above (Section 3.4), the Wedelsandstein Formation can be subdivided by a hardground (783.37 – 783.10 m) into a lower and an upper subinterval. The age of the two sub-intervals and therefore the whole Wedelsandstein Formation was dated by palynomorphs only because no ammonites were found. The lower subinterval until the hardground can be dated as Discites Zone and Ovale Zone with two palynosamples (785.55 m and 784.24 m). The lowermost two samples close to the base (786.53 m and 786.01 m) seem to have an age close to the stage boundary between the Aalenian to Bajocian (Concavum to questionably Discites Zone). The upper subinterval above the hardground was deposited during the Laeviuscula Zone (palynosamples at 782.98 m, 781.07 m and 779.43 m).

«Humphriesiolith Formation» (779.34 – 777.54 m)

The *lower boundary* of the «Humphriesiolith Formation» is set at 779.34 m at the base of an iron-oid and limonitic calcareous marl succession (779.34 – 778.88 m) covering an erosional surface. The onset of iron-ooids and limonitic components solely define the lithological lower boundary of the «Humphriesiolith Formation».

The *upper boundary* is set at 777.54 m, at the base of a bioclastic calcareous marl, covering a bioclastic argillaceous marl. The following 10.52 m thick, mainly bioclastic, calcareous succession seems to be a more basinal deposit that continues east into the mainly coral-bearing unit of the «Herrenwis Unit» in STA3-1 and BUL1-1 and therefore the mainly bioclastic succession was incorporated into the still informal «Herrenwis Unit». Both boundaries (lower and upper) are solely based on lithological criteria.

The age of the «Humphriesiolith Formation» in STA2-1 is defined by two palynomorph samples taken from the lower and upper part (779.13 m and 777.71 m). Both samples are still dated as Laeviuscula Zone, same as the three underlying ones from the upper part of the Wedelsandstein Formation.

«Herrenwis Unit» (777.54 – 767.02 m)

The *lower boundary* is set at 777.54 m at the base of the 10.52 m thick, bioclastic calcareous marl and limestone succession covering a bioclastic argillaceous marl (*cf.* Dossier III). The bioclastic succession appears to be the more basinal deposition of the corraligenous buildup and crinoidal limestone found further east, which was cored by the two drillings in STA3-1 and in BUL1-1. Therefore, the basinward wedging deposit, with reworking from the shallower platform indicated by coral clasts (Tab. 3-1), is also subsumed under the informal term «Herrenwis Unit».

The *upper boundary* is set at 767.02 m, at the top of a bored erosional surface with iron-stromatolitic clasts, which truncates the bioclastic succession towards the top. Above the sharp contact a bioclastic argillaceous marl was deposited. Both boundaries (lower and upper) are solely based on lithological criteria.

The age of the «Herrenwis Unit» in STA2-1 is mainly defined by six palynomorph samples taken from marlier interlayers and can be divided into three palynological intervals. The succession is overlying the «Humphriesiolith Formation», which is dated in the uppermost part (777.71 m) to

Laeviuscula Zone. The lower interval of the «Herrenwis Unit» (777.39 – 771.37 m) is dated by four samples as Sauzei Zone. The upper interval is somehow younger. The palynological sample at 768.76 m is interpreted Sauzei to Humphriesianum Zone and the uppermost sample at 767.40 m is interpreted as Niortense Zone. The two ammonites at 773.26 m and 773.23 m could not be prepared because there was no separation between the rock matrix and the fossil.

5 Conclusion

The present study documents data on microfacies analysis, ammonite stratigraphy and palynostratigraphy as well as detailed geochemical analyses (C, O and N isotopes). With this data collection, it was possible to predict the delimitation of the Mesozoic strata more accurately. Most of the important data for the boundaries in question were already present at the data-freeze (30.09.2021). Therefore, the present report complements the lithostratigraphic report of Dossier III for the deep borehole Stadel-2-1. The lithological boundaries, and therefore the stratigraphic profile, were mostly defined by lithological criteria. Nevertheless, the customary formal and informal formation boundaries were not always obvious in the drill cores, either because of the small core diameter or changing facies conditions. The exact location of specific formation boundaries led to discussions requiring additional data to determine the exact profile description and illustration. We are aware that certain boundaries are thus no longer based solely on lithological criteria, and that the definitions therefore also include chronostratigraphic criteria (ammonite stratigraphy, palyno- and chemostratigraphy).

6 References

- Bathurst, R.G.C. (1975): Carbonate sediments and their diagenesis (2nd ed.). Developments in Sedimentology, Amsterdam, Elsevier, 658 pp.
- Bloos, G., Dietl, G. & Schweigert, G. (2005): Der Jura Süddeutschlands in der Stratigraphischen Tabelle von Deutschland 2002. Newsletters on stratigraphy 41, 263-277.
- Bronn, G.H. (1842): Über die fossilen Gaviale der Lias-Formation und der Oolithe. Archiv für Naturgeschichte 8/1, 7-82.
- Buckman, S.S. (1887 – 1907): A Monograph of the ammonites of the Inferior Oolite Series. Palaeontographical Society Monographs, London, The Palaeontographical Society, 456 pp.
- Cariou, E. & Hantzpergue, P. (1997): Biostratigraphie du Jurassique ouest-européen et méditerranéen: zonations parallèles et distribution des invertébrés et microfossiles. Bull. Centre Rech. Elf Explor. Prod.
- Dickson, J.A. (1965): Modified staining technique for carbonates in thin section. Nature 205, 587.
- Dietze, V., Gräbenstein, S., Franz, M., Schweigert, G. & Wetzel, A. (2021): The Middle Jurassic Opalinuston Formation (Aalenian, Opalinus Zone) at its type locality near Bad Boll and adjacent outcrops (Swabian Alb, SW Germany). Palaeodiversity 14/1, 15-113.
- Dumortier, E. (1867 – 1874): Etudes paléontologiques sur les dépôts jurassiques du Bassin du Rhône. Bd IV, Lias supérieur. F. Savy, Paris, 335 pp.
- Emerson, S. & Hedges, J.I. (1988): Processes controlling the organic carbon content of open ocean sediments. Paleoceanography 3, 621-634.
- Feist, S. (1987): Palynologische Untersuchungen im Braunjura beta und unteren Braunjura gamma (oberes Aalenium bis unteres Bajocium) der Bohrungen Hausen, nordöstliche Schwäbische Alb. Diploma Thesis, University of Tübingen. 78pp.
- Feist-Burkhardt, S. & Monteil, E. (1997): Dinoflagellate cysts from the Bajocian stratotype (Calvados, Normandy, Western France). Bulletin Centre Rech. Elf Explor. Prod. 21/1, 31-105.
- Feist-Burkhardt, S. & Pross, J. (2010): Dinoflagellate cyst biostratigraphy of the Opalinuston Formation (Middle Jurassic) in the Aalenian type area in southwest Germany and north Switzerland. Lethaia 43, 10-31.
- Feist-Burkhardt, S. & Wille, W. (1992): Jurassic palynology in southwest Germany – state of the art. Cahiers de Micropaléontologie 7/1-2, 141-164.
- Fernandez, A., van Dijk, J., Müller, I.A. & Bernasconi, S.M. (2016): Siderite acid fractionation factors for sealed and open vessel digestions at 70°C and 100°C. Chemical Geology 444, 180-186.
- Gocht, H. (1964): Planktonische Kleinformen aus dem Lias/Dogger-Grenzbereich Nord- und Süddeutschlands. N. Jb. Geol. Paläont. Abh. 119/2, 113-133.

- Isler, A., Pasquier, F. & Huber, M. (1984): Geologische Karte der zentralen Nordschweiz 1:100'000. Herausgegeben von der Nagra und der Schweiz. Geol. Komm.
- Jordan, P. & Deplazes, G. (2019): Lithostratigraphy of consolidated rocks expected in the Jura Ost, Nördlich Lägern and Zürich Nordost regions. Nagra Arbeitsbericht NAB 19-14.
- Kuhn, O. & Etter, W. (1994): Der Posidonienschiefer der Nordschweiz: Lithostratigraphie, Biostratigraphie und Fazies. *Eclogae geol. Helv.* 87/1, 113-138.
- Kukal, Z. (1971): *Geology of recent sediments*. Academic Press, New York, 490 pp.
- Matter, A., Peters, Tj., Bläsi, H.-R., Meyer, J., Ischi, H. & Meyer, Ch. (1988): Sondierbohrung Weiach – Geologie (Textband und Beilagenband). Nagra Technischer Bericht NTB 86-01.
- Maubeuge, P.L. (1947): Sur quelques ammonites de l'Aalénien ferrugineux du Luxembourg et sur l'échelle stratigraphique de la Formation ferrifère Franco-Belgo-Luxembourgeoise. *Archives de l'Institut Grand-Ducal de Luxembourg, Section des Sciences naturelles, physique et mathématique, Nouvelle Série* 17, 73-87.
- Meyers, P.A. (1997): Organic geochemical proxies of paleoceanographic, paleolimnologic, and paleoclimatic processes. *Org. Geochem.* 27, 213-250.
- Meyers, P.A. & Bernasconi, S.M. (2005): Carbon and nitrogen isotope excursions in mid-Pleistocene sapropels from the Tyrrhenian Basin: Evidence for climate-induced increases in microbial primary production. *Marine Geology* 220, 41-58.
- Nagra (2014): SGT Etappe 2: Vorschlag weiter zu untersuchender geologischer Standortgebiete mit zugehörigen Standortarealen für die Oberflächenanlage. Geologische Grundlagen. Dossier II: Sedimentologische und tektonische Verhältnisse. Nagra Technischer Bericht NTB 14-02.
- Ogg, J.G., Ogg, G. & Gradstein, F.M. (2016): *The Concise Geologic Time Scale*. Cambridge University Press. 184 pp.
- Oppel, A. (1856–1858): The Juraformation Englands, Frankreichs, und des südwestlichen Deutschlands. *Ebner & Seubert, Stuttgart und Württ. Naturwiss. Jh.* 12-14, 857 pp.
- Oppel, A. (1863): Über jurassische Cephalopoden. *Paläontologische Mitteilungen des Museums des Königlichen Bayerischen Staates* 3, 163-266.
- Parsons, T.R. (1975): Particulate organic carbon in the sea. *In: Riey, J.P. & Skirrow, G. (eds.): Chemical oceanography*. Academic Press, London, 338-425.
- Pietsch, J. & Jordan, P. (2014): Digitales Höhenmodell Basis Quartär der Nordschweiz – Version 2013 (SGT E2) und ausgewählte Auswertungen. Nagra Arbeitsbericht NAB 14-02.
- Rais, P., Louis-Schmid, B., Bernasconi, S.M. & Weissert, H. (2007): Palaeoceanographic and palaeoclimatic reorganization around the Middle–Late Jurassic transition. *Palaeogeography, Palaeoclimatology, Palaeoecology* 251/3-4, 527-546.
- Reinecke, J.C.M. (1818): *Maris protogaei Nautilus et Argonautae vulga Cornua Ammonis in Agro Coburgico et vicinio reperiundos; descripsit et delineavit, simul Observationes de Fossilum Prototypis*. L.C.A. Ahlii imp., Coburg, 90 pp.

- Remane, J., Adatte, T., Berger, J.P., Burkhalter, R., Dall'Agnolo, S., Decrouez, D., Fischer, H., Funk, H., Furrer, H., Graf, H.R., Gouffon, Y., Heckendorn, W. & Winkler, W. (2005): Richtlinien zur stratigraphischen Nomenklatur. *Eclogae geol. Helv.* 98/3, 385-405.
- Ruebsam, W. & Al-Husseini, M. (2020): Calibrating the Early Toarcian (Early Jurassic) with stratigraphic black holes (SBH). *Gondwana Research* 82, 317-336.
- Schürch, P., Jordan, P., Schwarz, M., Naef, H., Felber, R., Ibele, T. & Gysi, M. (2023): TBO Stadel-3-1: Data Report – Dossier III: Lithostratigraphy. Nagra Arbeitsbericht NAB 22-01.
- Scheffer, F. & Schachtschnabel, P. (1984): *Lehrbuch der Bodenkunde*. Enke Verlag, Stuttgart.
- Smelror, M. (1988): Late Bathonian to Early Oxfordian dinoflagellate cyst stratigraphy of Jameson Land and Milne Land, East Greenland. *Rapport Grønlands Geologiske Undersøgelse* 137, 135-159.
- StrataBugs, version 2.1 (June 2016): StrataData Ltd., UK. <http://www.stratadata.co.uk>.
- Timescale Creator, version 7.0 (30. July 2016): Geologic TimeScale Foundation. <https://engineering.purdue.edu/Stratigraphy/tscreator/>
- Van Mooy, B.A.S., Keil, R.G. & Devol, A.H. (2002): Impact of suboxia on sinking particulate organic carbon: enhanced carbon flux and preferential degradation of amino acids via denitrification. *Geochim. Cosmochim. Acta* 66, 457-465.
- Voigt, E. (1968): Über Hiatus-Konkretionen (dargestellt an Beispielen aus dem Lias). *Geologische Rundschau* 58, 281-296.
- Wetzel, A. & Allia, V. (2000): The significance of hiatus beds in shallow-water mudstones: an example from the Middle Jurassic of Switzerland. *Journal of Sedimentary Research* 70/1, 170-180.
- Wohlwend, S., Bläsi, H.R., Feist-Burkhardt, S., Hostettler, B., Menkveld-Gfeller, U., Dietze, V. & Deplazes, G. (2023): TBO Stadel-3-1: Data Report – Dossier IV: Microfacies, Bio- and Chemostratigraphic Analysis. Nagra Arbeitsbericht NAB 22-01.
- Wohlwend, S., Bläsi, H.R., Feist-Burkhardt, S., Hostettler, B., Menkveld-Gfeller, U., Dietze, V. & Deplazes, G. (2022): TBO Bözberg-1-1: Data Report – Dossier IV: Microfacies, Bio- and Chemostratigraphic Analysis. Nagra Arbeitsbericht NAB 21-21.
- Wohlwend, S., Bläsi, H.R., Feist-Burkhardt, S., Hostettler, B., Menkveld-Gfeller, U., Dietze, V. & Deplazes, G. (2021a): TBO Bülach-1-1: Data Report – Dossier IV: Microfacies, Bio- and Chemostratigraphic Analysis. Nagra Arbeitsbericht NAB 20-08.
- Wohlwend, S., Bläsi, H.R., Feist-Burkhardt, S., Hostettler, B., Menkveld-Gfeller, U., Dietze, V. & Deplazes, G. (2021b): TBO Trüllikon-1-1: Data Report – Dossier IV: Microfacies, Bio- and Chemostratigraphic Analysis. Nagra Arbeitsbericht NAB 20-09.
- Wohlwend, S., Bläsi, H.R., Feist-Burkhardt, S., Hostettler, B., Menkveld-Gfeller, U., Dietze, V. & Deplazes, G. (2021c): TBO Marthalen-1-1: Data Report – Dossier IV: Microfacies, Bio- and Chemostratigraphic Analysis. Nagra Arbeitsbericht NAB 21-20.

- Wohlwend, S., Bernasconi, S.M., Deplazes, G. & Jaeggi, D. (2019): SO Experiment: Chemostratigraphic study of Late Aalenian to Early Bajocian. Mont Terri Technical Report TR 19-05. Federal Office of Topography (swisstopo), Wabern, Switzerland.
- Wohlwend, S., Hart, M. & Weissert, H. (2016): Chemostratigraphy of the Upper Albian to mid-Turonian Natih Formation (Oman) – How authigenic carbonate changes a global pattern. *The Depositional Record* 2/1, 97-117.
- Wood, G.D., Gabriel, A.M. & Lawson, J.C. (1996): Palynological techniques – processing and microscopy. *In*: Jansonius, J. & McGregor, D.C. (eds.): *Palynology, principles and applications*. American Association of Stratigraphic Palynologists Foundation 2, 29-50.
- Ziegler, B. (1958): Monographie der Ammonitengattung *Glochiceras* im epikontinentalen Weissjura Mitteleuropas. *Paläontographica* A/110, 93-164.
- Zieten, C.H. (1830): *Die Versteinerungen Württembergs*. Schweizerbart, Stuttgart, 102 pp.

Appendix A: List of all samples

Appendix A1: List of all thin sections from STA2-1
(1'225.80 – 521.15 m) A-2

Appendix A2: List of all sampled macrofossils from STA2-1
(915.45 – 718.61 m)..... A-3

Appendix A3: List of other provisionally determined conspicuous
macrofossils from STA2-1 (931.67 – 697.40 m)..... A-4

Appendix A4: List of all palynological samples from STA2-1
(905.83 – 726.25 m)..... A-5

Appendix A1: List of all thin sections from STA2-1 (1'225.80 – 521.15 m)

For the description and individual counting of the thin sections see Section 3.1; selected photos can be found in Appendix B.

Top [m]	Bottom [m]	Avg. depth [m]	Formation	Retrieval date [dd.mm.yyyy]	Sample ID
521.13	521.16	521.15	«Felsenkalk» + «Massenkalk»	21.06.2021	STA2-1-521.15-TS
673.53	673.57	673.55	Wildeggen Fm.	17.06.2021	STA2-1-673.55-TS
687.08	687.12	687.10	Wildeggen Fm.	17.06.2021	STA2-1-687.10-TS
726.44	726.48	726.46	Wildeggen Fm.	17.06.2021	STA2-1-726.46-TS
728.66	728.70	728.68	Wutach Fm.	17.06.2021	STA2-1-728.68-TS
739.88	739.92	739.90	«Park.-Württembergica-Sch.»	17.06.2021	STA2-1-739.90-TS
767.00	767.04	767.02	«Herrenwis Unit»	20.07.2021	STA2-1-767.02-TS
767.58	767.62	767.60	«Herrenwis Unit»	09.06.2021	STA2-1-767.60-TS
768.71	768.75	768.73	«Herrenwis Unit»	09.06.2021	STA2-1-768.73-TS
768.85	768.89	768.87	«Herrenwis Unit»	09.06.2021	STA2-1-768.87-TS
773.88	773.92	773.90	«Herrenwis Unit»	09.06.2021	STA2-1-773.90-TS
773.96	774.00	773.98	«Herrenwis Unit»	09.06.2021	STA2-1-773.98-TS
776.90	776.94	776.92	«Herrenwis Unit»	09.06.2021	STA2-1-776.92-TS
779.19	779.23	779.21	«Humphriesoolith Fm.»	09.06.2021	STA2-1-779.21-TS
786.76	786.80	786.78	Wedelsandstein Fm.	06.07.2021	STA2-1-786.78-TS
788.04	788.08	788.06	«Murchisonae-Oolith Fm.»	06.07.2021	STA2-1-788.06-TS
798.63	798.67	798.65	«Murchisonae-Oolith Fm.»	06.07.2021	STA2-1-798.65-TS
805.48	805.52	805.50	Opalinus Clay	06.07.2021	STA2-1-805.50-TS
805.84	805.88	805.86	Opalinus Clay	06.07.2021	STA2-1-805.86-TS
815.48	815.52	815.50	Opalinus Clay	06.07.2021	STA2-1-815.50-TS
819.18	819.22	819.20	Opalinus Clay	06.07.2021	STA2-1-819.20-TS
861.16	861.19	861.18	Opalinus Clay	06.07.2021	STA2-1-861.18-TS
953.70	953.73	953.72	Klettgau Fm.	20.07.2021	STA2-1-953.72-TS
960.67	960.71	960.69	Klettgau Fm.	20.07.2021	STA2-1-960.69-TS
965.00	965.04	965.02	Klettgau Fm.	20.07.2021	STA2-1-965.02-TS
1'033.86	1'033.89	1'033.88	Bänkerjoch Fm.	20.07.2021	STA2-1-1033.88-TS
1'049.95	1'049.99	1'049.97	Schinznach Fm.	31.08.2021	STA2-1-1049.97-TS
1'072.37	1'072.41	1'072.39	Schinznach Fm.	31.08.2021	STA2-1-1072.39-TS
1'080.12	1'080.16	1'080.14	Schinznach Fm.	31.08.2021	STA2-1-1080.14-TS
1'107.11	1'107.15	1'107.13	Schinznach Fm.	31.08.2021	STA2-1-1107.13-TS
1'113.85	1'113.89	1'113.87	Schinznach Fm.	31.08.2021	STA2-1-1113.87-TS
1'123.07	1'123.10	1'123.09	Zeglingen Fm.	31.08.2021	STA2-1-1123.09-TS
1'126.24	1'126.27	1'126.26	Zeglingen Fm.	31.08.2021	STA2-1-1126.26-TS
1'191.85	1'191.88	1'191.87	Kaiseraugst Fm.	03.09.2021	STA2-1-1191.87-TS
1'201.31	1'201.35	1'201.33	Kaiseraugst Fm.	03.09.2021	STA2-1-1201.33-TS
1'221.68	1'221.72	1'221.70	Kaiseraugst Fm.	03.09.2021	STA2-1-1221.70-TS
1'225.78	1'225.82	1'225.80	Dinkelberg Fm.	03.09.2021	STA2-1-1225.80-TS

Appendix A2: List of all sampled macrofossils from STA2-1 (915.45 – 718.61 m)

For the definitive determination of the individual macrofossils see Section 3.2 (Tab. 3-2).

Top [m]	Bottom [m]	Sample depth [m]	Formation	Retrieval date [dd.mm.yyyy]	Sample ID
718.61	718.65	718.61	Wildegge Fm.	14.07.2021	STA2-1-718.61-BS(MF)
725.00	725.05	725.00	Wildegge Fm.	17.06.2021	STA2-1-725.00-BS(MF)
727.06	727.08	727.08	Wildegge Fm.	17.06.2021	STA2-1-727.08-BS(MF)
727.49	727.55	727.51	Wutach Fm.	17.06.2021	STA2-1-727.51-BS(MF)
728.75	728.85	728.80	Wutach Fm.	17.06.2021	STA2-1-728.80-BS(MF)
729.54	729.61	729.58	Wutach Fm.	14.07.2021	STA2-1-729.58-BS(MF)
734.84	734.87	734.84	Variansmergel Fm.	17.06.2021	STA2-1-734.84-BS(MF)
773.21	773.28	773.24	«Herrenwis Unit»	09.06.2021	STA2-1-773.24-BS(MF)
774.00	774.09	774.05	«Herrenwis Unit»	09.06.2021	STA2-1-774.05-BS(MF)
795.09	795.13	795.11	«Murchisonae-Oolith Fm.»	06.07.2021	STA2-1-795.11-BS(MF)
805.48	805.54	805.52	Opalinus Clay	06.07.2021	STA2-1-805.52-BS(MF)
805.56	805.60	805.58	Opalinus Clay	06.07.2021	STA2-1-805.58-BS(MF)
850.54	850.57	850.57	Opalinus Clay	06.07.2021	STA2-1-850.57-BS(MF)
891.11	891.13	891.13	Opalinus Clay	06.07.2021	STA2-1-891.13-BS(MF)
894.31	894.34	894.34	Opalinus Clay	06.07.2021	STA2-1-894.34-BS(MF)
905.31	905.34	905.31	Staffelegg Fm.	06.07.2021	STA2-1-905.31-BS(MF)
905.81	905.84	905.84	Staffelegg Fm.	06.07.2021	STA2-1-905.84-BS(MF)
906.11	906.20	906.16	Staffelegg Fm.	06.07.2021	STA2-1-906.16-BS(MF)
906.39	906.45	906.42	Staffelegg Fm.	06.07.2021	STA2-1-906.42-BS(MF)
909.48	909.52	909.50	Staffelegg Fm.	06.07.2021	STA2-1-909.50-BS(MF)
909.92	909.97	909.95	Staffelegg Fm.	06.07.2021	STA2-1-909.95-BS(MF)
911.39	911.41	911.39	Staffelegg Fm.	06.07.2021	STA2-1-911.39-BS(MF)
915.41	915.49	915.45	Staffelegg Fm.	06.07.2021	STA2-1-915.45-BS(MF)

Appendix A3: List of other provisionally determined conspicuous macrofossils from STA2-1 (931.67 – 697.40 m)

Top [m]	Bottom [m]	Fossil	Determination (provisional)
697.40		Fragment of ammonite	Perisphinctidae indet.
698.17		Fragment of ammonite	Perisphinctidae indet.
698.63		Fragment of ammonite	Perisphinctidae indet.
704.19		Ammonite	Opeliidae indet.
704.57		Ammonite	Opeliidae indet.
717.26		Ammonite	Opeliidae indet.
721.15		Ammonite	indet.
737.00		Ammonite	<i>Parkinsonia</i> sp.
765.75		Ammonite	<i>Parkinsonia</i> sp. ?
773.23		Ammonite	indet.
773.26		Ammonite	indet.
774.10	774.90	2 echinids	<i>Stomechinus</i> sp. ?
785.72	785.91	Bivalves	<i>Gryphaea</i> sp.
890.83		Ammonite	<i>Leioceras</i> sp.
898.15		Ammonite	<i>Leioceras</i> sp.
906.25		Ammoniten	<i>Pleydellia</i> sp.
906.50		3 ammonites	<i>Pleydellia</i> sp.
908.39		Ammonite	<i>Grammoceras</i> sp. ?
912.41		Fragment of ammonite	indet.
914.56		Wood fragment ("gagat layer")	indet.
931.67		Ammonite	indet.

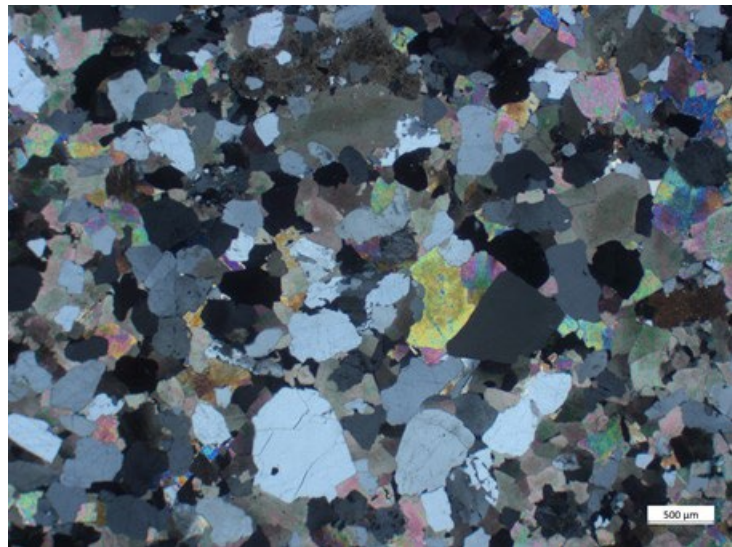

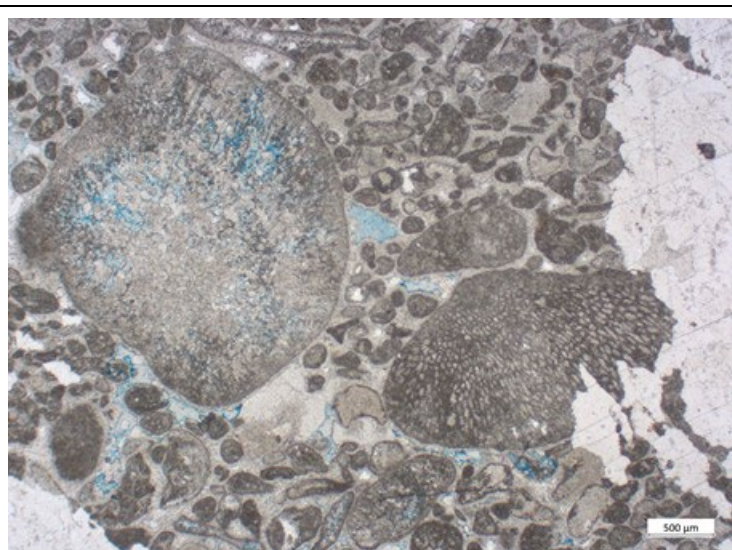
Appendix A4: List of all palynological samples from STA2-1 (905.83 – 726.25 m)

Palynological sample in grey was taken from ammonite sample retrieved at specific depth. Sampling was as close as possible to the ammonite at depth 905.84 m.

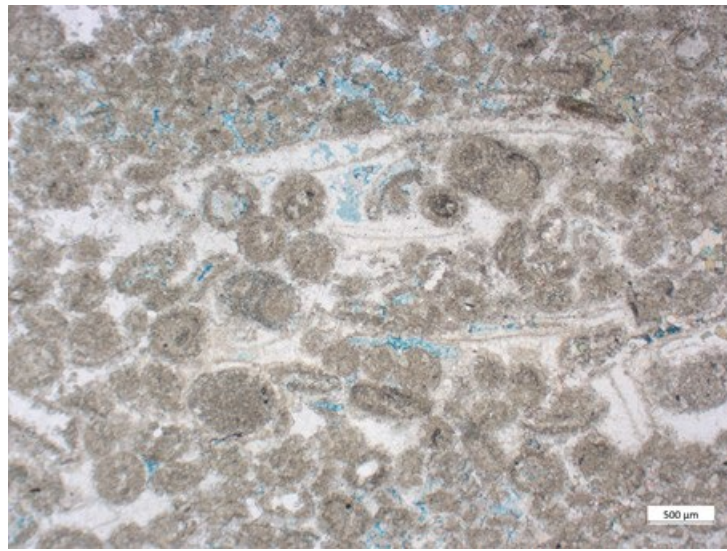

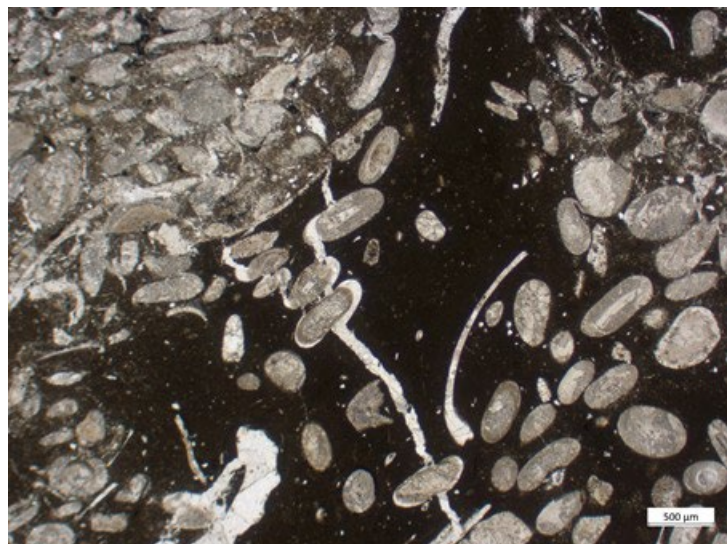
Top [m]	Bottom [m]	Avg. Depth [m]	Formation	Retrieval date [dd.mm.yyyy]	Sample ID
726.24	726.26	726.25	Wildeggen Fm.	14.07.2021	STA2-1-726.25-BS(PA)
728.45	728.47	728.46	Wutach Fm.	14.07.2021	STA2-1-728.46-BS(PA)
728.85	728.88	728.87	Wutach Fm.	14.07.2021	STA2-1-728.87-BS(PA)
731.75	731.77	731.76	Wutach Fm.	14.07.2021	STA2-1-731.76-BS(PA)
732.30	732.32	732.31	Variansmergel Fm.	14.07.2021	STA2-1-732.31-BS(PA)
734.65	734.67	734.66	Variansmergel Fm.	14.07.2021	STA2-1-734.66-BS(PA)
735.36	735.38	735.37	«Park.-Württembergica-Sch.»	14.07.2021	STA2-1-735.37-BS(PA)
744.26	744.28	744.27	«Park.-Württembergica-Sch.»	14.07.2021	STA2-1-744.27-BS(PA)
751.12	751.14	751.13	«Park.-Württembergica-Sch.»	14.07.2021	STA2-1-751.13-BS(PA)
759.35	759.36	759.36	«Park.-Württembergica-Sch.»	14.07.2021	STA2-1-759.36-BS(PA)
765.63	765.65	765.64	«Park.-Württembergica-Sch.»	09.06.2021	STA2-1-765.64-BS(PA)
766.94	766.96	766.95	«Park.-Württembergica-Sch.»	09.06.2021	STA2-1-766.95-BS(PA)
767.39	767.41	767.40	«Herrenwis Unit»	09.06.2021	STA2-1-767.40-BS(PA)
768.75	768.77	768.76	«Herrenwis Unit»	09.06.2021	STA2-1-768.76-BS(PA)
771.36	771.38	771.37	«Herrenwis Unit»	09.06.2021	STA2-1-771.37-BS(PA)
773.78	773.80	773.79	«Herrenwis Unit»	09.06.2021	STA2-1-773.79-BS(PA)
775.74	775.76	775.75	«Herrenwis Unit»	09.06.2021	STA2-1-775.75-BS(PA)
777.38	777.40	777.39	«Herrenwis Unit»	09.06.2021	STA2-1-777.39-BS(PA)
777.70	777.72	777.71	«Humphriesoolith Fm.»	09.06.2021	STA2-1-777.71-BS(PA)
779.12	779.14	779.13	«Humphriesoolith Fm.»	09.06.2021	STA2-1-779.13-BS(PA)
779.42	779.44	779.43	Wedelsandstein Fm.	09.06.2021	STA2-1-779.43-BS(PA)
781.05	781.08	781.07	Wedelsandstein Fm.	09.06.2021	STA2-1-781.07-BS(PA)
782.97	782.99	782.98	Wedelsandstein Fm.	14.07.2021	STA2-1-782.98-BS(PA)
784.23	784.25	784.24	Wedelsandstein Fm.	14.07.2021	STA2-1-784.24-BS(PA)
785.54	785.56	785.55	Wedelsandstein Fm.	14.07.2021	STA2-1-785.55-BS(PA)
786.00	786.02	786.01	Wedelsandstein Fm.	14.07.2021	STA2-1-786.01-BS(PA)
786.52	786.54	786.53	Wedelsandstein Fm.	14.07.2021	STA2-1-786.53-BS(PA)
787.03	787.05	787.04	«Murchisonae-Oolith Fm.»	14.07.2021	STA2-1-787.04-BS(PA)
787.94	787.96	787.95	«Murchisonae-Oolith Fm.»	14.07.2021	STA2-1-787.95-BS(PA)
789.00	789.02	789.01	«Murchisonae-Oolith Fm.»	14.07.2021	STA2-1-789.01-BS(PA)
795.06	795.08	795.07	«Murchisonae-Oolith Fm.»	14.07.2021	STA2-1-795.07-BS(PA)
795.78	795.80	795.79	«Murchisonae-Oolith Fm.»	14.07.2021	STA2-1-795.79-BS(PA)
799.10	799.12	799.11	«Murchisonae-Oolith Fm.»	14.07.2021	STA2-1-799.11-BS(PA)
799.54	799.56	799.55	«Murchisonae-Oolith Fm.»	14.07.2021	STA2-1-799.55-BS(PA)
799.89	799.90	799.90	Opalinus Clay	14.07.2021	STA2-1-799.90-BS(PA)
805.00	805.02	805.01	Opalinus Clay	14.07.2021	STA2-1-805.01-BS(PA)
806.61	806.63	806.62	Opalinus Clay	14.07.2021	STA2-1-806.62-BS(PA)
809.90	809.92	809.91	Opalinus Clay	14.07.2021	STA2-1-809.91-BS(PA)
820.29	820.31	820.30	Opalinus Clay	14.07.2021	STA2-1-820.30-BS(PA)
840.56	840.58	840.57	Opalinus Clay	14.07.2021	STA2-1-840.57-BS(PA)
860.69	860.71	860.70	Opalinus Clay	14.07.2021	STA2-1-860.70-BS(PA)
880.23	880.25	880.24	Opalinus Clay	14.07.2021	STA2-1-880.24-BS(PA)
899.82	899.84	899.83	Opalinus Clay	14.07.2021	STA2-1-899.83-BS(PA)
905.03	905.05	905.04	Opalinus Clay	14.07.2021	STA2-1-905.04-BS(PA)
905.81	905.84	905.83	Staffelegg Fm.	14.07.2021	STA2-1-905.83-BS(PA)

Appendix B: Photos microfacies



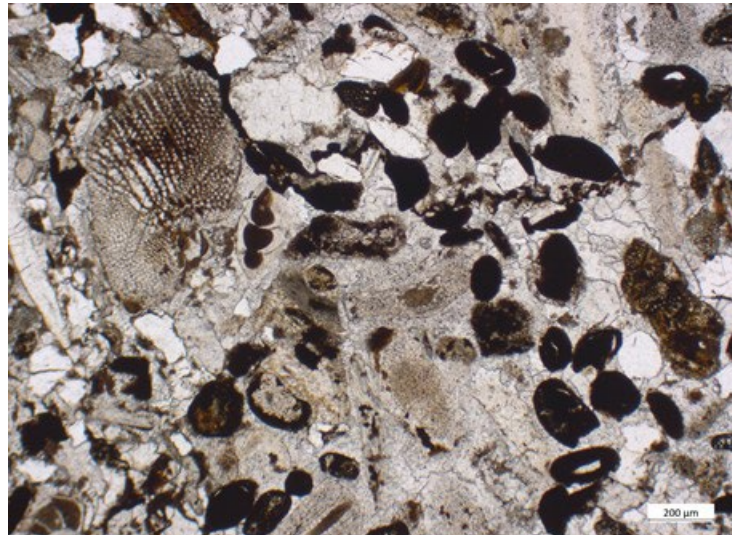
Fig. B-1:	Thin section STA2-1-1221-70, Kaiseraugst Fm.	B-2
Fig. B-2:	Thin section STA2-1-1201.33, Kaiseraugst Fm.	B-2
Fig. B-3:	Thin section STA2-1-1113.87, Schinznach Fm.	B-2
Fig. B-4:	Thin section STA2-1-1072.39, Schinznach Fm.	B-3
Fig. B-5:	Thin section STA2-1-861.18, Opalinus Clay	B-3
Fig. B-6:	Thin section STA2-1-819.20, Opalinus Clay	B-3
Fig. B-7:	Thin section STA2-1-815.50, Opalinus Clay	B-4
Fig. B-8:	Thin section STA2-1-805.50, Opalinus Clay	B-4
Fig. B-9:	Thin section STA2-1-798.65, «Murchisonae-Oolith Fm.»	B-4
Fig. B-10:	Thin section STA2-1-788.06, «Murchisonae-Oolith Fm.»	B-5
Fig. B-11:	Thin section STA2-1-786.78, Wedelsandstein Fm.	B-5
Fig. B-12:	Thin section STA2-1-779.21, «Humphriesiolith Fm.»	B-5
Fig. B-13:	Thin section STA2-1-773.98, «Herrenwis Unit»	B-6
Fig. B-14:	Thin section STA2-1-768.73, «Herrenwis Unit»	B-6
Fig. B-15:	Thin section STA2-1-767.60, «Herrenwis Unit»	B-6
Fig. B-16:	Thin section STA2-1-767.02, «Herrenwis Unit»	B-7
Fig. B-17:	Thin section STA2-1-739.90, «Parkinsoni-Württembergica-Sch.»	B-7
Fig. B-18:	Thin section STA2-1-521.15, Siderolithic infilling in «Massenkalk»	B-7

	<p>Fig. B-1:</p> <p>Dolomitic sandstone: quartz grains (grey to black) and dolomite cement (beige, also yellow, reddish, blue). Few dolomite crystals enclose an echinoderm skeletal element.</p> <p>Thin section photo, crossed nicols</p> <p>STA2-1-1221-70 Kaiseraugst Fm.</p>
	<p>Fig. B-2:</p> <p>Bioclastic limestone: thin bivalves with first generation calcite cement perpendicular on the shells (both red coloured). Second generation iron-calcite cement (violet) filling the pore space and dolomite (not coloured).</p> <p>Thin section photo TS stained for calcite=red</p> <p>STA2-1-1201.33 Kaiseraugst Fm.</p>
	<p>Fig. B-3:</p> <p>Bioclastic limestone with big codiacean green algae, micritic pellets, as well as echinoderms and bivalves, cemented by clear calcite and big anhydrite crystals (white)</p> <p>Thin section photo</p> <p>STA2-1-1113.87 Schinznach Fm.</p>


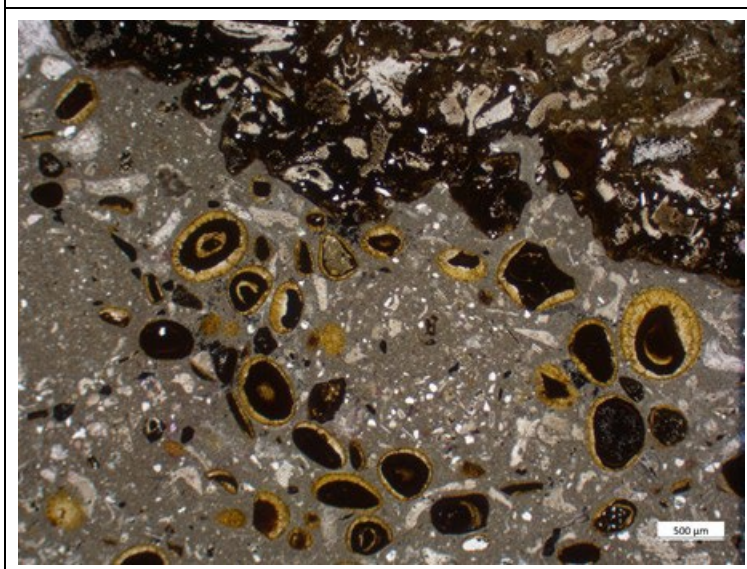
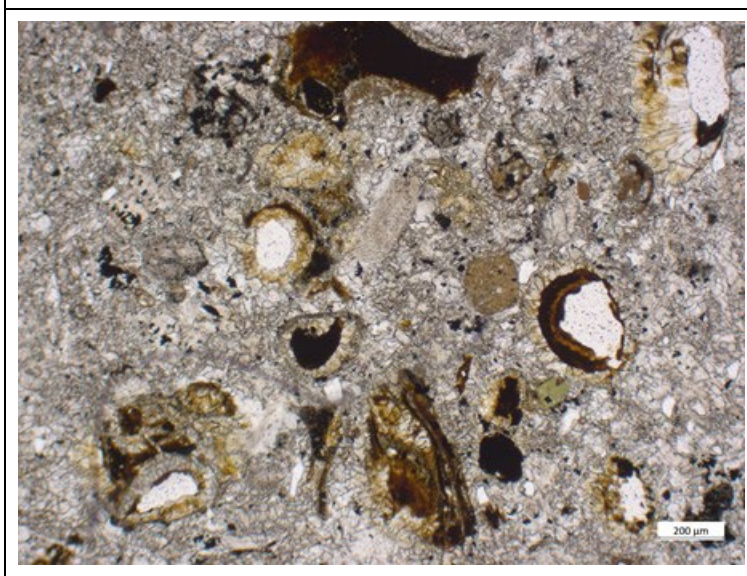
Selected photos of microfacies from Kaiseraugst Fm. and Schinznach Fm.

	<p>Fig. B-4:</p> <p>Dolomitic oolite: ooids and bivalves; all totally dolomitised, which generates some porosity (filled with blue coloured glue)</p> <p>Thin section photo</p> <p>STA2-1-1072.39 Schinznach Fm.</p>
	<p>Fig. B-5:</p> <p>"Hiatus bed" with banana shaped calcareous nodule in silty, bioclastic marl</p> <p>Thin section photo, Right third: TS stained for calcite = red</p> <p>STA2-1-861.18 Opalinus Clay</p>
	<p>Fig. B-6:</p> <p>Iron-oolitic (calcitic iron-ooids) limestone nodule as component in a multi-layered hardground</p> <p>Thin section photo</p> <p>STA2-1-819.20 Opalinus Clay</p>

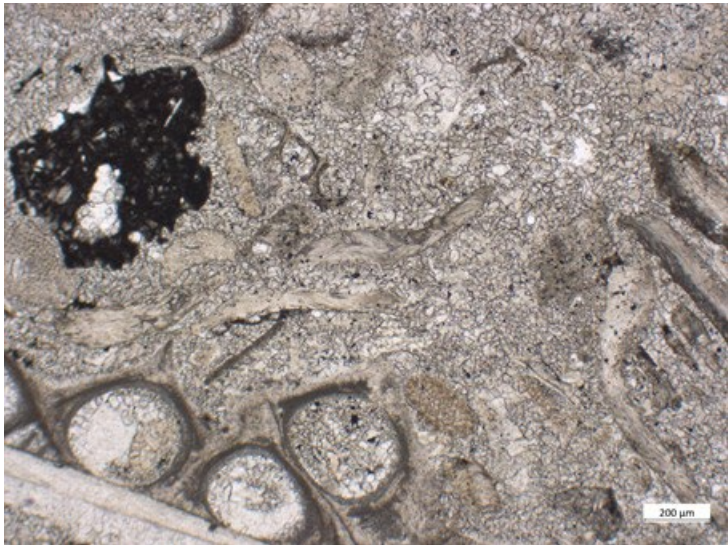

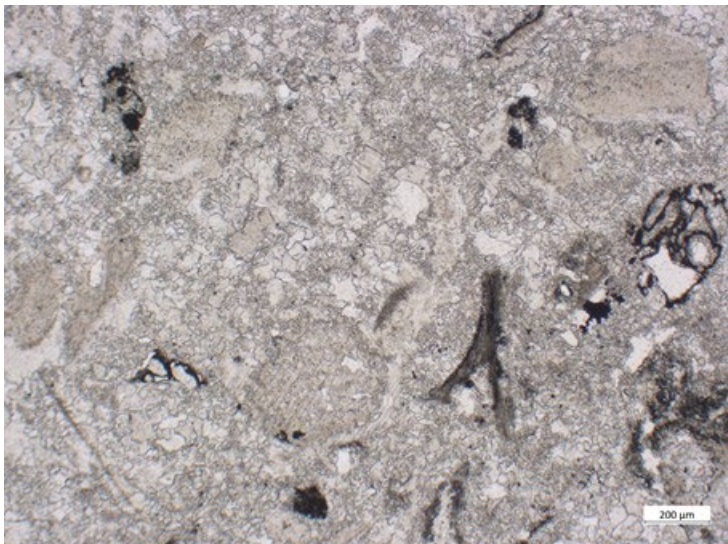
Selected photos of microfacies from Schinznach Fm. and Opalinus Clay

	<p>Fig. B-7:</p> <p>Sideritic nodule with iron-ooids, totally or partly replaced by calcite, and bivalves, lying in a sideritic, calcareous marl (bottom part).</p> <p>Thin section photo</p> <p>STA2-1-815.50 Opalinus Clay</p>
	<p>Fig. B-8:</p> <p>Hardground with 3 different lithologies: 1) limonitic, iron-oolitic, bioclastic limestone (left); 2) iron-stromatolite with quartz grains (middle); 3) sideritic, bioclastic limestone with "stellate calcite".</p> <p>Thin section photo</p> <p>STA2-1-805.50 Opalinus Clay</p>
	<p>Fig. B-9:</p> <p>Iron-oolitic, bioclastic limestone: consisting of small limonitic components, echinoderm skeletal elem., quartz grains and calcite cement. A part of the limonitic components are iron-ooids, another part are limonitic bioclasts and a third are limonitic pellets.</p> <p>Thin section photo</p> <p>STA2-1-798.65 «Murchisonae-Oolith Fm.»</p>

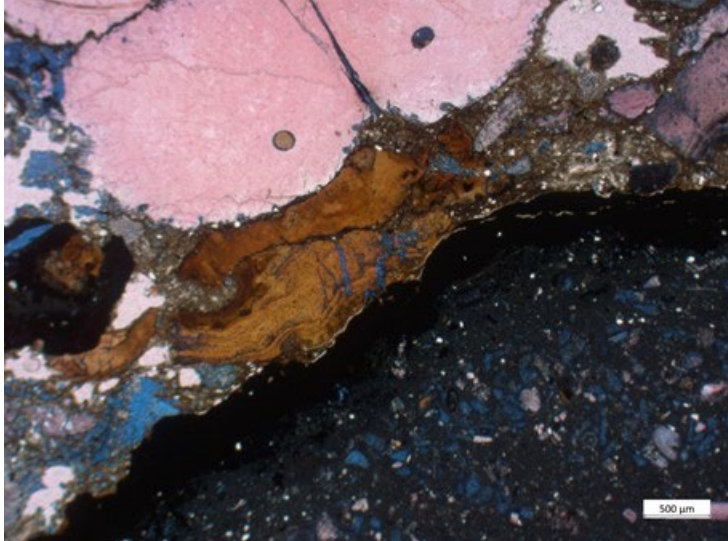
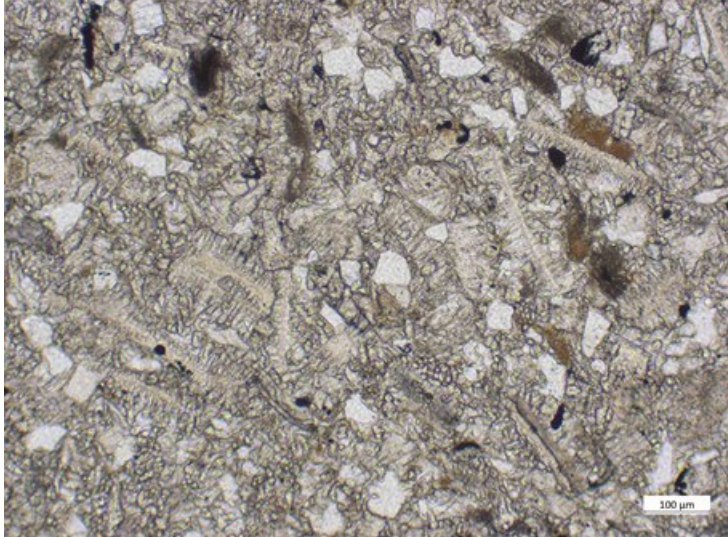
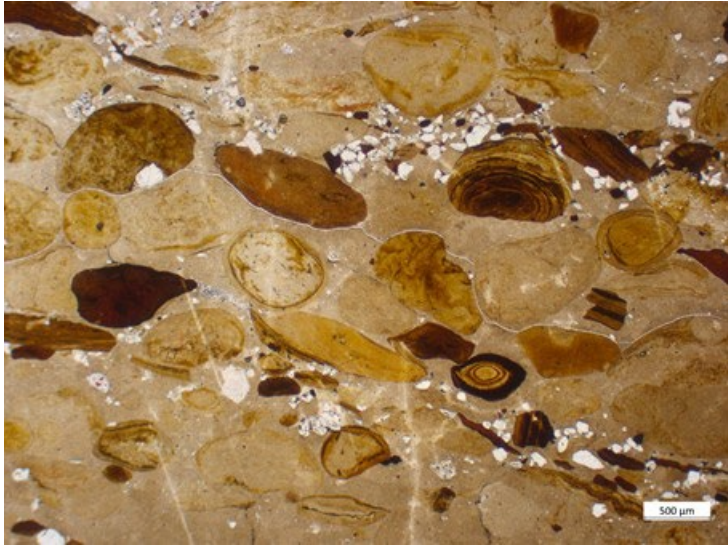
Selected photos of microfacies from Opalinus Clay and «Murchisonae-Oolith Fm.»

	<p>Fig. B-10:</p> <p>Special "iron-ooids" – limonitic echinoderm "bioclasts" with a small ooidal cortex – in a bioclastic limestone (sandy)</p> <p>Thin section photo</p> <p>STA2-1-788.06 «Murchisonae-Oolith Fm.»</p>
	<p>Fig. B-11:</p> <p>Iron-oolitic, bioclastic limestone with limonitic, bioclastic limestone nodule (upper part). The iron-ooids show limonitic calcite cement rims.</p> <p>Thin section photo</p> <p>STA2-1-786.78 Wedelsandstein Fm.</p>
	<p>Fig. B-12:</p> <p>"Hiatus bed": bioclastic limestone with some limonitic bioclasts and iron-ooids surrounded by "stellate calcite". The white spots are holes, generated by thin section preparation.</p> <p>Thin section photo</p> <p>STA2-1-779.21 «Humphriesioolith Fm.»</p>

Selected photos of microfacies from «Murch.-O. Fm.», Wedelsst. Fm. and «Humphriesiool. Fm.»

	<p>Fig. B-13:</p> <p>Bioclastic limestone, consisting mostly of bivalves and serpulids, as well as few small pyrite nodules, and microsparitic matrix.</p> <p>Thin section photo</p> <p>STA2-1-773.98 «Herrenwis Unit»</p>
	<p>Fig. B-14:</p> <p>Bioclastic, calcareous marl: bivalves and echinoderm skeletal elements with marly matrix. The bioclasts are closely packed due to strong pressure solution.</p> <p>Thin section photo</p> <p>STA2-1-768.73 «Herrenwis Unit»</p>
	<p>Fig. B-15:</p> <p>Bioclastic limestone: Clasts of corals, bivalves and echinoderms with microsparitic matrix. Few of the biogene components contains pyrite (black).</p> <p>Thin section photo</p> <p>STA2-1-767.60 «Herrenwis Unit»</p>

Selected photos of microfacies from «Herrenwis Unit»

	<p>Fig. B-16:</p> <p>Top of the «Herrenwis Unit» (right bottom corner), partly overlain by a limonitic crust and then a bed of bioclasts with a lot of belemnites (rosa coloured).</p> <p>Thin section photo TS stained for calcite=red</p> <p>STA2-1-767.02 «Herrenwis Unit»</p>
	<p>Fig. B-17:</p> <p>"Hiatus bed": silty, bioclastic limestone, consisting of small clasts of bivalves, echinoderms and pellets, embedded in "stellate calcite".</p> <p>Thin section photo</p> <p>STA2-1-739.90 «Parkinsoni-Württembergica-Sch.»</p>
	<p>Fig. B-18:</p> <p>Sandy claystone: spherical claystone components, with limonitic clasts, few iron-pisoids (Bohnerz) and quartz sand (white). Karst filling within the «Massenkalk» limestone</p> <p>Thin section photo</p> <p>STA2-1-521.15 Siderolithic infilling in «Felsenkalke» and «Massenkalk»</p>

Selected photos of microfacies from «Herrenwis U.», «Park.-Württem.-Sch.» and «Massenkalk»

Appendix C: Plates of ammonites and other macrofossils

Plate I: STA2-1 (915.45 m, core pictures)C-3

Plate II: STA2-1 (915.45 m).....C-5

Plate III: STA2-1 (911.39 – 905.84 m).....C-7

Plate IV: STA2-1 (905.31 – 850.57 m).....C-9

Plate V: STA2-1 (805.58 – 774.05 m).....C-11

Plate VI: STA2-1 (734.84 – 728.84 m).....C-13

Plate VII: STA2-1 (727.08 – 718.61 m).....C-15

Plate I STA2-1 (915.45 m)

Fig. 1: Planar photograph (*cf.* Dossier II) from the section 915.53 – 914.91 m with the location of the «Unterer Stein» and the location of the sampled crocodile at 915.45 m.

Fig. 2: 360° photograph from the same section as Fig. 1.

Both core photographs are illustrated with the same scales; in Fig. 2 the depth 915.0 m and 915.5 m are marked on the yellow line.

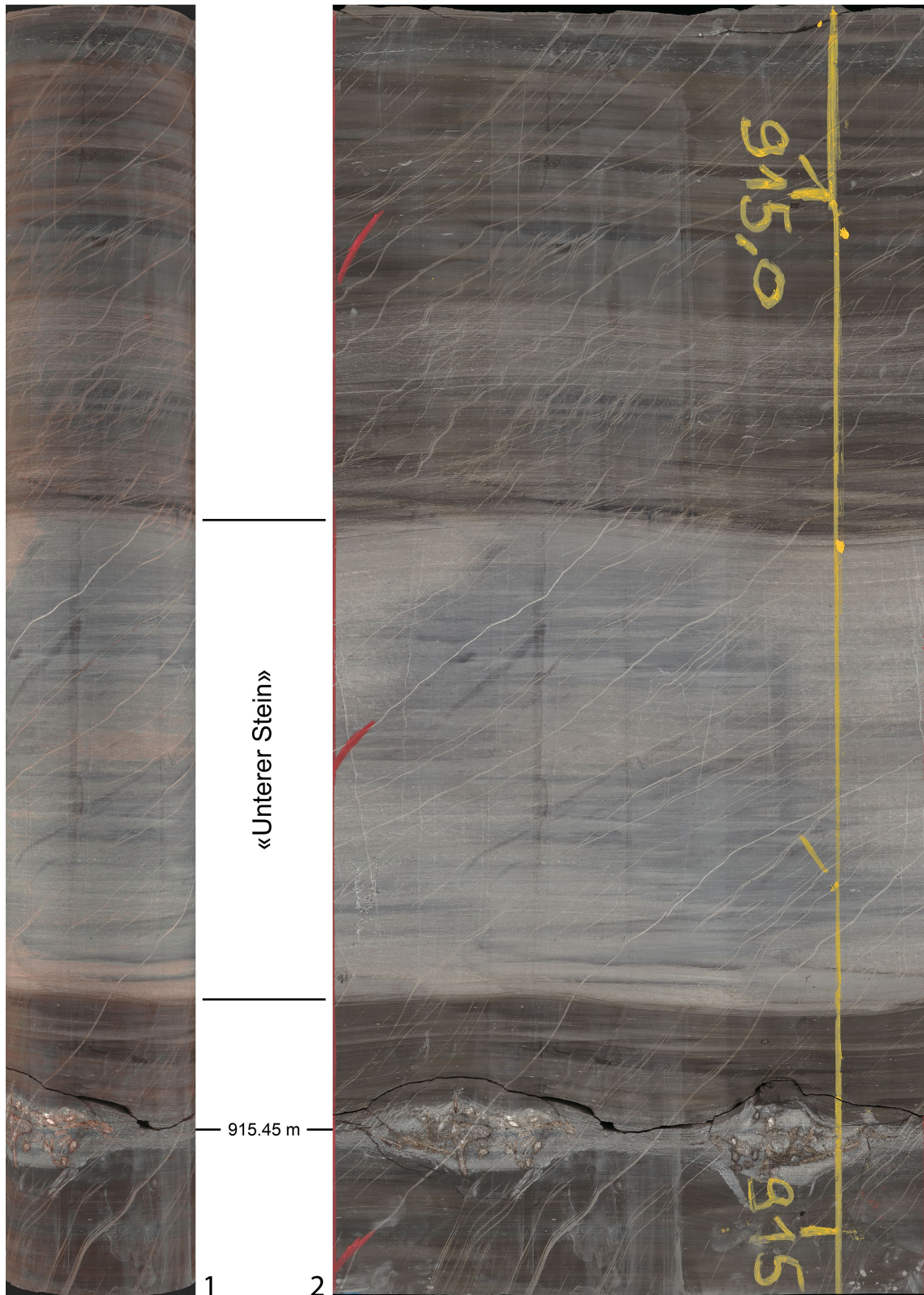


Plate I: STA2-1 (915.45 m, core pictures)

Plate II STA2-1 (915.45 m)

Fig. 1: *Pelagosaurus typus* (Bronn, 1842), depth: 915.45 m, Staffelegg Fm. (Rietheim Mb.), Early Toarcian, after 7 hours of preparation.

Figs. 2 to 5: *Pelagosaurus typus* (Bronn, 1842), depth: 915.45 m, Staffelegg Fm. (Rietheim Mb.), Early Toarcian, after 46 hours of preparation.

All figures are illustrated in the same scales; black bar indicate approximatly 1 cm.

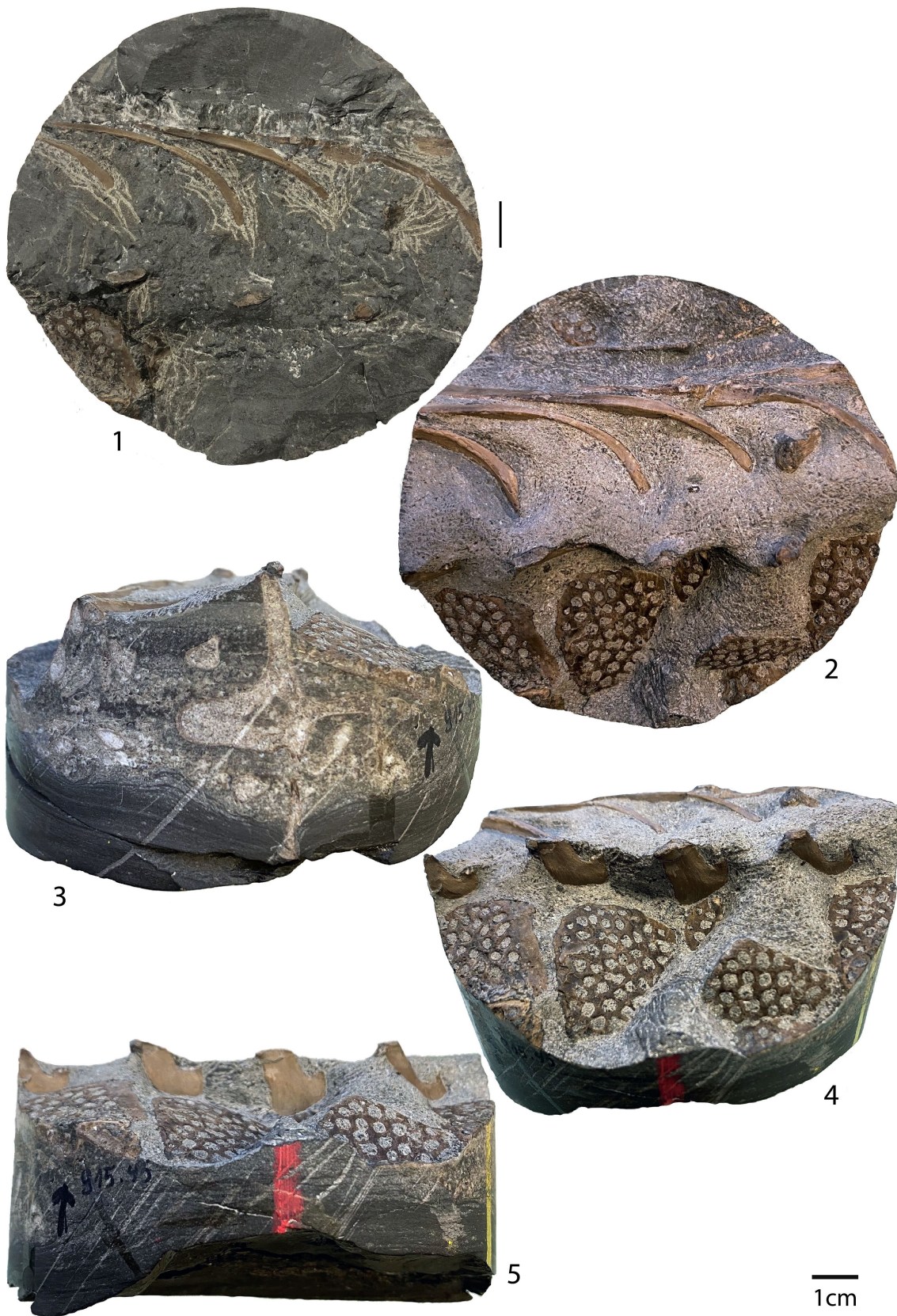


Plate II: STA2-1 (915.45 m)

Plate III STA2-1 (911.39 – 905.84 m)

- Fig. 1: *Dactylioceras* sp., depth: 911.39 m, Staffelegg Fm. (Rietheim Mb.), probably Falciferum Zone.
- Figs. 2a, 2b: *Hildoceras* sp.?, depth: 909.95 m, Staffelegg Fm. (Gross Wolf Mb.), probably Variabilis Zone, Fig. 2a: lateral view, Fig. 2b: cross section.
- Fig. 3: *Cotteswoldia* ex gr. *aalensis* (Zieten, 1830), pathogenic specimen, depth: 906.42 m, Staffelegg Fm. (Gross Wolf Mb.), Aalensis Zone, Aalensis Subzone.
- Fig. 4: *Cotteswoldia* sp., depth: 906.16 m, Staffelegg Fm. (Gross Wolf Mb.), Aalensis Zone, probably Aalensis Subzone.
- Fig. 5: *Cotteswoldia* aff. *fluitans* (Dumortier, 1874), depth: 905.84 m, Staffelegg Fm. (Gross Wolf Mb.), Aalensis Zone, Aalensis Subzone.

All figures are illustrated in individual scales; black bars indicate 1 cm.

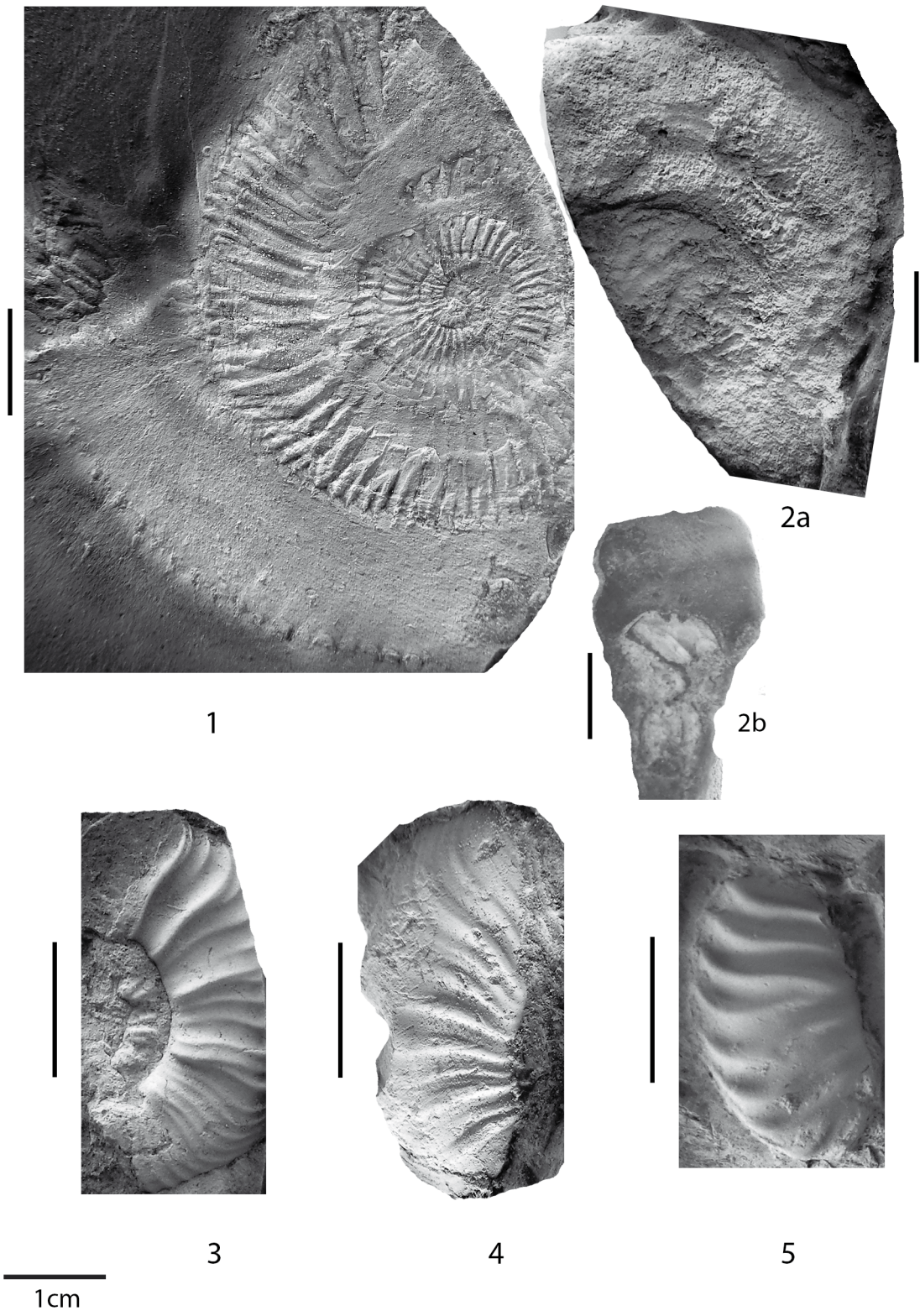


Plate III: STA2-1 (911.39 – 905.84 m)

Plate IV STA2-1 (905.31 – 850.57 m)

- Fig. 1: *Pleydellia* ex gr. *buckmani* (Maubeuge, 1947), two specimens, microconchs, depth: 905.31 m, Staffelegg Fm. (Gross Wolf Mb.), Aalensis Zone, Torulosum Subzone.
- Fig. 2: *Leioceras* ex gr. *subglabrum* (Buckman, 1902), depth: 894.34 m, Opalinus Clay, Opalinum Zone, Opalinum Subzone.
- Fig. 3: *Leioceras* ex gr. *opalinum* (Reinecke, 1818), depth: 891.13 m, Opalinus Clay, Opalinum Zone, Opalinum Subzone.
- Fig. 4: *Leioceras* ex gr. *subglabrum* (Buckman, 1902), depth: 850.57 m, Opalinus Clay, Opalinum Zone, Opalinum Subzone.

All figures are illustrated in individual scales; black bars indicate 1 cm.

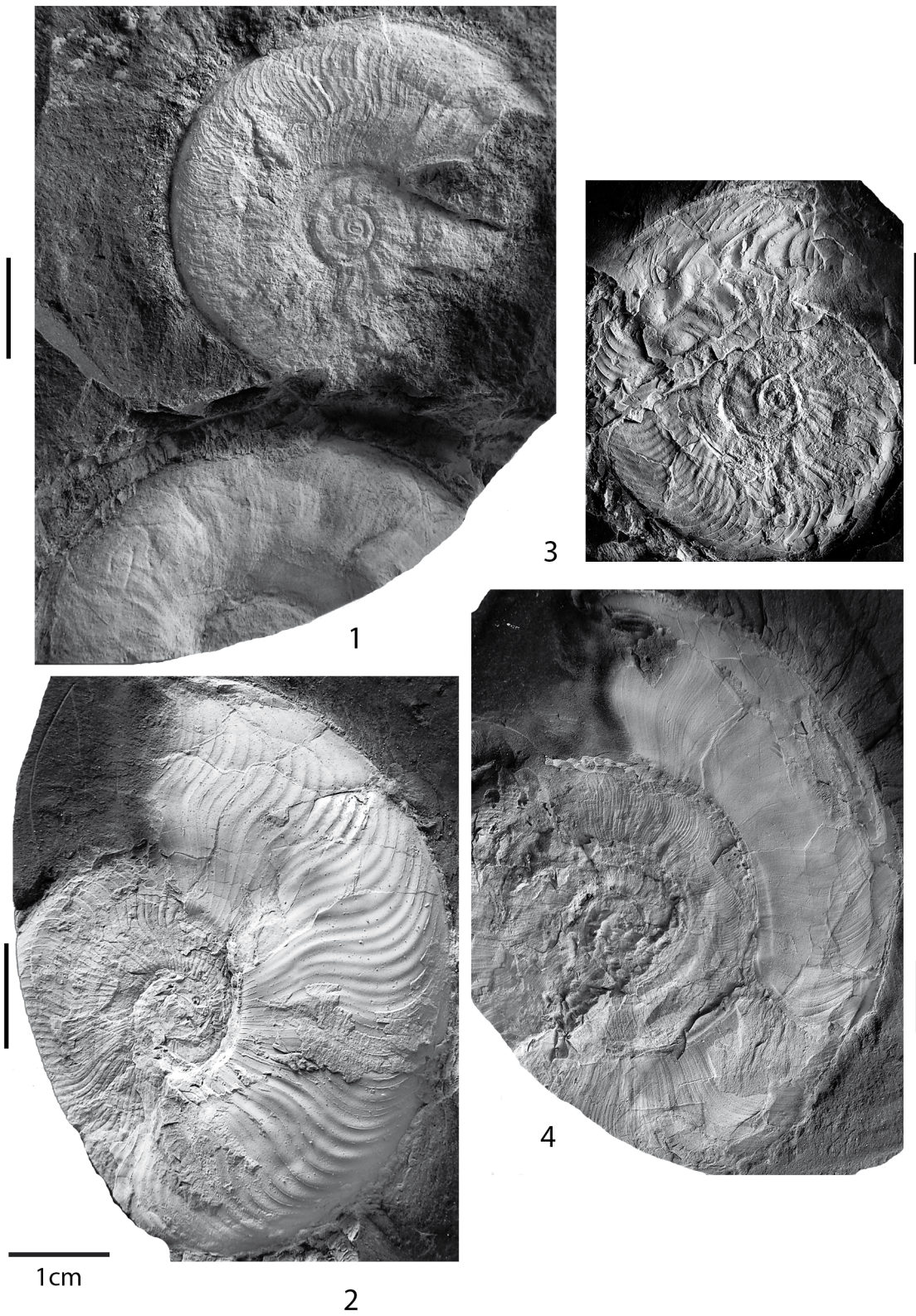


Plate IV: STA2-1 (905.31 – 850.57 m)

Plate V STA2-1 (805.58 – 774.05 m)

- Fig. 1: *Leioceras* ex gr. *bifidatum*? (Buckman, 1899), depth: 805.58 m, Opalinus Clay, Opalinum Zone, probably Bifidatum Subzone.
- Figs. 2a, 2b: *Staufenia* ex gr. *staufensis*? (Oppel, 1856), depth: 795.11 m, «Murchisonae-Oolith Fm.», probably Bradfordensis Zone, probably Bradfordensis Subzone, Fig. 2a: lateral view, Fig. 2b: cross section.
- Fig. 3: *Pedina* sp., depth: 774.05 m, «Herrenwis Unit», Bajocien.

All figures are illustrated in individual scales; black bars indicate 1 cm.

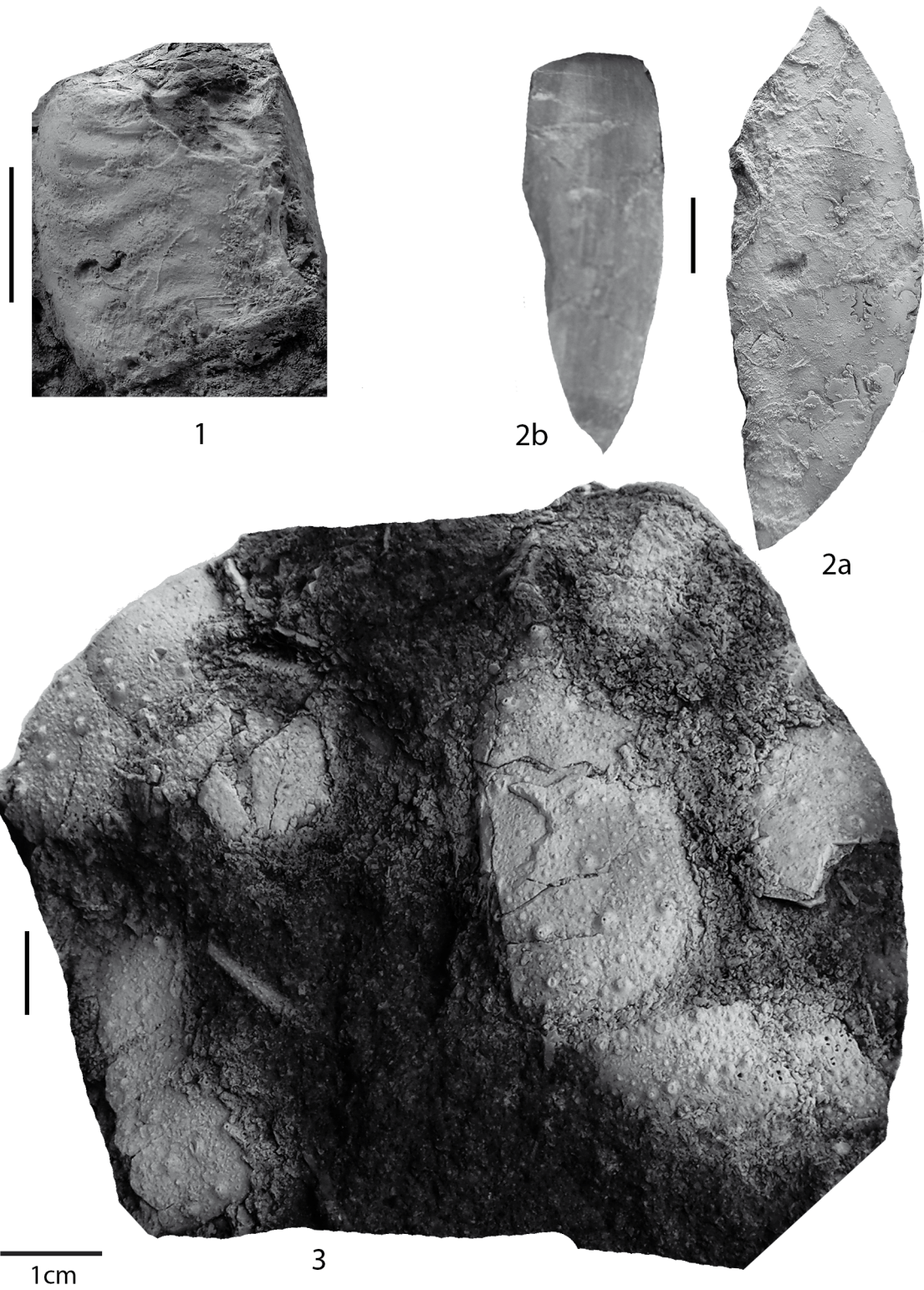


Plate V: STA2-1 (805.58 – 774.05 m)

Plate VI STA2-1 (734.84 – 728.84 m)

Fig. 1: *Parkinsonia (Oraniceras)* sp., depth: 734.84 m, «Parkinsoni-Württembergica-Schichten», Zigzag Zone.

Figs. 2a, 2b: *Macrocephalites* sp., depth: 728.80 m, Wutach Fm., Fig. 2a: lateral view, Fig. 2b: cross section.

All figures are illustrated in individual scales; black bars indicate 1 cm.

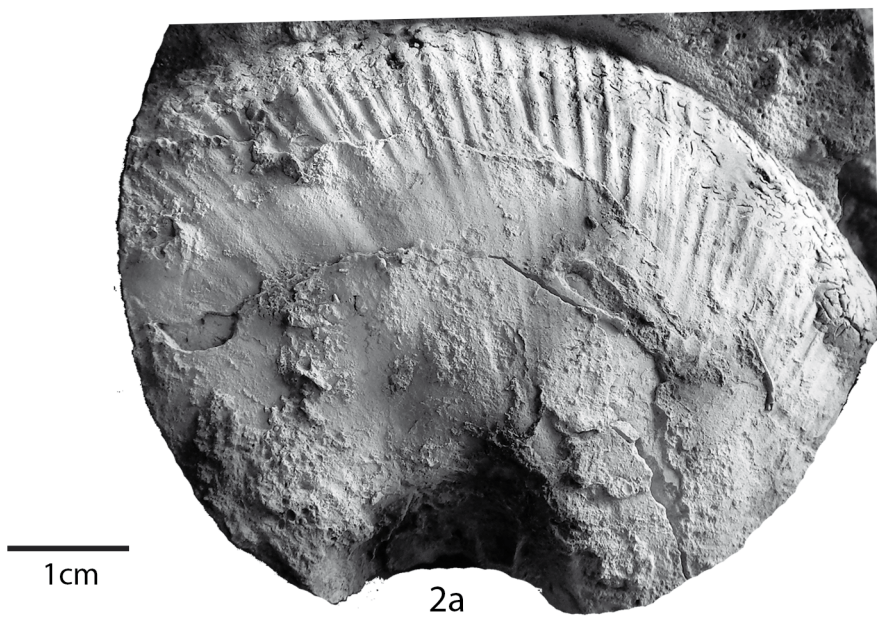
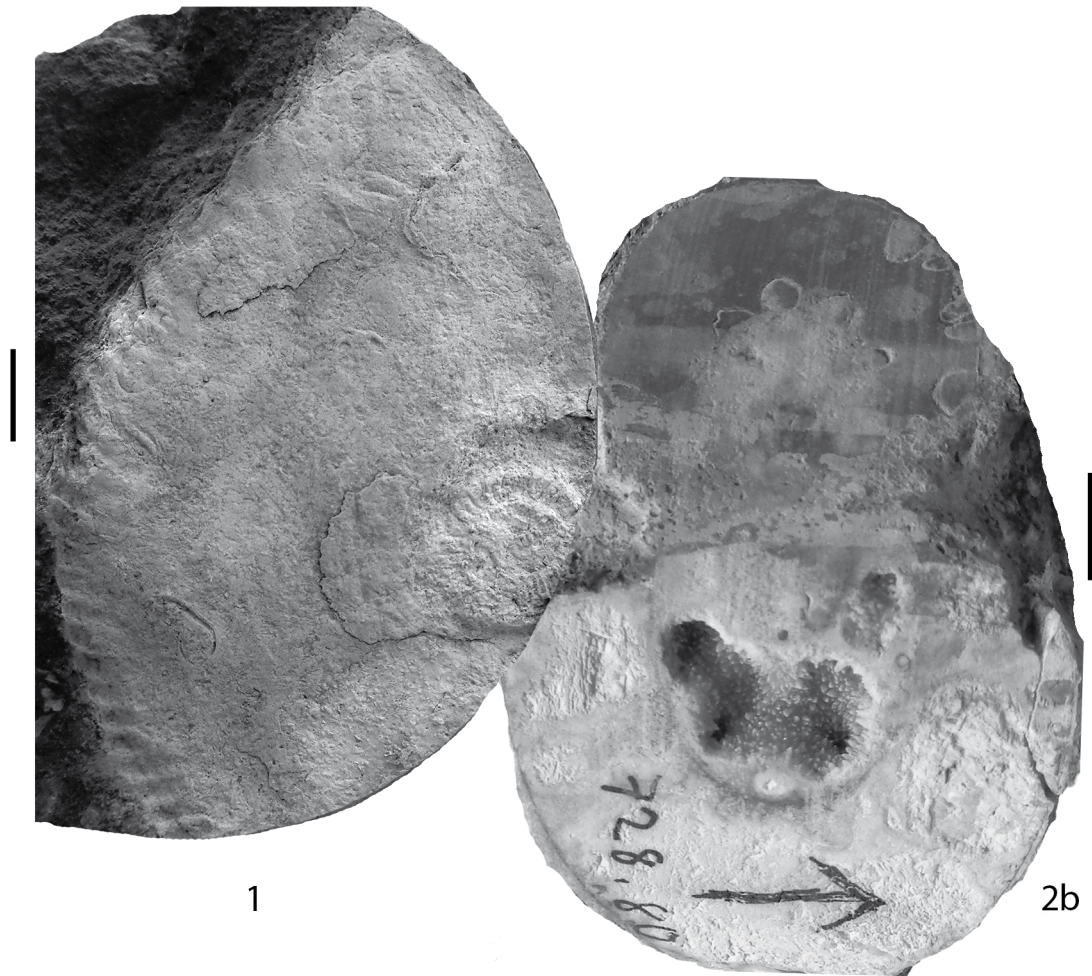


Plate VI: STA2-1 (734.84 – 728.84 m)

Plate VII STA2-1 (727.08 – 718.61 m)

- Fig. 1: *Trimarginites* ex gr. *arolicus*? (Oppel, 1863), depth: 727.08 m, Wildegge Fm. (Birmenstorf Mb. and «Glaukonitsandmergel Bed»), Transversarium or Bifurcatus Zone.
- Fig. 2: *Perisphinctes* sp., depth 725.00 m, Wildegge Fm. (Effingen Mb.), Transversarium Zone.
- Fig. 3: *Glochiceras* ex gr. *tectum* (Ziegler, 1958), depth 718.61 m, Wildegge Fm. (Effingen Mb.), Transversarium or Bifurcatus Zone.

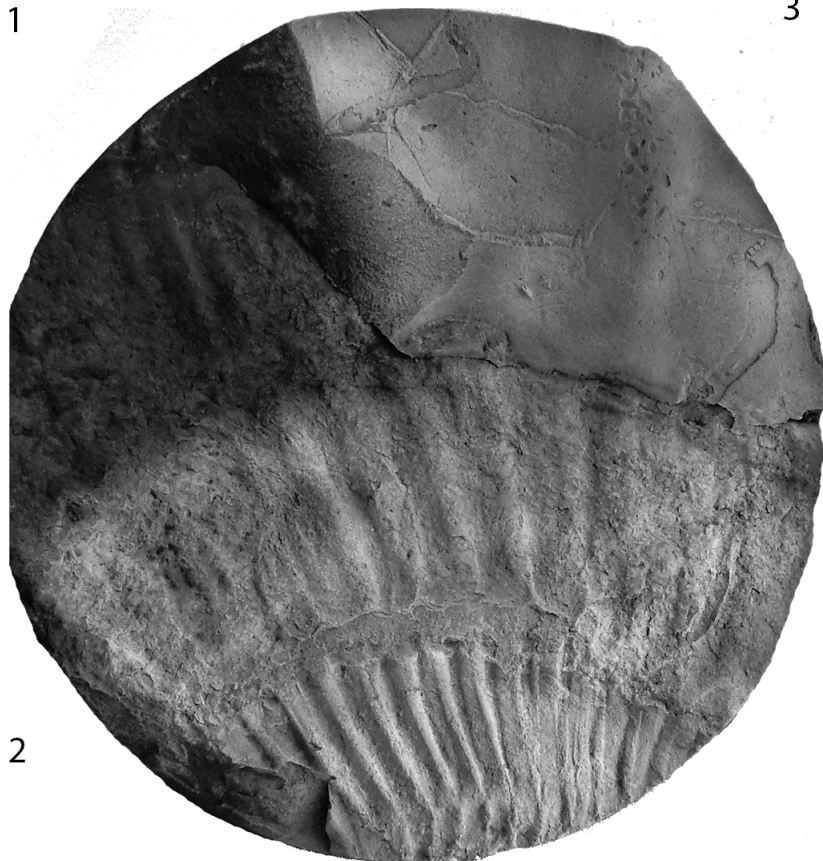
All figures are illustrated in individual scales; black bars indicate 1 cm.



1



3



2

1cm

Plate VII: STA2-1 (727.08 – 718.61 m)

Appendix D: Palynostratigraphy

Appendix D1: Range Chart: Quantitative stratigraphic distribution of Middle Jurassic palynomorphs in the Stadel-2-1 borehole

Appendix D2: Depth/Age plot: Stadel-2-1 borehole

Note: The appendices are only included in the digital version of this report (PDF) and can be found under the paper clip symbol.

Appendix E: Chemostratigraphy

Appendix E1: List of all geochemical samples and results mainly drilled
from specific calcareous beds in the Opalinus Clay and its
confining unitsE-2

Appendix E1: List of all geochemical samples and results mainly drilled from specific calcareous beds in the Opalinus Clay and its confining units

Data are discussed in Section 3.4 and partly illustrated in Fig. 3-4 (part of the data points lie outside the presented scale for the $\delta^{13}\text{C}_{\text{carb}}$): HB: drilled from a "hiatus bed" (for definition of HB see Section 2.1), CC: drilled from a calcareous concretion, SC: drilled from a sideritic concretion or nodule, SN: drilled from a septarian nodule, MF: drilled from macrofossil, TS: drilled directly from thin section sample (see microfacies description in Section 3.1).

Depth [m]	Description of sample		TS	$\delta^{13}\text{C}_{\text{carb}}$ [‰ VPDB]	$\delta^{18}\text{O}_{\text{carb}}$ [‰ VPDB]	Carbonate [wt.-%]
739.05	Septarian nodule	SN		-19.65	-0.90	87.0
779.21	Bioclastic limestone	HB	×	-1.48	-3.10	82.3
783.20	Calcareous concretion	CC		0.59	-1.38	79.6
785.80	Gryphaea	MF		3.02	-0.71	95.0
785.82	Bioclastic limestone (limonitic)	HB		0.16	-3.00	60.1
786.78	Bioclastic limestone (iron-oolitic)		×	-1.57	-2.34	66.4
788.06	Bioclastic marly (limonitic)			-1.20	-7.55	46.7
799.50	Limestone (iron-oolitic)			-2.81	-3.33	91.2
805.50	Iron-stromatolitic horizon	HB	×	-0.69	-3.11	83.1
805.86	Bioclastic limestone		×	-2.40	-3.53	86.7
815.45	Calcareous concretion	CC		-6.48	-1.13	70.9
815.50	"Hiatus bed" (marly and bioclastic)	HB	×	-2.78	-4.05	81.1
816.87	Septarian nodule	SN		-25.32	-1.19	77.5
819.02	Sideritic concretion	SC		-19.11	-1.26	82.1
819.20	Sideritic layer or concretion	SC	×	-8.71	-3.70	67.1
823.56	Sideritic concretion	SC		-3.44	-2.65	61.4
891.32	Calcareous concretion	CC		-19.24	-1.71	82.4
892.01	Septarian nodule	SN		-31.14	-1.36	83.7
914.00	«Oberer Stein» (Rietheim Mb.)			-0.09	-6.09	84.2
914.75	«Homog. Kalkbank» (Rietheim Mb.)			-1.17	-2.86	83.4
915.25	«Unterer Stein» (Rietheim Mb.)			-2.18	-3.13	94.8